UNIVERSIDADE FEDERAL DE SANTA MARIA
CENTRO DE TECNOLOGIA
PROGRAMA DE PÓS-GRADUAÇÃO EM ENGENHARIA QUÍMICA

Susanne Pedroso Druzian

DESENVOLVIMENTO DE MATERIAIS A BASE DE QUITINA PARA APLICAÇÃO NA ADSORÇÃO DE CORANTES

Santa Maria, RS
2021

Susanne Pedroso Druzian

DESENVOLVIMENTO DE MATERIAIS A BASE DE QUITINA PARA APLICAÇÃO NA ADSORÇÃO DE CORANTES

Tese apresentada ao curso de Doutorado do Programa de Pós-Graduação em Engenharia Química, da Universidade Federal de Santa Maria (UFSM), como requisito parcial para a obtenção do título de **Doutora em Engenharia Química**.

Orientador: Profº Drº. Guilherme Luiz Dotto
Coorientadora: Drª. Janaína Oliveira Gonçalves

Santa Maria, RS
2021

Susanne Pedroso Druzian

DESENVOLVIMENTO DE MATERIAIS A BASE DE QUITINA PARA APLICAÇÃO NA ADSORÇÃO DE CORANTES

Tese apresentada ao curso de Doutorado do Programa de Pós-Graduação em Engenharia Química, da Universidade Federal de Santa Maria (UFSM, RS), como requisito parcial para a obtenção do título de **Doutora em Engenharia Química**.

Aprovado em 24 de fevereiro de 2021:

_____
Guilherme Luiz Dotto, Dr. (UFSM)
(Presidente, Orientador)

_____
Eric da Cruz Severo, Dr. (INT)

_____
Gabriela Carvalho Collazzo, Dra. (UFSM)

_____
Maria Amélia Zazycki, Dra. (UFN)

_____
Fernanda de Castilhos, Dra. (UFSM)

Santa Maria, RS
2021

DEDICATÓRIA

Dedico este trabalho à minha mãe, Oneide Pedroso Druzian, que é a minha maior incentivadora e minha melhor amiga. Luz da minha vida.

AGRADECIMENTOS

Primeiramente, a Deus, por me conceder saúde e força para chegar até aqui;

À minha mãe, Oneide Pedroso Druzian, por todo apoio e amor. Por me proporcionar todas as condições para que eu pudesse estudar. Por ser a grande responsável por esta conquista e o meu maior amor;

À minha tia, Solange Pedroso Denardi, por ser minha segunda mãe e me dar também todo apoio que eu precisava para concluir essa etapa;

Ao meu pai, Gilberto Forgiarini Druzian (*in memoriam*), por ter sido meu exemplo de integridade;

Ao meu orientador e amigo, prof. Dr. Guilherme Luiz Dotto, pelos ensinamentos e competência que oportunizaram o meu crescimento profissional e, principalmente, pela compreensão e apoio nos momentos difíceis que passei durante essa jornada. Tens minha gratidão e admiração tanto pelo profissional, quanto pela pessoa que és;

Ao programa de Pós-graduação em Engenharia Química da Universidade Federal de Santa Maria, pela oportunidade de desenvolver este projeto;

Às alunas de iniciação científica, Natalia Pollon Zanatta e Renata König Borchardt, pela colaboração no desenvolvimento dos experimentos de laboratório;

Aos funcionários, Marcos Mello, Mariana Bassaco, Margiani Fortes e Liége Abelin, por toda ajuda prestada durante o desenvolvimento deste trabalho e por serem sempre profissionais muito competentes e dispostos a ajudar;

Aos colegas da pós, por sempre proporcionarem um ambiente harmonioso e divertido;

Aos amigos para a vida que a pós me proporcionou, Angélica Streit, Enrique Chaves, Fabíola Dalla Nora, Gabriel Porto, Isaac Nunes, Juliano Missau, Larissa Ricardo e Lauren Marcilene Machado, que tornaram meus dias mais alegres. E principalmente aos amigos Eric Severo e Letícia Côrtes que foram meus companheiros inseparáveis durante esses quatro anos;

Ao meu namorado, Lucas Gerhard, por todo amor e suporte que me deu, principalmente nas etapas finais da conclusão deste trabalho;

Aos meus familiares, por todo amor e apoio;

Às minhas amigas de longa data, Cátia Armany, Izabel Freitas, Lauren Machado e Paola Ferigolo, por toda amizade e incentivo durante todos esses anos;

A CAPES pelo apoio financeiro;

RESUMO

Os problemas ambientais em virtude da industrialização acelerada das últimas décadas têm despertado na sociedade a necessidade de desenvolvimento de novas tecnologias para o tratamento dos resíduos industriais. A indústria têxtil se destaca devido ao alto consumo de água no seu processo produtivo e aos grandes volumes de efluentes gerados contendo compostos contaminantes, como corantes, com grande potencial para a poluição de corpos d`água. Em função disso, uma extensa pesquisa vem sendo realizada visando o desenvolvimento de tecnologias para o tratamento de efluentes contendo corantes, dentre as quais a adsorção se destaca por seu baixo custo e alta eficiência. A quitina é um biopolímero biodegradável e renovável que pode ser utilizado como base para o desenvolvimento de materiais adsorventes. Nesse contexto, o presente trabalho teve como objetivo desenvolver materiais a partir da quitina para aplicação na remoção do corante violeta cristal de soluções aquosas por adsorção. Primeiramente, quitina foi obtida a partir de resíduos de camarão, e através da hidrólise ácida da quitina obtida, nanowhiskers foram sintetizados. Ambos os materiais foram caracterizados e aplicados para estudos de adsorção. A caracterização dos materiais mostrou que os nanowhiskers apresentaram forma de haste e um maior tamanho médio de poros quando comparada a quitina. Os testes de adsorção mostraram que a adsorção foi favorecida utilizando-se 5 g L^{-1} de nanowhiskers e pH da solução igual a 8. O modelo de pseudossegunda ordem foi o mais adequado para representar os dados cinéticos e o modelo de Sips o que melhor representou as curvas de equilíbrio. O processo foi endotérmico, espontâneo e favorável. A capacidade máxima de adsorção do violeta cristal foi 59,52 mg g^{-1}, o que corroborou o potencial dos nanowhiskers para ser utilizado como adsorvente no tratamento de efluentes coloridos. Um novo aerogel também foi sintetizado a partir da quitina. Este aerogel foi obtido pela criodessecação de um gel de quitina e psyllium. O material desenvolvido foi caracterizado e aplicado para estudos de adsorção. A caracterização mostrou que o aerogel apresenta uma estrutura típica de materiais amorfos com uma estrutura porosa e interconectada aleatoriamente que se assemelha a uma rede de poros abertos. A adsorção foi favorecida utilizando-se 2,5 g L^{-1} de aerogel e pH da solução igual a 8. Os modelos de pseudossegunda ordem e Freundlich descreveram satisfatoriamente os dados cinéticos e de equilíbrio, respectivamente. A capacidade máxima de adsorção do violeta cristal foi 227,11 mg g^{-1}, o que indica que o aerogel é muito eficiente e competitivo com diversos outros adsorventes descritos na literatura para remover violeta cristal de soluções aquosas. Os testes utilizando aerogel para tratar efluente têxtil simulado mostraram que este material tem grande potencial para tratar efluentes coloridos reais. Em síntese, pode-se concluir que o desenvolvimento de adsorventes a partir da quitina contribui fortemente para as pesquisas sobre desenvolvimento de tecnologias para o tratamento de efluentes contendo corantes.

Palavras-chave: Adsorção, quitina, violeta cristal, nanowhiskers, aerogel.

ABSTRACT

The environmental problems due to the accelerated industrialization of the last decades have caused in society the need to develop new technologies for the treatment of industrial waste. The textile industry stands out due to the high consumption of water in its production process and the large volumes of effluents generated containing contaminating compounds, such as dyes, with great potential for the pollution of water bodies. As result, an extensive research has been carried out to develop technologies for the treatment of effluents containing dyes, among which adsorption stands out for its low cost and high efficiency. Chitin is a biodegradable and renewable biopolymer that can be used as a basis for the development of adsorbent materials. In this context, the present work aimed to develop materials from chitin for application in the removal of crystal violet dye from aqueous solutions by adsorption. First, chitin was obtained from shrimp residues, and by acid hydrolysis of the obtained chitin, nanowhiskers were synthesized. Both materials were characterized and applied for adsorption studies. The characterization of the materials showed that the nanowhiskers had a rod shape and a larger average pore size when compared to chitin. The adsorption tests showed that the adsorption was favored using 5 g L^{-1} of nanowhiskers and solution with a pH of 8. The pseudo-second order model was the most adequate to represent the kinetic data and the Sips model the best represented the equilibrium curves. The process was endothermic, spontaneous and favorable. The maximum adsorption capacity of crystal violet was 59.52 mg g^{-1}, which corroborated the potential of nanowhiskers to be used as an adsorbent in the treatment of colored effluents. A new aerogel was also synthesized from chitin. This aerogel was obtained by the freeze-drying of a gel of chitin and psyllium. The developed material was characterized and applied for adsorption studies. The characterization showed that the aerogel has a typical structure of amorphous materials with a porous and randomly interconnected structure that resembles an open pore network. The adsorption was favored using 2.5 g L^{-1} of aerogel and solutions with a pH of 8. The pseudo-second order and Freundlich models satisfactorily described the kinetic and equilibrium data, respectively. The maximum adsorption capacity of crystal violet was 227.11 mg g^{-1}, which indicates that aerogel is very efficient and competitive with several other adsorbents described in the literature for removing crystal violet from aqueous solutions. Tests using aerogel to treat simulated textile effluents showed that this material has great potential to treat real colored effluents. In summary, it can be concluded that the development of adsorbents from chitin contributes strongly to research on the development of technologies for the treatment of effluents containing dyes.

Keywords: Adsorption, chitin, crystal violet, nanowhiskers, aerogel.

LISTA DE ILUSTRAÇÕES

CAPÍTULO 2

CAPÍTULO 3

3.1 – ARTIGO 1

3.2 – ARTIGO 2

LISTA DE QUADROS

CAPÍTULO 2

LISTA DE TABELAS

CAPÍTULO 3

3.1 ARTIGO 1

3.2 ARTIGO 2

LISTA DE ABREVIATURAS, SIGLAS E SÍMBOLOS

%R - Percentagem de remoção de corante (%)
$\Delta G°$- Variação da Energia Livre de Gibbs Padrão (kJ mol^{-1})
$\Delta H°$- Variação da Entalpia Padrão (kJ mol^{-1})
$\Delta S°$- Variação da Entropia Padrão (kJ mol^{-1} K^{-1})
$1/n_F$- Fator de Heterogeneidade
AIC - Critério de informação de Akaike
ANOVA- Análise de variância
ARE - Erro médio relativo (%)
BET- Brunauer, Emmett e Teller
BJH- Barret, Joyner e Halenda
C_0- Concentração inicial de corante na solução (mg L^{-1})
C_e- Concentração de corante na solução no equilíbrio (mg L^{-1})
C_f- Concentração final de corante na fase líquida (mg L^{-1})
Ch - Quitina
ChNW - Nanowhiskers de quitina
C_t - Concentração de corante na solução no tempo (mg L^{-1})
CV - violeta cristal
d_p- Diâmetro de partícula (mm)
DRX- Difração de Raios-X
DSC - Calorimetria Exploratória Diferencial
EMR- Erro Médio Relativo (%)
FT-IR- Espectroscopia no Infravermelho com Transformada de Fourier
k_1- Coeficiente cinético de PPO (min^{-1})
k_2- Coeficiente cinético de PSO (g $mg^{-1}min^{-1}$)
k_{AV}- Constante de Avrami (min^{-1})
K_D- Constante de Hill (mg $L^{-1})^{nH}$
K_e- Constante de equilíbrio (L g^{-1})
K_F- Constante de Freundlich (mg g^{-1}(L $mg^{-1})^{1/n}$)
K_L- Constante de Langmuir (L mg^{-1})
k_n- Coeficiente cinético de PnO (min^{-1}(g $mg^{-1})^{n-1}$)
K_S - Constante de Sips (L mg^{-1})
m - Massa de adsorvente (g)
m_S- Expoente do modelo de Sips
MEV- Microscopia Eletrônica de Varredura
n - número de pontos experimentais
n_{AV}-Expoente do modelo de Avrami
n_H- coeficiente de cooperatividade de Hill
p - Número de parâmetros do modelo ajustado
PnO - Pseudo-n Ordem
PPO- Pseudoprimeira Ordem
PSO- Pseudossegunda Ordem
q_1- Capacidade de adsorção para PPO (mg g^{-1})
q_2- Capacidade de adsorção para PSO (mg g^{-1})
q_{AV}- Capacidade de adsorção de Avrami (mg g^{-1})
q_e- Capacidade de adsorção no equilíbrio (mg g^{-1})
q_H- Máxima capacidade de adsorção correspondente à saturação dos sítios (mg g^{-1})
$q_{i,exp}$- Capacidade de adsorção obtida experimentalmente (mg g^{-1})
$q_{i,model}$ - Capacidade de adsorção estimada através do modelo (mg g^{-1})

q_m - Máxima capacidade de adsorção (mg g^{-1})
q_{mS}- Máxima capacidade de adsorção do modelo de Sips (mg g^{-1})
q_n- Capacidade de adsorção para PnO (mg g^{-1})
q_t- Capacidade de adsorção no tempo (mg g^{-1})
R - Constante universal, (kJ mol^{-1} K^{-1})
R^2- Coeficiente de determinação
$R^2_{ajustado}$- Coeficiente de determinação ajustado
R_L- Fator de equilíbrio
SEM - Microscopia Eletrônica de Varredura
SSE - Soma dos erros ao quadrado
t - Tempo (min)
T- Temperatura (K)
TEMPO - 2,2,6,6-tetrametilpiperidina-1-oxil
V - Volume da solução (L)
XRD - Difração de raios-x
ρ - Massa específica (kg m^{-3})
ϕ - Esfericidade

SUMÁRIO

CAPÍTULO 1: CONSIDERAÇÕES INICIAIS

1.1 INTRODUÇÃO

A poluição do meio ambiente é um dos grandes problemas enfrentados pela sociedade atual, causada pela atividade humana desenfreada, rápida urbanização e industrialização. A poluição das águas vem gerando grande preocupação, devido ao esgotamento de recursos hídricos, que já começam a dar sinais de escassez. Especialistas afirmam que em 2050, como consequência do aumento da demanda de água em razão da atividade econômica e crescimento populacional, poderá haver cerca de 1,8 bilhões de pessoas vivendo sob estresse hídrico no mundo, inclusive em países em desenvolvimento (GOSWAMI & PHUKAN, 2017; NATAJARAN et al., 2017; SCHLOSSER et al., 2014).

A indústria têxtil é globalmente conhecida por ser um dos setores que mais contribuem para a poluição de águas, devido aos grandes volumes de efluentes gerados contendo corantes. Em sua grande maioria, os corantes são moléculas tóxicas, carcinogênicas e não biodegradáveis (KHATRI et al., 2015; CHRISTIE, 2007; RODRIGUES FILHO, 2012; BELBEL et al., 2018). Em face deste problema, normas ambientais vêm sendo implantadas a fim de diminuir os impactos causados por esse tipo de indústria. A fiscalização está cada vez mais atuante e as leis mais rigorosas, o que consequentemente gerou uma maior procura por tecnologias eficazes e de baixo custo para o tratamento de efluentes contendo cor (GOSWAMI & PHUKNAN, 2017).

Corantes sintéticos são um problema sério de contaminação, pois causam danos tanto ao meio ambiente quanto à saúde pública e, em função disso, é fundamental a remoção efetiva desses corantes de águas residuais para garantir o descarte seguro de efluentes em cursos d'água (TAN et al., 2015). O violeta cristal é um corante catiônico amplamente usado como agente de coloração de tecidos pela indústria têxtil (BRIÃO et al., 2017). Quando presente em efluentes, mesmo que em baixas concentrações, torna necessário o tratamento destes efluentes visando minimizar os riscos toxicológicos oferecidos a flora, fauna e seres humanos (BORTOLUZZI, 2015). Diante disso, há uma grande necessidade de se desenvolver meios eficazes e de baixo custo para o tratamento de soluções aquosas contendo violeta cristal.

Existe uma grande dificuldade em remover corantes de águas residuais em função de suas propriedades inerentes. Quando há baixas concentrações destes contaminantes, os métodos convencionais tornam-se desvantajosos devido ao alto custo do processo (WAN NGAH et al., 2011; CRINI & BADOT, 2008). Pesquisas vêm sendo realizadas recentemente para remover corantes de águas. Vários métodos de tratamento vêm sendo relatados,

incluindo coagulação-floculação (CAI et al., 2015), adsorção (MOURA et al., 2016; SILVA et al., 2017; DOTTO et al., 2017), degradação fotocatalítica (ROSU et al., 2017), separação por membranas (WANG et al., 2017), osmose reversa (NATARAJ et al., 2009), entre outros. Entre estes métodos, a adsorção destaca-se como um dos mais eficazes empregados pela indústria para a remoção de contaminantes presentes em águas residuais, devido relevantes vantagens como a possibilidade do uso de diversos materiais como adsorventes (KANT, 2013; ZAZYKI et al., 2018).

A quitina é um biopolímero biodegradável e renovável que contém grupos hidroxil e n-acetil em sua estrutura (CRINI & BADOT, 2008). Sua utilização como adsorvente de corantes é benéfica para a proteção ambiental, pois além de contribuir para o tratamento de efluentes coloridos, também contribui para a gestão de resíduos sólidos, uma vez que este polissacarídeo é obtido de resíduos de indústrias de frutos do mar (DOTTO et al., 2012;CRINI & BADOT, 2008; VAKILI et al., 2014). Materiais a base de quitina vêm sendo amplamente estudados, nos últimos anos, no tratamento de águas residuais (LI et al., 2019). Porém a quitina, em seu estado natural, é pouco utilizada na adsorção devido a características como baixa porosidade e baixa área de superfície (DOTTO et al., 2015b). Em função disto, alguns estudos têm buscado a melhoria das propriedades da quitina utilizando diferentes tecnologias como, por exemplo, supercrítica e ultrassônica, a fim de aumentar sua aplicabilidade como adsorvente de corantes (DOTTO et al., 2015a,b; DOTTO 2016a).

Partículas rígidas em nanoescala como nanotubos de carbono e nanowhiskers de celulose têm despertado grande interesse nas pesquisas desenvolvidas recentemente (SÁ et al., 2015). Nanowhiskers de quitina são uma classe de nanomateriais considerados muito interessantes devido aos seus grupos funcionais presentes em sua estrutura e sua alta razão área de superfície por volume. Este material pode ser obtido pela hidrólise ácida da quitina e apresenta potencial para remover violeta cristal de águas contaminadas (DOMARD, 2011;GOPI et al., 2016). Aerogéis, por sua vez, são materiais sólidos sintetizados a partir da extração controlada do solvente presente na rede de um gel (FONSECA, 2019). Este material foi produzido pela primeira vez em 1931, a partir da sílica, e desde então vários materiais precursores vêm sendo utilizados para sua produção. Devido a características como baixa densidade, alta área superficial específica e alta porosidade, os aerogéis têm as mais diversas aplicações, podendo ser utilizados inclusive na adsorção de corantes, como o violeta cristal (KISTLER, 1931; ZAMAN et al., 2020; TIAN et al., 2019).

Baseando-se nestes aspectos, este trabalho buscou desenvolver materiais alternativos, como nanowhiskers e aerogéis, a partir da quitina para a aplicação na remoção de violeta cristal de soluções aquosas através de adsorção.

1.2 OBJETIVOS

1.2.1 Objetivo geral

O objetivo principal deste trabalho foi desenvolver materiais a partir da quitina para aplicação na remoção do corante violeta cristal de soluções aquosas através de adsorção.

1.2.2 Objetivos específicos

- Obter quitina partir de resíduos de camarão-rosa;
- Preparar nanowhiskers de quitina a partir de hidrólise ácida;
- Preparar aerogel a base de quitina através de criodessecação;
- Caracterizar a quitina, os nanowhiskers e o aerogel através de difração de raios-x (DRX), isotermas de N_2 (BET e BJH), calorimetria diferencial de varredura (DSC), microscopia eletrônica de varredura (MEV) e espectroscopia no infravermelho por transformada de Fourier (FT-IR);
- Estudar a adsorção do corante violeta cristal utilizando os três materiais (quitina, nanowhiskers e aerogel) em relação ao o efeito da dosagem de adsorvente, efeito do pH inicial da solução, comportamento cinético, isotermas de equilíbrio, termodinâmica e aplicação no tratamento de efluentes simulados.

CAPÍTULO 2: REVISÃO BIBLIOGRÁFICA

2.1 EFLUENTES TÊXTEIS

A indústria têxtil é um setor de grande importância na economia mundial e brasileira, em termos de produção e mercado de trabalho gerado. Segundo informações da Associação Brasileira da Indústria Têxtil e de Confecção (ABIT), só no Brasil conta com mais de 32 mil empresas, e corresponde a quinta maior do mundo, a segunda maior em produção de jeans e a terceira em produção de malhas (ABIT, 2017). De acordo com o IEMI – Inteligência de mercado, a produção de têxteis em 2017, teve um aumento de 5,4%, comparada ao ano de 2016 (IEMI, 2017).

As etapas produtivas da indústria têxtil demandam uma grande quantidade de água, onde podem ser consumidos até 400 L de água para a produção de 1 kg de tecido (PERUZZO, 2003). Como consequência desse alto consumo de água, há também a geração de grandes volumes de águas residuais contendo substâncias contaminantes orgânicas e inorgânicas (MARÍN, 2015). Metais pesados e compostos orgânicos tóxicos são alguns exemplos de contaminantes comumente presentes em efluentes têxteis (TÜFEKCI et al., 2007).

Efluentes têxteis podem apresentar diversos constituintes que dificultam seu tratamento, principalmente por seu alto grau de não biodegradabilidade causado principalmente pela presença de compostos orgânicos de estrutura complexa, como os corantes (BALAN, 2002). Estes compostos, mesmo em baixas concentrações, podem causar impactos negativos sobre os corpos d'água, representando um sério problema ambiental devido ao alto potencial de poluição, o que causa danos tanto ao meio ambiente quanto à saúde pública (ABBASIAN et al., 2017; TAN et al., 2015, KAMMRADT, 2004).

Devido ao potencial poluidor dos efluentes têxteis, há necessidade de remover corantes de águas residuais de forma eficiente antes do seu descarte em corpos receptores. Em função disso, são descritos na literatura inúmeros métodos físicos, químicos e biológicos para o tratamento para efluentes coloridos, como coagulação-floculação (CAI et al., 2015), degradação fotocatalítica (ROSU et al., 2017), osmose reversa (NATARAJ et al., 2009), separação por membranas (WANG et al., 2017), adsorção (MOURA et al., 2016;SILVA et al., 2017; DOTTO et al., 2017), entre outros. Entre estes métodos, a adsorção se mostra como um dos mais vantajosos devido ao baixo custo energético, baixo custo de operação e implementação, simplicidade de operação e alta eficiência (DOTTO et al., 2015b).

2.2 CORANTEVIOLETA CRISTAL

Violeta Cristal é um corante pertencente ao grupo dos triarilmetanos, também conhecido como Violeta de Metila 10B, Violeta genciana ou Violeta básico 3, cuja molécula possui propriedades antissépticas, antifúngicas, anti-helmínticas e antibacterianas (MITTAL et al., 2010; SHOJAEIPOOR et al., 2017). Também conhecido como cloreto de hexa-metil-pararosanilina, o violeta cristal é um corante básico catiônico, cujas características gerais estão apresentadas no Quadro 1 e a estrutura química na Figura 1 (BERTOLINI et al., 2014).

Quadro 1 – Características gerais do violeta cristal

Características gerais	**Violeta cristal**
Nome genérico	CI 42555
Grupos cromóforos	-C=C-; -C=N-; Anel quinóide
Absorbância máxima (nm)	590
Massa molecular (g mol^{-1})	408
Fórmula química	$C_{25}H_{30}N_2Cl$
Classe	Básico
Tipo	Catiônico

Fonte: BERTOLINI, 2014.

O violeta cristal possui grande importância na microbiologia, onde é amplamente empregado na caracterização de certos tipos de bactérias pela metodologia de coloração de Gram (SANTOS et al., 2005). Este corante também é utilizado como indicador de pH, desinfetante, aditivo de rações animais e, principalmente, como agente de coloração de tecidos em indústrias têxteis (BERTOLINI, 2014; KUMAR et al., 2010; CHAKRABORTY et al., 2011). Logo, este corante é muito encontrado nos resíduos industriais, os quais necessitam de tratamento adequado para o descarte seguro em rios e lagos.

Figura 1 – Estrutura química do corante violeta cristal.

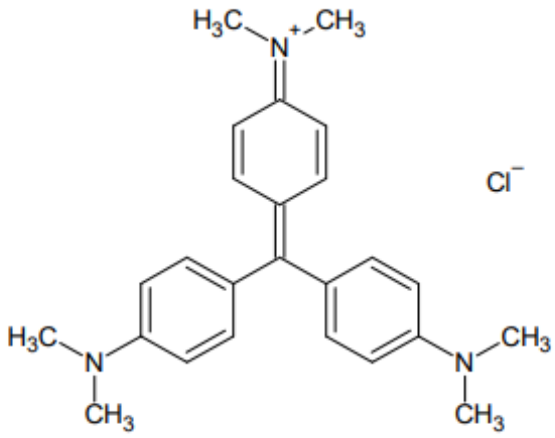

Fonte: a autora.

O violeta cristal é persistente em diversos ambientes, não biodegradável e considerado uma molécula recalcitrante (CHAKRABORTY et al.; 2011). Em função disto, na literatura existem diversos estudos nos últimos cinco anos que buscam por tecnologias de baixo custo e eficiência, objetivando remover este contaminante de efluentes industriais. Tahir et al. desenvolveram compósitos de polianilina, amido, polipirrol, anilina/quitosana e pirrol/quitosana utilizando resíduo de amendoim para serem utilizados na remoção por adsorção de violeta cristal, e obtiveram uma capacidade máxima de adsorção do violeta cristal de 100,6 mg g^{-1} (compósito de resíduo de amendoim e anilina/quitosana) (TAHIR et al., 2016). Outro compósito de quitosana/carvão ativado de *Typha latifólia* foi desenvolvido por Kumari et al. para o mesmo fim, o qual apresentou uma capacidade de adsorção de 15,0 mg g^{-1} (KUMARI et al., 2017). Abdel-Salam et al. investigaram o potencial adsorvente de nanopartículas de Ag (AgNPLs) quimicamente imobilizada em carvão ativado (AC-AgNPLs), assim como Sharma et al. (2018) estudaram o potencial adsorvente de nano-hidrogel de goma arábica e poliacrilamida para tratar violeta cristal em meio aquoso e obtiveram, respectivamente, capacidades máximas de adsorção de 87,2 e 90,9 mg g^{-1} (ABDEL-SALAM et al., 2017). Ghazali et al. e Chahinez et al. apresentaram novas informações sobre a adsorção de violeta cristal utilizando folhas de tamareira e biochar derivado de pecíolo de palma, com capacidades de adsorção máxima de 37,7 e 209,0 mg g^{-1}, respectivamente (GHAZALI et al., 2018; CHAHINEZ et al., 2020).

2.3 QUITINA

A quitina é o segundo polissacarídeo mais abundante do planeta após a celulose e pode ser encontrada no exoesqueleto de crustáceos, em invertebrados terrestres, em algas e nas paredes celulares de leveduras e outros fungos. Este biopolímero caracteriza-se por ser biodegradável, não tóxico, renovável e pode ser obtido em abundância a partir de resíduos de indústrias de frutos do mar (GUINESI et al., 2007; JAYAKUMAR et al., 2010; MINCEA et al., 2012). Na Figura 2 é apresentada a quitina em forma de pó.

Figura 2 – Quitina em pó.

Fonte: A autora.

A quitina, cuja fórmula molecular é β-(1-4)-N-acetil-D-glucosamina, ocorre na natureza como três alomorfas: a α-quitina, a β-quitina e a γ-quitina. A α-quitina é facilmente encontrada em camarões, caranguejos, lagostas, fungos entre outros, enquanto a β-quitina é raramente encontrada na natureza. A γ-quitina tem sido proposta como uma estrutura intermediária entre as outras duas alomorfas (RINAUDO, 2006; CARDOSO, 2008; PILLAI et al., 2009; MOURA et al., 2011; CADAVAL JR et al., 2012; YOUNES & RINAUDO, 2015). Na Figura 3 é apresentada a estrutura primária da quitina, onde n é o grau de polimerização.

Figura 3 – Estrutura da quitina.

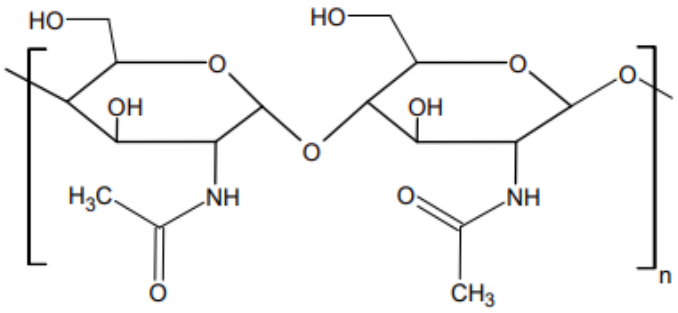

Fonte: A autora.

A quitina apresenta grupos como N-acetil e hidroxil em sua estrutura, que são capazes de se ligar com íons em meios aquosos, ou seja, grupos que podem ser sítios ativos de adsorção. Em função desses grupos presentes em sua estrutura, a quitina pode ser utilizada como adsorvente para o tratamento de efluentes coloridos por adsorção, o que também contribui para o gerenciamento de resíduos sólidos de indústrias de frutos do mar (CRINI & BADOT, 2008; CÔRTES et al., 2015; DOTTO et al., 2015a; DOTTO et al., 2015b).

A quitina possui características como baixa porosidade e baixa área superficial limitam seu potencial como adsorvente (CRINI & BADOT, 2008; DOTTO et al., 2012; VAKILI et al., 2014; DOTTO et al., 2015a). Neste contexto, nanowhiskers e aerogéis desenvolvidos a partir da quitina surgem como uma alternativa para contornar as limitações desta, uma vez que essas formas mantêm as mesmas propriedades como funcionalidade, biodegradabilidade e potencial de adsorção (GOPI et al., 2017).

2.3.1 Nanowhiskers

Nanowhiskers de quitina são cristalitos em forma de haste que possui dimensões em escala nanométrica e é obtido a partir da quitina pela remoção de domínios amorfos (FAN et al., 2008). Na Figura 4, são apresentados os nanowhiskers de quitina em forma de pó. Na literatura, são descritos vários métodos para a preparação de nanowhiskers de quitina, como ultrasonicação, eletrofiação, oxidação mediada por radical 2,2,6,6-tetrametilpiperidina-1-oxil (TEMPO), tratamento mecânico e hidrólise ácida (KADOKAWA et al., 2011). Na preparação por hidrólise ácida, há uma diminuição na fase amorfa da quitina pela dissolução das regiões laterais de pouca ordenação de cadeias, ocasionando um aumento na cristalinidade dos nanowhiskers de quitina (MOL, 2014; JI et al., 2017).

Figura 4 – Nanowhiskers de quitina em pó.

Fonte: A autora.

Os nanowhiskers de quitina preservam as propriedades adsortivas da quitina, porém adquirem vantagens de nanomateriais, como áreas de superfície grandes e ativas (ZHANG et al., 2016, MORIN & DUFRESNE, 2002). Dhananasekaran et al. (2016) estudaram o processo de adsorção dos corantes azul de metileno, azul de bromofenol e azul de Coomassie utilizando nanopartículas de quitina, e verificaram que este adsorvente é adequado para a remoção desses corantes de efluentes, pois é um material biodegradável simples, de reação rápida e baixo custo. Nanowhiskers de quitina também foram utilizadas para o desenvolvimento de uma membrana funcional ativa de fluoreto de polivinilideno (PVDF). Os resultados obtidos mostraram que a membrana contendo os nanowhiskers de quitina apresentaram maior eficiência de remoção (88,9%) e capacidade de adsorção (72,6 mg g^{-1}) na adsorção do corante índigo carmim, quando comparadas a membrana contendo apenas PVDF (GOPI et al., 2017).

Gopi et al. investigaram a utilização de nanowhiskers de quitina na adsorção do corante violeta cristal, avaliando a eficiência de remoção e capacidade de adsorção. Os resultados obtidos mostraram que os nanowhiskers de quitina apresentam grande potencial para a remoção do corante violeta cristal de águas contaminadas, com maiores valores de eficiência de remoção (79,13%) e capacidade de adsorção (39,56 mg g^{-1}) quando comparados a quitina-Fe_3O_4, celulose e celulose-Fe_3O_4 (GOPI et al., 2016).

2.3.2 Aerogel

Aerogéis são materiais sólidos sintetizados através da secagem no ponto crítico, utilizando CO_2 supercrítico, ou através de secagem por sublimação (liofilização). Esses materiais são altamente porosos e ultraleves, e do ponto de vista morfológico, se apresentam como uma rede muito fina formada por um aglomerado de nanopartículas (PEREIRA, 2018; CHEN et al., 2011). Na Figura 5 é apresentado um aerogel feito a partir de quitina e psyllium por liofilização.

Figura 5 – Aerogel de quitina e psyllium.

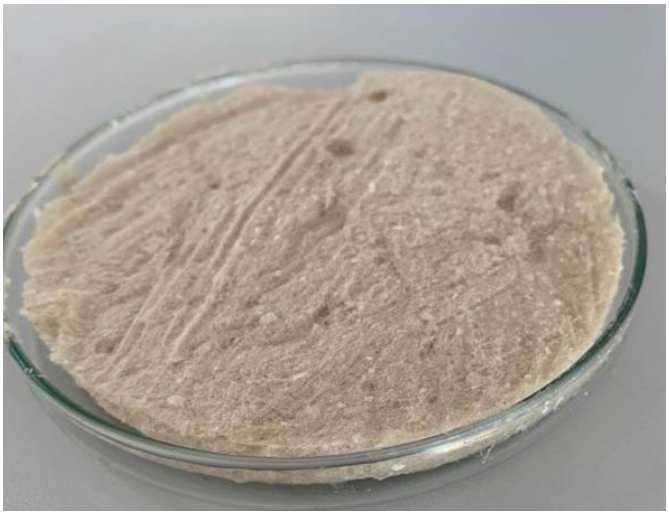

Fonte: A autora.

O primeiro aerogel foi produzido em 1931, por secagem supercrítica de hidrogéis de sílica, e desde então há na literatura um vasto estudo de aerogéis produzidos a partir de vários materiais precursores e utilizados nas mais variadas aplicações (KISTLER, 1931; ZAMAN et al., 2020; TIAN et al., 2019). Estes materiais apresentam propriedades como baixa densidade e alta área superficial específica, o que pode ser muito interessante para processos como a adsorção (ZHAO et al., 2018).

Lim et al. (2020) produziram aerogéis funcionalizados com carvão ativado e dietilenotriamina a partir de fibras de folhas de abacaxi e os aplicaram na adsorção de gás etileno e íons de níquel (II). O aerogel funcionalizado com carvão ativado apresentou uma excelente capacidade máxima de adsorção de etileno (1,08 mmol g^{-1}), que superou os valores de capacidade dos adsorventes comerciais de etileno. O aerogel funcionalizado com dietilenotriamina apresentou boa capacidade de adsorção dos íons de níquel (II), apresentando uma capacidade máxima de adsorção de 0,835 mmol g^{-1}.

Liu et al. (2020) sintetizaram aerogéis de sílica calcinada na intenção de remover corantes orgânicos de águas residuais têxteis, como os corantes azul de metileno, verde malaquita e violeta cristal. Os testes apresentaram uma porcentagem de remoção máxima de 98%, o que indica que o aerogel de sílica calcinada pode ser um eficiente adsorvente para a remoção de corantes de águas residuais.

Um novo aerogel de óxido de grafeno/lignina aminada foi desenvolvido para a remoção do corante verde malaquita de águas residuais por Chen. et al. (2020). Os resultados dos testes de adsorção mostraram que esse novo aerogel apresentou uma capacidade de adsorção máxima de 113,5 mg g^{-1} e um bom potencial para ser utilizado no tratamento de águas residuais.

2.4 ADSORÇÃO

A adsorção é uma operação de transferência de massa na qual um sólido possui a habilidade de concentrar em sua superfície moléculas presente em soluções líquidas ou gasosas devido a forças de atração entre o sólido e as moléculas. O sólido em cuja superfície ocorre o fenômeno de adsorção denomina-se adsorvente e as espécies químicas retidas na superfície do sólido denominam-se adsorbatos (GOMIDE, 1980). A Figura 6 apresenta simplificadamente um esquema de adsorção/dessorção em uma dada matriz.

Figura 6 – Esquema de adsorção/dessorção em um material adsorvente.

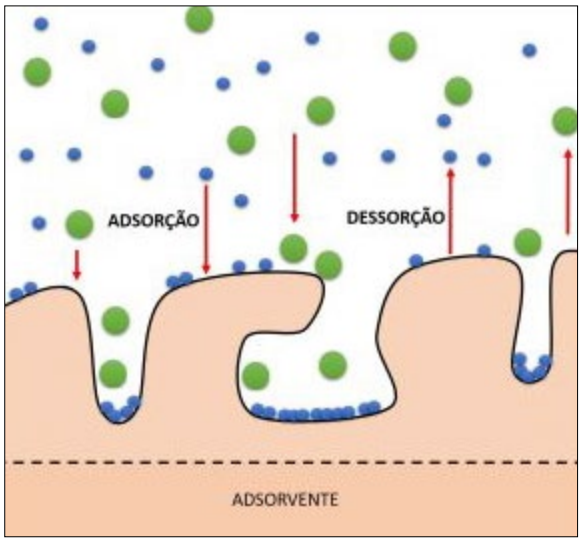

Fonte: GPQuim, 2017.

A adsorção pode ser classificada em física (fisissorção) ou química (quimissorção), dependendo da natureza das forças envolvidas. Na fisissorção, as forças de atração entre o adsorbato e o adsorvente são relativamente fracas, envolvendo principalmente forças de Van der Walls. Diferentemente, na quimissorção ocorre uma reação química, ou seja, ocorre a troca ou partilha de elétrons entre a superfície do adsorvente e moléculas do adsorbatos, o que resulta em uma ligação mais forte (VIDAL et al., 2014). No Quadro 2 são apresentadas características gerais que distinguem fisissorção e quimissorção.

Quadro 2 – Características gerais de fisissorção e quimissorção.

Fisissorção	**Quimissorção**
Baixo calor de adsorção (< 2 ou 3 vezes o calor latente de evaporação) Monocamada ou multicamadas	Alto calor de adsorção (> 2 ou 3 vezes o calor latente de evaporação) Preferencialmente monocamada
Não ocorre dissociação das espécies adsorvidas	Pode envolver dissociação
Significativa apenas em temperaturas relativamente baixas	Possível através de uma ampla faixa de temperatura
Rápida e reversível	Pode ser lenta e irreversível
Não compartilhamento ou transferência de elétrons	Ocorre uma combinação química entre a superfície do material adsorvente e do adsorbato

Fonte: Adaptado de CARDOSO, 2012.

2.4.1 Cinética de adsorção

A cinética de adsorção descreve a taxa de remoção do adsorbato da solução, a qual determina o tempo de residência para que o adsorbato se acumule na interface sólido-líquido (TONUCCI, 2014). Em função disto, o estudo da cinética é muito importante, pois leva ao entendimento de possíveis mecanismos de adsorção e auxilia a prever a velocidade com que ocorre a adsorção, o que possibilita o desenvolvimento de sistemas adequados de tratamento (ZHU et al., 2005).

O mecanismo da cinética de adsorção envolve quatro etapas principais (RUTHVEN, 1984):

(i) Transferência de massa até a camada limite;

(ii) Transferência de massa da camada limite até a superfície externa do adsorvente;

(iii) Difusão intrapartícula;

(iv) Adsorção das moléculas do adsorbato nos sítios ativos do adsorvente.

Na Figura 7 são ilustradas as quatro etapas principais do mecanismo da cinética de adsorção.

Figura 7 – Principais etapas do mecanismo de cinética de adsorção.

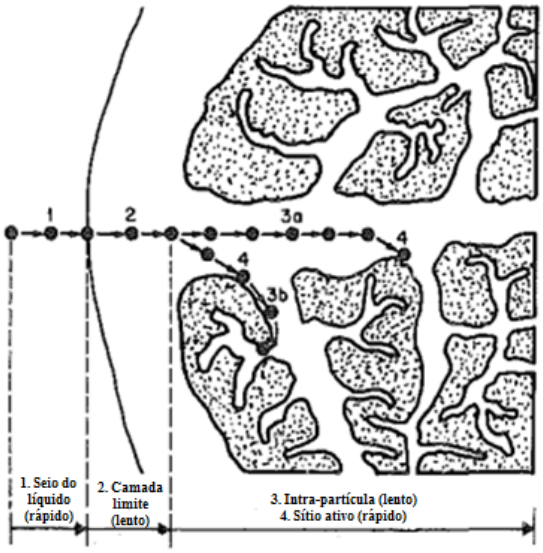

Fonte: Adaptado de WEBER, 1984.

A etapa de transferência de massa externa, que corresponde à transferência do adsorbato do seio do fluido até a camada limite, pode ser facilmente manipulada pela agitação e pela concentração de adsorbato na solução. A última etapa, que corresponde à adsorção propriamente dita, também corresponde a uma etapa rápida e não significativa para o processo, na maioria das vezes. Em contrapartida, as etapas de difusão do adsorbato pela camada limite e pelo interior dos poros são geralmente as etapas limitantes do processo adsortivo, especialmente no caso de difusão intrapartícula de adsorvente microporosos (WEBER, 1984).

O modelo cinético utilizado para descrever o mecanismo controlador do processo de adsorção deve ser simples matematicamente, para facilitar o tratamento dos dados, e complexo o bastante para apresentar as características do sólido e sua influência no processo (DO, 1998). Na literatura, vários modelos cinéticos são reportados para verificar o mecanismo

que controla o processo de adsorção, como a transferência de massa, difusão ou reação química. Entre os modelos, pode-se citar o de pseudoprimeira ordem (PPO), de pseudossegunda ordem (PSO), pseudo-n ordem (PnO) e Avrami que podem fornecer uma resposta prática e interessante para certos conjuntos de dados (ÖNAL, 2006).

2.4.1.1 Modelo de pseudoprimeira ordem

O modelo cinético de pseudoprimeira ordem se baseia na Lei de resfriamento de Newton e foi desenvolvido por Lagergren em 1898. Este modelo descreve o mecanismo cinético de adsorção da fase sólido-líquido e assume que a adsorção ocorre devido a um gradiente de concentração entre a solução e a superfície do adsorvente. Na Equação 1 é expresso o modelo de pseudoprimeira ordem proposto por Lagergren (QIU et al., 2009):

$$\frac{dq_t}{dt} = k_1(q_e - q_t) \tag{1}$$

Onde q_t (mg g^{-1}) corresponde a capacidade de adsorção no tempo t, q_e (mg g^{-1}) corresponde a capacidade de adsorção no equilíbrio e k_1 corresponde a constante cinética de pseudoprimeira ordem (min^{-1}).

Considerando q_t=0 em t=0 e q_t=q_t em t=t, e rearranjando, a Equação 1, chega-se à Equação 2 (QIU et al., 2009):

$$q_t = q_1(1 - exp(-k_1 t) \tag{2}$$

Onde q_1 (mg g^{-1}) corresponde ao valor teórico da capacidade de adsorção obtido através do modelo de pseudoprimeira ordem.

2.4.1.2 Modelo de pseudossegunda ordem

O modelo cinético de pseudossegunda ordem assume que a força motriz para ocorrer a adsorção é proporcional à fração de sítios ativos disponíveis no adsorvente e é geralmente mais adequado em operações de adsorção química (HO, 2006; HO & McKAY, 1998). Este modelo é expresso de acordo com a Equação 3 (WU et al., 2009):

$$\frac{dq_t}{dt} = k_2(q_e - q_t)^2 \tag{3}$$

Onde k_2 (g mg^{-1} min^{-1}) corresponde a constante cinética de pseudossegunda ordem.

Considerando $q_t=0$ em $t=0$ e $q_t=q_t$ em $t=t$, e rearranjando, a Equação 3 pode ser representada pela Equação 4 (HO e MCKAY, 1998):

$$q_t = \frac{t}{(1/k_2 q_2^2) + (t/q_2)} \quad (4)$$

Onde q_2 (mg g^{-1}) corresponde ao valor teórico da capacidade de adsorção obtido através do modelo de pseudossegunda ordem.

2.4.1.3 Modelo de Pseudo-n ordem

O modelo de pseudo-n ordem é a generalização do modelo proposto por Largergren, e também considera a adsorção como uma reação (ALENCAR et al., 2012; PERES et al., 2018;ALMEIRA, 2014). Este modelo é representado pela Equação 5.

$$q_t = q_n - \frac{q_n}{[k_n (q_n)^{n-1} t(n-1) + 1]^{1/(n-1)}} \quad (5)$$

Onde q_n (mg g^{-1}) é a capacidade de adsorção para o modelo de PnO; k_n(min^{-1}(g mg^{-1})$^{n-1}$)é o coeficiente cinético de PnO e n é a ordem da reação.

2.4.1.4 Modelo de Avrami

O modelo de Avrami é um modelo semi-empírico bastante utilizado a fim de explicar a cinética de adsorção. Este modelo foi proposto por Avrami, em 1939, e se baseia em uma cinética de decomposição térmica (DOTTO, 2012; LOPES et al., 2003). O modelo de Avrami pode ser representado pela Equação 6.

$$q_t = q_{AV}\{1 - \exp[-(k_{AV} t)]^{n_{AV}}\} \quad (6)$$

Onde q_{AV} (mg g^{-1}) é a capacidade de adsorção de Avrami, k_{AV} (min^{-1}) é a constante de Avrami e n_{AV} é o expoente do modelo de Avrami.

2.4.2 Equilíbrio de adsorção

Quando uma determinada quantidade de material adsorvente entra em contato com um fluido contendo um soluto adsorbível, este soluto tende a fluir do seio da fase fluida para a superfície do material adsorvente até que a concentração do soluto na fase fluida permaneça constante, ou seja, até que o equilíbrio termodinâmico do sistema seja atingido (SUZUKI, 1990). O equilíbrio termodinâmico na adsorção ocorre quando as velocidades com que as

moléculas adsorvem e dessorvem se igualam, e o seu estudo é muito importante para o planejamento de qualquer sistema de adsorção, pois a partir dele obtêm-se informações importantes para o projeto e análise do processo (MELO et al., 2014; CARDOSO, 2012).

O equilíbrio de adsorção é avaliado através das isotermas de adsorção, que são comumente descritas por modelos matemáticos físicos e empíricos (SUZUKI, 1990).

2.4.2.1 Isoterma de Langmuir

A isoterma de Langmuir foi proposta por Langmuir em 1918 e corresponde a uma das equações mais utilizadas para descrever o processo de adsorção. Este modelo considera que a adsorção ocorre em monocamada e que existe um número definido de sítios, com energia equivalente, na superfície do adsorvente. A Equação 7 corresponde a representação matemática da isoterma de Langmuir (LANGMUIR, 1918):

$$q_e = \frac{q_m k_L C_e}{1 + k_L C_e} \tag{7}$$

Onde q_e (mg g^{-1}) é a capacidade de adsorção no equilíbrio, q_m (mg g^{-1}) é a capacidade máxima de adsorção, k_L é é a constante de Langmuir (L mg^{-1}) e C_e (mg L^{-1}) é a concentração do adsorbato remanescente na fase líquida no equilíbrio.

O fator de separação ou fator de equilíbrio (R_L) indica a natureza favorável da adsorção, ou seja, os valores de R_L indicam se a isoterma é favorável ($0<R_L<1$), desfavorável ($R_L>1$), linear ($R_L=1$) ou irreversível ($R_L=0$). Este fator é calculado de acordo com a Equação 8 (HAMDAOUI & NAFFRECHOUX, 2007):

$$R_L = \frac{1}{1 + k_L C_0} \tag{8}$$

Onde C_0 corresponde à concentração inicial de adsorbato na fase líquida (mg L^{-1}).

2.4.2.2 Isoterma de Freundlich

Outro exemplo de equação frequentemente utilizada para descrever o processo de adsorção é a isoterma de Freundlich. Este modelo é uma descrição empírica da relação entre a concentração do adsorbato no equilíbrio na fase líquida e a capacidade de adsorção do adsorvente (INGLEZAKIS & POULOPOULOS, 2006). O modelo de Freundlich,

representado pela Equação 9, pode ser utilizado para adsorção em multicamada, sistemas não ideais e que ocorram em superfícies heterogêneas (FREUNDLICH, 1906).

$$q_e = k_F {C_e}^{1/n_F} \quad (9)$$

Onde k_F é a constante de Freundlich ((mg g^{-1})(mg L^{-1})$^{-1/nF}$) e $1/n_F$ é o fator de heterogeneidade.

2.4.2.3 Isoterma de Sips

O modelo de isoterma de Sips é uma forma combinada dos modelos de isotermas de Freundlich e Langmuir e, por isso, é também conhecido isoterma de Langmuir-Freundlich. Em concentrações baixas de adsorbato, a isoterma de Sips se comporta como a isoterma de Freundlich, e em concentrações altas, prevê adsorção em monocamada, assim como a isoterma de Langmuir. (FOO& HAMEED, 2010;ALMEIDA, 2014). Na Equação 10, há a representação matemática da isoterma de Sips (SIPS, 1948).

$$q_e = \frac{q_{m_S}(k_S C_e)^{m_S}}{1 + (k_S C_e)^{m_S}} \quad (10)$$

Onde k_S é a constante de Sips (L mg^{-1}), m_S é o expoente do modelo de Sips e q_{mS} é a capacidade de adsorção máxima de Sips (mg g^{-1}).

2.4.2.4 Isoterma de Hill

O modelo de isoterma de Hill assume a adsorção como um fenômeno cooperativo, pois considera que a ligação em um sítio da macromolécula é influenciada pelas ligações em diferentes sítios da mesma macromolécula. A representação matemática da isoterma de Hill é apresentada na Equação 11 (FOO & HAMEED, 2010; RINGOT et al., 2007).

$$q_e = \frac{q_H {C_e}^{n_H}}{k_D + {C_e}^{n_H}} \quad (11)$$

Onde q_H é a capacidade de adsorção máxima de Hill (mg g^{-1}); n_H é o coeficiente de cooperatividade de Hill e k_D é a constante de Hill (mg L^{-1})^{nH}.

2.4.3 Termodinâmica de adsorção

A estimação dos parâmetros termodinâmicos de adsorção é essencial para se obter informações relevantes sobre o processo, como espontaneidade e mecanismo predominantes, entre outras (FAUST & ALY, 1986). Os parâmetros termodinâmicos de adsorção, como variação da energia livre de Gibbs padrão (ΔG°) (kJ mol^{-1}), variação da entalpia padrão (ΔH°) (kJ mol^{-1}) e variação da entropia padrão (ΔS°) (kJ mol^{-1} K^{-1}), podem ser estimados a partir dos dados de equilíbrio e são obtidos através das Equações 12-14, respectivamente (DOTTO et al., 2016b):

$$\Delta G° = -RTln(\rho K_e) \tag{12}$$

$$\Delta G° = \Delta H° - T\Delta S° \tag{13}$$

$$\ln(\rho K_e) = \frac{\Delta S°}{R} - \frac{\Delta H°}{RT} \tag{14}$$

Onde T é temperatura (K), R é 8,31x10^{-3}(kJ mol^{-1} K^{-1}), K_e é a constante de equilíbrio (L g^{-1}) e ρ é a densidade da solução (g L^{-1}).

A espontaneidade do processo pode ser avaliada através do valor obtido de variação de energia livre de Gibbs padrão. Processos espontâneos são processos nos quais a energia deixa o sistema e apresentam valores de ΔG° negativos. Contrariamente, nos processos não espontâneos a energia aporta no sistema e os valores de ΔG° são positivos (LIMA et al., 2014). O valor obtido de variação de entalpia padrão indica se o processo é exotérmico ou endotérmico. Valores negativos de ΔH° indicam que há liberação de energia (processo exotérmico) e valores positivos de ΔH° indicam que há absorção de energia (processo endotérmico) (SENTURK et al., 2009; KULA et al., 2008). Valores negativos de variação de entropia padrão (ΔS°<0) indicam uma diminuição do número de graus de liberdade do sistema, ou seja, há uma diminuição na aleatoriedade na interface adsorvente/solução em consequência das interações entre o adsorvente e adsorbato (KULA et al., 2008).

REFERÊNCIAS

ABBASIAN, M. et al. Grafting of aniline derivatives onto chitosan and their applications for removal of reactive dyes from industrial effluents. **Int. J. Biol. Macromol.**, v. 95, p. 393-403, 2017.

ABDEL-SALAM, A. H. et al. Silver nanoparticles immobilized on the activated carbon as efficient adsorbent for removal of crystal violet dye from aqueous solutions. A kinetic study. **J. Mol. Liq.**, v. 248, p. 833-841, 2017.

ABIT - ASSOCIAÇÃO BRASILEIRA DA INDÚSTRIA TÊXTIL E DE CONFECÇÃO, 2017. Disponível em: <http://www.abit.org.br>. Acesso em: Nov. 2017.

ALENCAR, W. S. et al. Application of aqai stalks as biosorbents for the removal of the dye Procion Blue MX-R from aqueous solution. **Sep. Sci. Technol.**, v. 47, p. 513- 526, 2012.

ALMEIDA, F. T. R. de. **Adsorção de cátions metálicos e oxiânions em solução aquosa usando novos materiais bifuncionalizados a partir da celulose e da quitosana**. 2014. Dissertação (Mestrado em Engenharia Ambiental)–Universidade Federal de Ouro Preto, Ouro Preto, 2014.

BALAN, D. S. L. **A Indústria Têxtil e o Meio Ambiente, Tecnologia Limpa e Controle Ambiental**. Faculdade de Tecnologia de Americana. Revista Química Têxtil, Rio Claro, 2002.

BELBEL, A. et al. Preparation and characterization of homoionic montmorillonite modified with ionic liquid: Application in dye adsorption. **Colloids Surf. A Physicochem. Eng. Asp.**, v. 558, p. 219-227, 2018.

BERTOLINI, T. C. R. **Estudo comparativo sobre a adsorção de diferentes classes de corantes em zeólitas de cinzas de carvão: Modelagem cinética e de equilíbrio**. 2014. Dissertação (Mestre em Ciências na Área de Tecnologia Nuclear – Materiais)–Universidade de São Paulo, São Paulo, SP, 2014.

BORTOLUZZI, B. M. A. **Remoção dos corantes azul de metileno e cristal violeta de solução aquosa utilizando epicarpo (casca) de uva Niágara rosada (*Vitis labrusca*) como adsorvente**. 2015. Dissertação (Mestre em Engenharia)–Universidade Federal do Pampa, Bagé, 2015.

BRIÃO, G.V. et al. Adsorption of Crystal Violet Dye onto a Mesoporous ZSM–5 Zeolite Synthetized using Chitin as Template. **J. Colloid Interface Sci.**, v. 508, p. 313-322, 2017.

CADAVAL JR, T. R. S.; CAMARA, A. S.; DOTTO, G. L.; PINTO, L. A. de A. Adsorption of Cr (VI) by chitosan with different deacetylation degrees. **Desalin. Water Treat.**, v. 51, p. 7690-7699, 2012.

CAI, T. et al. Efficient flocculation of an anionic dye from aqueous solutions using a cellulose-based flocculent. **Cellulose**, v. 22, n. 2, p. 1439–1449, 2015.

CARDOSO, M. B. **Contribuição ao estudo da reação de desacetilação de quitina: Estudos da desacetilação assistida por ultrassom de alta potência**. 2008. Tese (Doutorado em Química)–Universidade de São Paulo, Instituto de Química de São Carlos, São Carlos, SP, 2008.

CARDOSO, N. F. **Adsorção de corantes têxteis utilizando biossorventes alternativos**. 2012. Tese (Doutorado em Química)–Universidade Federal do Rio Grande do Sul, Instituto de Química, Porto Alegre, RS, 2012.

CHAHINEZ, H-O.et al. One-stage preparation of palm petiole-derived biochar: Characterization and application for adsorption crystal violet dye in water. **Environ. Technol. Inno.**, 100872, 2020.

CHAKRABORTY, S. et al. Adsorption of Crystal Violet from aqueous solution onto NaOH-modified rice husk. **Carbohyd. Polym.**, v. 86, n. 4, p. 1533-1541, 2011.

CHEN, H. et al. Novel graphene oxide/aminated lignin aerogels for enhanced adsorption of malachite green in wastewater. **Colloids Surf. A Psycochem. Eng. Asp.**, n. 603, 125281, 2020.

CHEN, W. et al. Ultralight and highly flexible aerogels with long cellulose I nanofibers. Soft.Matter., v. 7, n. 21, 10360, 2011.

CHRISTIE, R. M. **Environmental aspects of textile dyeing**. 1. Ed., Manchester: Woodhead Publishing LTD, 2007.

CÔRTES, L. N. et al. Biosorption of gold from computer microprocessor leachate solutions using chitin. **Waste Management**, v. 45, p. 272-279, 2015.

CRINI, G. & BADOT, P. M. Application of chitosan, a natural aminopolysaccharide, for dye removal from aqueous solutions by adsorption processes using batch studies: a review of recent literature. **Prog. Polym. Sci.**, v. 33, p. 399–447, 2008.

DHANANASEKARAN, S. et al. Adsorption of methylene blue, bromophenol blue, and Coomassie brilliant blue by α-chitin nanoparticles. **J. Adv. Res.**, v. 7, n. 1, p. 113-124, 2016.

DO, D. D. **Adsorption analysis:** Equilibria and Kinetics. Series on Chemical Engineering. v. 2, London: Imperial College Press, 1998.

DOMARD, A.A perspective on 30 years research on chitin and chitosan. **Carbohyd. Polym.**, p. 84, n. 2, p. 696–703, 2011.

DOTTO, G. L. **Biossorção de corantes alimentícios utilizando nanopartículas de *Spirulina platensis***. 2012. Tese (Doutorado em Engenharia e Ciência de Alimentos) – Universidade Federal do Rio Grande, Rio Grande, RS, 2012.

DOTTO, G. L. et al. Development of chitosan/bentonite hybrid composite to remove hazardous anionic and cationic dyes from colored effluents. **J. Environ. Chem. Eng.**, v. 4, n. 3, p. 3230-3239, 2016b.

DOTTO, G. L. et al. Ultrasound-assisted treatment of chitin: evaluation of physicochemical characteristics and dye removal potential. **E-Polymers**, v. 16, p. 49-56, 2016a.

DOTTO, G. L. et al. Adsorption of methylene blue by ultrasonic surface modified chitin. **J. Colloid Interface Sci.**, v. 446, p. 133-140, 2015b.

DOTTO, G. L. et al. Fixed Bed adsorption of methylene blue by ultrasonic surface modified chitin supported on sand. **Chem. Eng. Res. Des.**, v. 100, p. 302-310, 2015a.

DOTTO, G. L. et al. Chitosan/polyamide nanofibers prepared by Forcespinning technology: A new adsorbent to remove anionic dyes from aqueous solutions. **J. Clean. Prod.**, v. 144, p. 120–129, 2017.

DOTTO, G. L. et al. Kinetics and mechanism of tartrazine adsorption onto chitin and chitosan. **Ind. Eng. Chem. Res.**, v. 51, p. 6862–6868, 2012.

FAUST, S. D. & ALY, O. M. **Adsorption processes for water treatment**. Oxford: Butterworth-Heinemann, 1986.

FONSECA, F. A. A. da. **Síntese e estudo espectrocóspico de aerogéis baseados em compósitos de alumina e sílica dopados com íons Eu^{3+}**. Dissertação (Mestrado em Química)-Universidade de São Paulo, Ribeirão Preto, 2019.

FOO, K. Y. & HAMEED, B. H. Insights into the modeling of adsorption isotherm systems. **Chem. Eng. J.**, v. 156, p. 2-10, 2010.

FREUNDLICH, H. M. F. Über die adsorption in lösungen. **J. Phys. Chem.**, v. 57, p. 385-470, 1906.

GHAZALI, A. et al. Optimization of crystal violet adsorption onto date palm leaves as a potent biosorbent from aqueous solutions using response surface methodology and ant colony. **J. Environ. Chem. Eng.**, v. 6, n. 4, p. 3942-3950, 2018.

GOMIDE, R. **Operações Unitárias**, São Paulo: Edição do Autor, 1980.

GOPI, S. et al. Chitin nanowhiskers (ChNW)-functionalized electrospun PVDF membrane for enhanced removal of Indigo carmine. **Carbohyd. Polym.**, v. 165, p. 115-122, 2017.

GOPI, S. et al. Enhanced adsorption of crystal violet by synthesized and characterized chitin nano-whiskers from shrimp shell. **J. Water Proc. Engineering**, v. 14, p. 1-8, 2016.

GOSWAMI, M. & PHUKAN, P. Enhanced adsorption of cationic dyes using sulfonic acid modified activated carbon. **J. Environ. Chem. Eng.**, v. 5, n. 4, p. 3508–3517, 2017.

GPQuim - **GRUPO DE PESQUISA EM QUÍMICA**, 2017. Disponível em: <http://gpquim.com.br>. Acesso em: Nov. 2017.

GUINESI, L. S. et al. Adsorção de íons cobre (II) pela quitosana usando coluna em sistema sob fluxo hidrodinâmico. **Quim. Nova**, v. 30, n. 4, p. 809-814, 2007.

HAMDAOUI, O. & NAFFRECHOUX, E. Modeling of adsorption isotherms of phenol and chlorophenols onto granular activated carbon Part I. Two-parameter models and equations allowing determination of thermodynamic parameters. **J. Hazard. Mater.**, v. 147, p. 381-394, 2007.

HO, Y. S. & McKAY, G. Kinetic models for the sorption of dye from aqueous solution bywood. **Process Saf. Environ. Prot.**, v. 76, p. 183-191, 1998.

IEMI – **Inteligência de Mercado**, 2017. Disponível em: <http://iemi.com.br>.
Acesso em: Nov. 2017.

INGLEZAKIS V. J. & POULOPOULOS S.G. **Adsorption, ion exchange and catalysis – design of operations and environmental applications**. Amsterdam: Elsevier, 2006.

JAYAKUMAR, R. et al. Novel chitin and chitosan nanofibers in biomedical applications. **Biotechnol. Adv.**, v. 28, p. 142-150, 2010.

JI, N. et al. Effects of chitin nano-whiskers on the gelatinization and retrogradation of maize and potato starches. **Food Chem.**, v. 214, p. 543-549, 2017.

KADOKAWA, J. et al. Preparation of chitin nanowhiskers using an ionic liquid and their composite materials with poly(vinyl alcohol). **Carbohyd. Polym.**, v. 84, p. 1408-1412, 2011.

KAMMRADT, P. B. **Remoção de cor de efluentes de tinturarias industriais através de processo de oxidação avançada.** 2004. Dissertação (Mestrado em Engenharia de Recursos Hídricos e Ambiental) – Universidade Federal do Paraná, Curitiba, 2004.

KANT, R. Adsorption of dye olive BGL using two different samples of activated carbon by static batch method. **Asian J. Chem.**, v. 25, n.4, p. 1905–1908, 2013.

KHATRI, A. et al. A review on developments in dyeing cotton fabrics with reactive dyes for reducing effluent pollution. **J. Clean. Prod.**, v. 87, p. 50-57, 2015.

KISTLER, S. Coherent Expanded Aerogels and Jellies. **Nature**, v. 127, p. 741-741, 1931.

KULA, I. et al. Adsorption of Cd(II) ions from aqueous solutions using activated carbon prepared from olive stone by $ZnCl_2$ activation. **Bioresour. Technol.**, v. 99, p. 492-501, 2008.

KUMAR, P. S. et al. Adsorption of dye from aqueous solution by cashew nut shell: Studies on equilibrium isotherm, kinetics and thermodynamics of interactions. **Desalination**, v. 261, p. 52-60, 2010.

KUMARI, H. J. et al. An efficient removal of crystal violet dye from waste water by adsorption onto TLAC/Chitosan composite: A novel low cost adsorbent. **Int. J. Biol. Macromol.**, v. 96, p. 324-333, 2017.

LANGMUIR, I. The adsorption of gases on plane surfaces of glass, mica and platinum. **J. Am. Chem. Soc.**, v. 40, p. 1361-1403, 1918.

LI, Z. et al. Adsorption of indium (III) from aqueous solutions on raw, ultrasound- and supercritical-modified chitin: Experimental and theoretical analysis. **Chem. Eng. J.**, v. 373, p. 1247-1253, 2019.

LIMA, A. C. A. de et al. **Termodinâmica de Adsorção**. In: NASCIMENTO, R. F. do et al. **Adsorção: Aspectos teóricos e aplicações ambientais**, Fortaleza: Imprensa Universitária, 2014.

LIM, Z. E. et al. Functionalized pineapple aerogels for ethylene gas adsorption and nickel (II) íon removal applications. **J. Environ. Chem. Eng.**, v. 8, 104524, 2020.

LIU, Q. et al. Adsorption of cationic dyes from aqueous solution using hydrophilic silica aerogel via ambient pressure drying. **Chin. J. Chem. Eng.**, v. 29, n. 9, p. 2467-2473, 2020.

LOPES, E. C. N. et al. An alternative Avrami equation to evaluate kinetic parameters of the interaction of Hg (II) with thin chitosan membranes. **J. Colloid Interface Sci.**, v. 263, p. 542-547, 2003.

MARÍN, S. L. A. **Remoção dos corantes têxteis C.I. reactive blue 203 e C.I. reactive red 195 mediante o uso de bagaço de maçã como adsorvente**. 2015. Dissertação (Mestrado em Tecnologia de Processos Químicos e Bioquímico)- Universidade Tecnológica Federal do Paraná, Pato Branco, 2015.

MELO, D. de Q. et al. **Equilíbrio de Adsorção**. In: NASCIMENTO, R. F. do et al. **Adsorção: Aspectos teóricos e aplicações ambientais**, Fortaleza: Imprensa Universitária, 2014.

MINCEA, M. et al. Preparation, modification, and applications of chitin nanowhiskers: A review. **Review on Advanced Materials Science**, v. 30, p. 225-242, 2012.

MITTAL, A. et al. Adsorption of hazardous dye crystal violet from wastewater by waste materials.**J. Colloid Interface Sci.**, v. 343, p. 463-473, 2010.

MOL, A. de S. **Preparação e funcionalização de nano fibras (whiskers) de quitina e sua aplicação como agente de recuperação de propriedades em polímeros reciclados**. 2014. Tese (Doutorado em Engenharia de Materiais)- Universidade Federal de Minas Gerais, Belo Horizonte, 2014.

MORIN, A. & DUFRESNE, A. Nanocomposites of chitin whiskers from riftia tubes and poly(caprolactone). **Macromolecules**, v. 35, n. 6, p. 2190-2199, 2002.

MOURA, C. M. de M.; MOURA, J. M. de; SOARES, N. M.; PINTO, L. A. de A. Evaluation of molar weight and deacetylation degree of chitosan during chitin deacetylation reaction: Used to produce biofilm. **Chemical Engineering and Processing: Process Intensification**, v. 50, p. 351-355, 2011.

MOURA, J. M. et al. Comparison of chitosan with different physical forms to remove Reactive Black 5 from aqueous solutions. **J. Environ. Chem. Eng.**, v. 4, n.2, p. 2259–2267, 2016.

NATARAJ, S. K. et al. Nanofiltration and reverse osmosis thin film composite membrane module for the removal of dye and salts from the simulated mixtures. **Desalination**, v. 249, n. 1, p. 12–17, 2009.

ÖNAL, Y. Kinetics of adsorption of dyes from aqueous solution using activated carbon prepared from waste apricot. **J. Hazard. Mater.**, v. 137, n. 3, p. 1719-1728, 2006.

PEREIRA, A. L. S. Aerogéis de nanocelulose funcionalizados para absorção seletiva de solventes orgânicos. Tese (Doutorado em Química) – Universidade Federal do Ceará, Fortaleza, CE, 2018.

PERES, E. C. et al. Microwave synthesis of sílica nanoparticles and its application for methylene blue adsorption. **J. Environ. Chem. Eng.**, v. 6, n. 1, p. 649-659, 2018.

PERUZZO, L. C. **Influência de agentes auxiliares na adsorção de corantes de efluentes da indústria têxtil em colunas de leito fixo**. Dissertação (Mestrado em Engenharia Química)- Universidade Federal de Santa Catarina, Florianópolis, SC, 2003.

PILLAI, C. K. S. et al. Chitin and chitosan polymers: chemistry, solubility and fiber formation. **Prog. Polym. Sci.**, v. 34, p. 641–678, 2009.

QIU, H. et al. Critical review in adsorption kinetic models. **J. Zhejiang Univ. Sci. A**, v. 10, p. 716-724, 2009.

RINAUDO, M. Chitin and chitosan: properties and applications. **Prog. Polym. Sci.**, v. 31, n. 7, p. 603–632, 2006.

RINGOT, D. et al. *In vitro* biosorption of ochratoxin A on the yeast industry by-products: Comparison of isotherm models. **Bioresour. Technol.**, v. 98, p. 1812-1821, 2007.

RODRIGUES FILHO, G. M. **Adsorção do corante amarelo reativo BF-G4 200% por argila esmectita**. 2012. Tese (Doutorado em Engenharia Química)–Universidade Federal do Rio Grande do Norte, Natal, 2012.

ROSU, M. C. et al. Azo dyes degradation using TiO2-Pt/graphene oxide and TiO2-Pt/reduced graphene oxide photocatalysts under UV and natural sunlight irradiation. **Solid State Sci.**, v. 70, p. 13–20, 2017.

RUTHVEN, D. M. **Principles of adsorption and adsorption Processes**. John Wiley & Sons, 1984.

SÁ, R. M. de et al. Preparation and characterization of nanowhiskers cellulose from fiber arrowroot (*Maranta arundinacea*). **Mat. Res.**, v. 18, n. 2, p. 225-229, 2015.

SANTOS, G. da S. et al. identification and characterization of crystal violet in *Cassava spirits* (tiquira). **Quim. Nova**, v. 28, n. 4, p. 583-586, 2005.

SCHLOSSER, C. A. et al. The future of global water stress: An integrated assessment. **Earth's Future**, v. 2, n. 8, p. 341-361, 2014.

SENTURK, H. B. et al. Removal of phenol from aqueous solutions by adsorption onto organomodified Tirebolu bentonite: Equilibrium, kinetic, and thermodynamic study. **J. Hazard. Mater.**, v. 172, p. 353-362, 2009.

SHOJAEIPOOR, F. et al. Aminopropyl-containing ionic liquid based organosilica as a novel and efficient adsorbent for removal of crystal violet from wastewaters. **Chin. J. Chem. Eng.**, v. 25, n. 9, p. 1294-1302, 2017.

SILVA, J. M. et al. Development of chitosan/Spirulina bio-blend films and its biosorption potential for dyes. **J. Appl. Polym. Sci.**, v. 134, n. 11, p. 1–8, 2017.

SIPS, R.The structure of a catalyst surface. **J. Chem. Phys.**, v. 16, p. 490–495, 1948.

SUZUKI, M. **Adsorption Engineering**. Kodansha, Tóquio, 1990.

TAHIR, n. ET AL. Biopolymers composites with peanut hull waste biomass and application for crystal Violet adsorption. **Int. J. Biol. Macromol.**, v. 94, p. 210-220, 2017.

TAN, K. B. et al. Adsorption of dyes by nanomaterials: Recent developments and adsorption mechanisms. **Sep. Purif. Technol.**, v. 150, p. 229–242, 2015.

TIAN, X. et al. Adsorption of antibiotics from aqueous solution by different aerogels. **J. Non. Cryst. Solids.**, v. 505, p. 72-78, 2019.

TONUCCI, M. C. **Adsorção de diclofenaco, estradiol e sulfametoxazol em carvões ativados e nanotubos de carbono: Estudos cinéticos e termodinâmicos**. 2014. Dissertação (Mestrado em Engenharia Ambiental)- Universidade Federal de Ouro Preto, Ouro Preto, MG, 2014.

TÜFEKCI, N. et al. Pollutants of textile industry wastewater and assessment of its discharge limits by water quality standards. **Turkish J. Fish. Aquat. Sci.**, v. 7, p. 97-103, 2007.

VAKILI, M. et al. Application of chitosan and its derivatives as adsorbents for dye removal from water and wastewater: A review. **Carbohyd. Polym.**, v. 26, p. 115-130, 2014.

VIDAL, C. B. et al. Princípios básicos. In: NASCIMENTO, R. F. do et al. **Adsorção: Aspectos teóricos e aplicações ambientais**, Fortaleza: Imprensa Universitária, 2014.

WAN NGAH, W. S. et al. Adsorption of dyes and heavy metal ions by chitosan composites: A review. **Carbohydr. Polym.**, v. 83, n. 4, p. 1446–1456, 2011.

WANG, J. et al. Enzymatic construction of antibacterial ultrathin membranes for dyes removal. **Chem. Eng. J.**, v. 323, p. 56–63, 2017.

WEBER, W. J. Evolution of a technology. **J. Environ. Eng.**, v. 110, n. 5, 889-917, 1984.

WU, F. C. et al. Characteristics of pseudosecond order kinetic model for liquid-phase adsorption: A mini review. **Chem. Eng. J.**, v. 151, p. 1-9, 2009.

YOUNES, I. & RINAUDO, M. Chitin and chitosan preparation from marine sources. Structure, properties and applications. **Mar. Drugs**, v.13, n. 13, p. 1133–1174, 2015.

ZENG, J. B. et al. Chitin whiskers: An Overview. **Biomacromolecules**, v. 13, n. 1, p. 1-11, 2012.

ZAMAN, A. et al. Preparation, properties and applications of natural cellulosic aerogels: A review. **Energy and Built Environment**, v. 1, n. 1, p. 60-76,2019.

ZAZYCKI, M. A. et al. New biochar from *pecan nutshells* as an alternative adsorbent for removing reactive red 141 from aqueous solutions. **J. Clean. Prod.**, v. 171, p. 57-65, 2018.

ZHAO, S. et al. Biopolymer Aerogels and Foams: Chemistry, Properties, and Applications. **Angew. Chem. Int. Ed.**, v. 57, n. 57, p. 2-31, 2018.

ZHANG, C. et al. Chitin nanowhisker-supported sulphonated poly(ether sulfone) proton exchange for fuel cell applications. **Carbohyd. Polym.**, v. 140, p. 195-201, 2016.

ZHU, M. et al. Sorption of an anionic dye by uncalcined and calcined layered double hydroxides: A case study. **J. Hazard. Mater.**, v. 120, p. 163–171, 2005.

CAPÍTULO 3: RESULTADOS E DISCUSSÃO

Os resultados deste trabalho estão apresentados em forma de dois artigos.

- ARTIGO 1: Preparation of chitin nanowhiskers and its application for crystal violet dye removal from wastewaters. (Publicado na revista “Environmental Science and Pollution Research”)

- ARTIGO 2: Chitin-psyllium based aerogel for the efficient removal of crystal violet from aqueous solutions. (Aceito pela revista “International Journal of Biological Macromolecules”).

3.1 ARTIGO 1

Preparation of chitin nanowhiskers and its application for crystal violet dye removal from wastewaters

Susanne Pedroso Druzian[1], Natalia Pollon Zanatta[1], Letícia Nascimento Côrtes[1], Angélica Fátima Mantelli Streit[1], Guilherme Luiz Dotto[1]

[1]Chemical Engineering Department, Federal University of Santa Maria, UFSM, Roraima Avenue, 1000, 97105–900, Santa Maria, RS, Brazil.

Abstract Chitin (Ch) and chitin nanowhiskers (ChNW) were prepared, characterized and applied as adsorbent to remove the crystal violet (CV) dye from aqueous solutions. Ch was obtained from shrimp wastes and ChNW were synthetized by acid hydrolysis. The increase in average pore size and the rod–like shape of ChNW were probably the main characteristics which contributed to the increase in adsorption potential when compared with raw Ch. The adsorbent dosage considered more adequate was 5 g L^{-1} and the most suitable pH was 8.0. Pseudo–second order model was adequate to represent the kinetic profile and Sips model was suitable to fit the equilibrium curves. The maximum adsorption capacity of CV on ChNW was 59.52 mg g^{-1} and the process was endothermic, favorable and spontaneous. These findings indicated that ChNW have potential to be used as adsorbent in the treatment of colored wastewaters.

Keywords chitin nanowhiskers; chitin; adsorption; crystal violet; cationic dye.

3.1.1 Introduction

Water pollution is one of the main social problems nowadays, which is caused by the rapid urbanization and industrialization. Among the main recalcitrant compounds that cause water pollution, synthetic dyes are considered hazardous contaminants due to their stable nature and non–biodegradability that make it difficult to remove from wastewater (FORGACS et al., 2004; GOSWANI & PHUKAN, 2017). Synthetic dyes are a serious pollution problem because they cause damage to both, environment and public health. Therefore, in order to ensure the safe discharge of treated effluents into watercourses, the effective removal of dyes from residual waters is crucial (TAN et al., 2015). Crystal violet is a cationic dye widely used as a coloring agent in many production processes. This may cause adverse effects to human health and may lead to the depletion of water resources when. Thus

the removal of this contaminant from water bodies is extremely important and requires great attention (GOPI et al., 2016; FABRYANTY et al., 2017).

It is very difficult to treat dye containing wastewaters because their inert properties and resistance to aerobic digestion. Another factor that hinders the treatment of colored wastewaters is the low concentration of dyes, which makes conventional methods unfavorable (WAN NGAH et al., 2011; CRINI & BADOT, 2008). An extensive research has been conducted recently to remove dyes from wastewaters. Several treatment methods have been reported, including flocculation (CAI et al., 2015), adsorption (MOURA et al., 2016; DOTTO et al., 2017; CADAVAL et al., 2015a), photocatalytic degradation (ROSU et al., 2017), membrane separation (WANG et al., 2017), reverse osmosis (NATARAJ et al., 2009) and others. Among these, adsorption presents some advantages as low cost and high efficiency that makes it one of the most effective processes for removing dyes from colored wastewaters (YAGUB et al., 2014).

Chitin is a biodegradable, renewable and low cost biopolymer which contains hydroxyl and n–acetyl groups in its structure. Its use as an adsorbent is eco–friendly, once this contributes to the treatment of colored wastewater and also contributes to the solid wastes management, since this polysaccharide is obtained from seafood industry wastes (CRINI & BADOT, 2008; DOTTO et al., 2015a). However, the application of raw chitin presents some drawbacks, since the biopolymer has low surface area, pore volume and average pore size. In this way, modifications in the chitin structure are required to improve its potential (Dotto et al., 2015a). Chitin nanowhiskers for example, are a class of nanomaterials considered very interesting due to their functional groups and high surface to volume ratio. This nanomaterial can be obtained by acid hydrolysis of native chitin (GOPI et al., 2016).

Therefore, this work aimed to prepare chitin nanowhiskers and evaluate its application as adsorbent for crystal violet removal from aqueous solution. Chitin was obtained from shrimp shells and chitin nanowhiskers were prepared by acid hydrolysis. Chitin and chitin nanowhiskers were characterized by X–ray diffraction (XRD), Fourier transform infrared spectroscopy (FT–IR), specific surface area, pore volume and average pore radius (BET and BJH methods), differential scanning calorimetry (DSC) and scanning electron microscopy (SEM). In the adsorption studies, adsorbent dosage effect, pH effect, kinetic, equilibrium and thermodynamic studies were addressed.

3.1.2 Material and methods

3.1.2.1 Reagents

Crystal violet dye (color index 42555, λ_{max} = 584 nm, purity 99.0% and molar weight of 407.98 g mol^{-1}) was purchased from INLAB (Brazil). The analytical grade reagents HCl (99.0%), NaOH (98.0%) and NaClO (active chlorine content of 10–12%) were purchased from G. Gotuzzo and Cia Ltda (Brazil) and Interglas (Brazil). Shrimp (*Penaeus brasiliensis*) wastes were obtained from a fishery industry located in the Brazil southern. All solutions were prepared using deionized water and all reagents were of analytical grade.

3.1.2.2 Chitin obtainment

Chitin was obtained from shrimp wastes through the demineralization, deproteinization and deodorization stages, respectively, according to the methodology proposed by Dotto et al. (DOTTO et al., 2016). Thereon chitin was oven dried, ground and sieved to obtain particles in the size range from 425 to 850 μm.

3.1.2.3 Chitin nanowhiskers preparation

Chitin nanowhiskers were prepared using chitin as precursor material, according to the methodology proposed by Pereira et al. (PEREIRA et al., 2014), with some modifications. Chitin was hydrolyzed with hydrochloric acid 3 mol L^{-1} solution for 90 min under stirring and at boiling point conditions. For each 1 g of chitin, 30 mL of acid solution was used. The resulting dispersion was cooled to room temperature and diluted by addition of deionized water. The suspension was centrifuged (LGI Scientific, DLC802B, Brazil) at 4000 rpm for 20 min for phase separation. The precipitate was washed and centrifuged several times until remaining solution has near–neutral pH and freeze–dried (Liobras, l108, Brazil) for 1 day to obtain chitin nanowhiskers.

3.1.2.4 Characterization of chitin and chitin nanowhiskers

Chitin and chitin nanowhiskers characteristics were determined by X–ray diffraction (XRD), infrared spectroscopy (FT–IR), N_2 adsorption–desorption isotherms (BET and BJH), differential scanning calorimetry (DSC) and scanning electron microscopy (SEM).

The information about the crystallographic structure of Ch and ChNW were verified by XRD (Rigaku, Miniflex 300, Japan) (Al–Sagheer et al., 2009). The functional groups of the samples were identified by FT–IR (Prestige, 21210045, Japan) (Silverstein et al., 2005). The values of specific surface area (m^2 g^{-1}), pore volume (cm^3 g^{-1}) and average pore radius (Å)

were determined by N_2 adsorption–desorption isotherms using the BET and BJH methods (Quantachrome Instruments, New Win 2, USA) (THOMMES et al., 2015). The thermal profile of the samples was determined by DSC (DSC, TA instruments) (BROWN, 2001). The morphological and textural characteristics were observed by SEM (Jeol, JSM –6610LV, Japão) (GOLDSTEIN et al., 2003).

3.1.2.5 Adsorption experiments

The adsorption experiments were carried out in batch operation and using a thermostatic shaker (Marconi, MA 093, Brazil), in order to evaluate and compare the adsorption capacity of Ch and ChNW. Solutions of CV were prepared by diluting a stock of solution of 1 g L^{-1} of CV.

First, the adsorbent dosage effect (adsorbent dosage ranging from 1.25 to 5 g L^{-1}) was evaluated. The assays were performed in Erlenmeyer flasks at the original pH of the solution (pH=8.0), 298 K, 250 rpm, CV initial concentration of 25 mg L^{-1} and contact time of 2 h. After the determination of adsorbent dosage, the pH effect (pH 2.0, 3.0, 4.0, 5.0, 6.0, 7.0, 8.0, 9.0 and 10.0) was studied. NaOH and HCl 0.1 mol L^{-1} solutions were used to adjust the solution pH. The experiments were performed using 5 g L^{-1} of adsorbent dosage, under the same conditions of temperature, agitation, initial concentration and contact time used in the previous assay. Kinetic curves were constructed with a contact time of 5, 10, 15, 20, 30, 60, 90, 120, 150 and 180 min, initial dye concentrations of 25, 50, 100, 150 and 200 mg L^{-1}, temperature of 298 K, stirring rate of 250 rpm and with the more adequate values of adsorbent dosage and pH previously defined. The equilibrium curves were constructed with temperatures of 298, 308 and 318 K, initial dye concentrations of 25, 50, 100, 150 and 200 200 mg L^{-1}, stirring rate of 250 rpm and the more adequate values of adsorbent dosage and pH previously defined. The equilibrium was considered when the concentration of CV dye was constant in the liquid phase, that is, after three equal consecutive measurements of dye concentration in liquid phase with intervals of 30 min.

For all assays, separation of the solid phase and the remaining solution was performed by centrifugation (Centribio, 80–2B, Brasil) at 4000 rpm for 15 min. The quantification of CV in the liquid phase was performed by spectrophotometric method at the wavelength of maximum absorption (584 nm), using a spectrophotometer (Biospectro, SP–22, Brasil). Blank and triplicate tests were performed in order to ensure the reliability of the results. The CV removal percentage (R, %) (CADAVAL et al., 2015a) (Eq. 1), the adsorption capacity at time

"t" (q_t, mg g^{-1}) (FRANTZ et al., 2016) (Eq. 2) and the equilibrium adsorption capacity (q_e, mg g^{-1}) (DOTTO et al., 2016a) (Eq. 3) were determined by the following equations.

$$R = \frac{(C_0 - C_t)}{C_0} 100 \quad (1)$$

$$q_t = \frac{V(C_0 - C_t)}{m} \quad (2)$$

$$q_e = \frac{V(C_0 - C_e)}{m} \quad (3)$$

where C_0 is the initial CV concentration in liquid phase (mg L^{-1}), C_t is the CV concentration in liquid phase at time "t" (mg L^{-1}), C_e is the equilibrium CV concentration in liquid phase (mg L^{-1}), V is the volume of solution (L) and m is the adsorbent amount (g)

3.1.2.6 Kinetic evaluation

The kinetic behavior of CV adsorption was evaluated by adjusting the experimental curves by the pseudo–first order (QIU et al., 2009) (Equation 4) and pseudo–second order (WU et al., 2009) (Equation 5) models.

$$q_t = q_1\left(1 - exp(-k_1 t)\right) \quad (4)$$

$$q_t = \frac{t}{\left(\frac{1}{k_2 q_2^2}\right) + \left(\frac{t}{q_2}\right)} \quad (5)$$

where k_1 (min^{-1}) and k_2 (g mg^{-1} min^{-1}) are the rate constants of pseudo–first order and pseudo–second order models, respectively; q_1 (mg g^{-1}) and q_2 (mg g^{-1}) are the theoretical values for the adsorption capacity obtained by the pseudo–first order and pseudo–second order models, respectively and t (min) is the time.

3.1.2.7 Equilibrium

The equilibrium models of Langmuir (Equation 6) (Langmuir, 1918), Freundlich (Equation 7) (FREUNDLICH, 1906), Sips (Equation 8) (SIPS, 1948) and Hill (Equation 9) (RINGOT et al., 2007; FOO&HAMEED, 2010) were used to estimate the equilibrium parameters.

$$q_e = \frac{q_m k_L C_e}{1 + k_L C_e} \quad (6)$$

$$q_e = k_F C_e^{\frac{1}{n_F}} \quad (7)$$

$$q_e = \frac{q_{mS}(k_S C_e)^{m_S}}{1 + (k_S C_e)^{m_S}} \quad (8)$$

$$q_e = \frac{q_H C_e^{n_H}}{K_D + C_e^{n_H}} \quad (9)$$

where q_m (mg g^{-1}) is the maximum adsorption capacity; k_L (L mg^{-1}) is the Langmuir constant; k_F ((mg g^{-1})(mg $L^{-1})^{-1/nF}$) is the Freundlich constant; $1/n_F$ is the heterogeneity factor; q_{mS} (mg g^{-1}) is the maximum adsorption capacity of Sips; k_S (L mg^{-1}) is the Sips constant; msis the fractional exponent; q_H (mg g^{-1}) is the maximum specific uptake corresponding to sites saturation; n_H is the Hill cooperativity coefficient of the binding interaction and K_D (mg L^{-1}) is the Hill constant.

3.1.2.8 Thermodynamics

The adsorption thermodynamic parameters, as Gibbs free energy (ΔG^0, kJ mol^{-1}), enthalpy (ΔH^0, kJ mol^{-1}) and entropy (ΔS^0, kJ mol^{-1} K^{-1}) changes, were estimated from the Equations 10–12 (BRIÃO et al., 2017).

$$\Delta G° = -RTln(\rho K_e) \quad (10)$$

$$\Delta G° = \Delta H° - T\Delta S° \quad (11)$$

$$ln(\rho K_e) = \frac{\Delta S°}{R} - \frac{\Delta H°}{RT} \quad (12)$$

Where T is the temperature (K), ρ is the solution density (g L^{-1}), K_e is the equilibrium constant (L g^{-1}) and R is 8.31 x 10^{-3} kJ mol^{-1} K^{-1}.

3.1.2.9 Modeling and parameters estimation

The kinetic and equilibrium parameters were determined by non–linear regression of the experimental data, based on the minimization of least squares function, using Statistic 10.0 software (Statsoft, EUA). The fit quality was evaluated by the coefficient of determination (R^2), adjusted coefficient of determination (R^2_{adj}) and the average relative error (ARE) (DOTTO et al., 2013).

3.1.3 Results and discussions

3.1.3.1 Characteristics of chitin and chitin nanowhiskers

Chitin nanowhiskers were characterized by XRD, FT–IR, BET, BJH, DSC and SEM. Raw chitin was also characterized in order to verify the possible modifications that occurred during the hydrolysis.

The information about the crystallographic structure of Ch and ChNW are obtained by XRD measurements. In Figure 1 are illustrated the X–Ray patterns of the Ch and ChNW samples. It can be observed that Ch and ChNW samples showed sharp crystalline reflections near to9.3°, 19.2°, 31.5°, 34.1° and 35.9° that are peaks related to orthorhombic crystal structure of the shrimp (Al–SAGHEER et al., 2009). It can be observed that the intensity of the peaks of ChNW increases when compared with Ch. This occurs due to the removal of amorphous domains of Ch during the acid hydrolysis (ZENG et al., 2012).

The main functional groups of Ch and ChNW were identified by FT–IR. The FT–IR spectra for the two materials can be visualized in Figure 2. Observing the FT–IR spectra of Ch and ChNW, we can verify that these spectra are very similar and present the same bands. In both spectra, a broad band centered around 3400cm^{-1} was observed, corresponding to the vibration of the O–H and N–H stretching. The IR band around 2900 cm^{-1} can be attributed to the CH_2 and CH_3 stretching. At 1650 and 1550 cm^{-1}, it can be seen the IR bands corresponding to amide I and amide II, respectively. At 1450 cm^{-1}, the characteristic band of the CHx deformation can be observed. In the range of 1250–820 cm^{-1}, the observed bands can be attributed to the C–O and C–O–C stretching (DOTTO et al., 2016b; DOTTO et al., 2015a).

The N_2 adsorption/desorption isotherms for Ch and ChNW are presented in Figure 3. According to the IUPAC classification, both isotherms for Ch and ChNW are Type II. This type of isotherm is typical of nonporous or macroporous adsorbents and its shape is the result of unrestricted monolayer–multilayer adsorption. An adsorption hysteresis is presented in the adsorption/desorption isotherm of ChNW (Fig. 3b), which is characteristic of the presence of mesopores (THOMMES et al., 2015). The values of BET surface area, total pore volume and average pore size determined by the BET and BJH methods were 2.07 $m^2\ g^{-1}$, 0.0060 $cm^3\ g^{-1}$ and 17.16 nm for ChNW and 2.93 $m^2\ g^{-1}$, 0.0069 $cm^3\ g^{-1}$ and 8.58 nm for Ch, respectively.

Fig. 1 XRD patterns of Ch and ChNW.

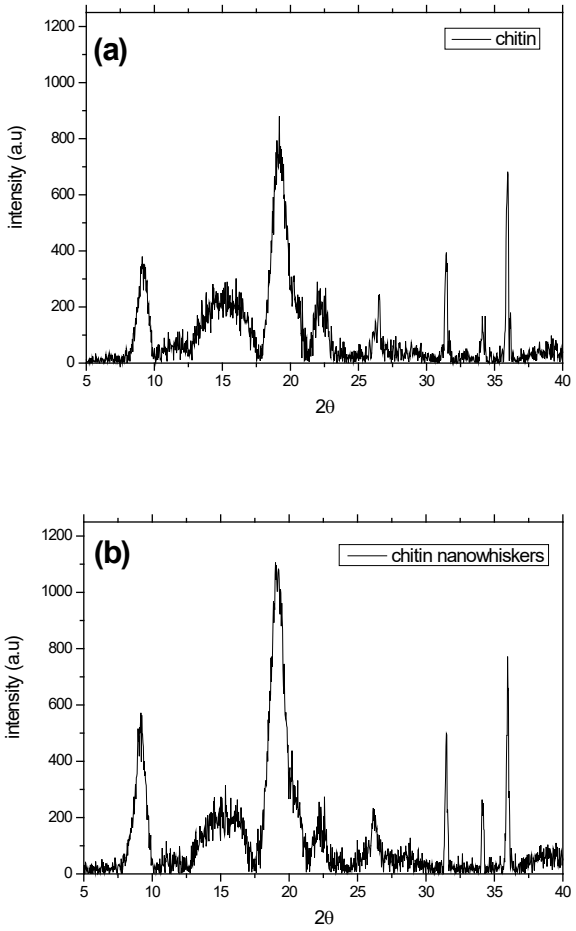

Fig. 2 FT–IR vibrational spectra of Ch and ChNW.

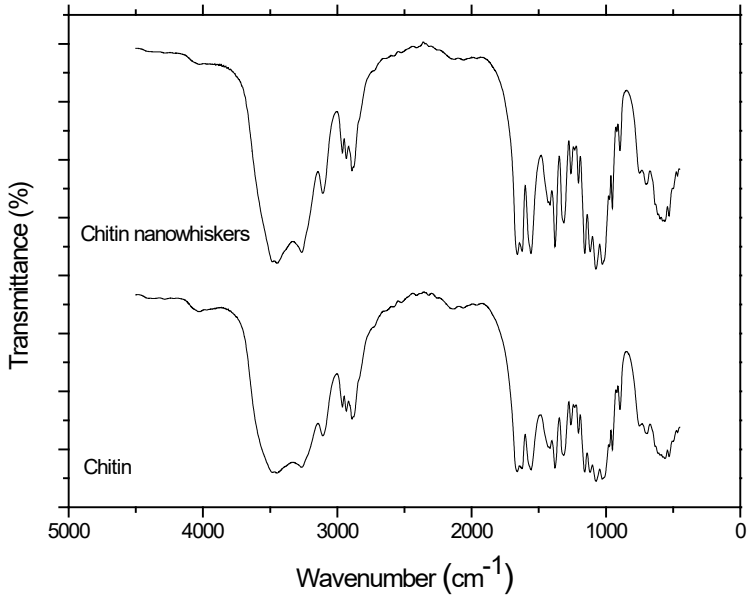

The ChNW presented BET surface area and total pore volume values relatively similar to the Ch. However, a significant increase was observed in the average pore size values of the ChNW, which improves adsorption since it facilitates intraparticle diffusion of the dye molecules.

Fig. 3 N_2 adsorption–desorption isotherms of (a) Ch and (b) ChNW.

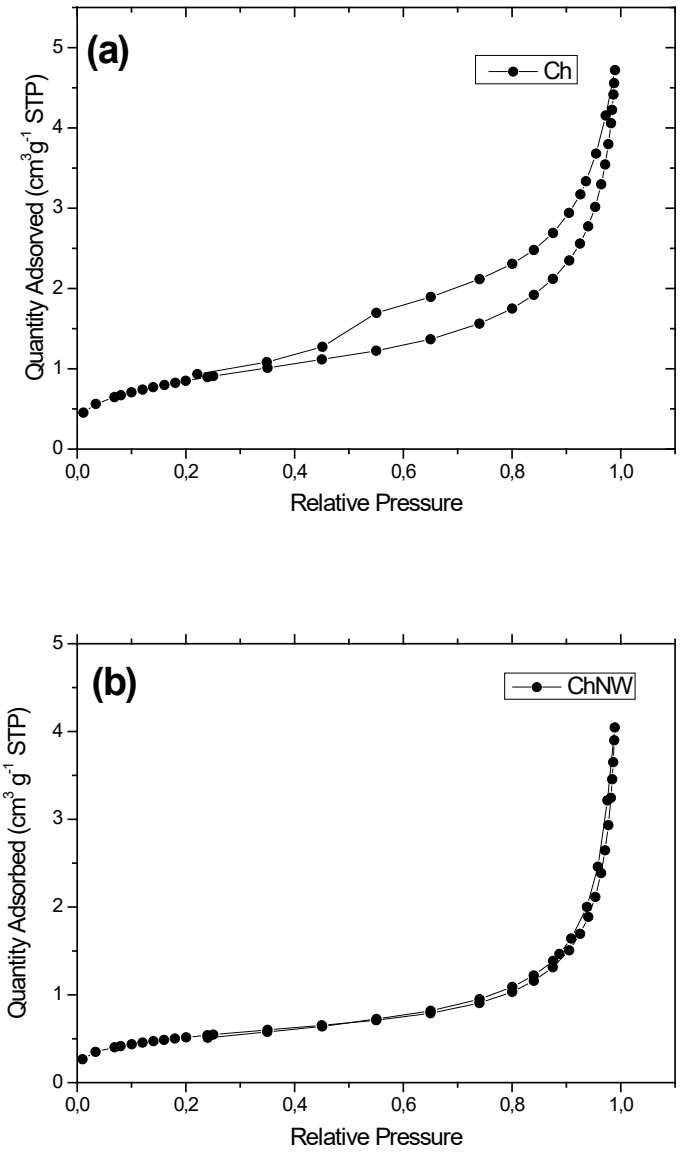

In Figure 4 are presented the DSC curves of Ch and ChNW, respectively, in the temperature range from 25 to 400°C. Both Ch and ChNW DSC curves showed endothermic peaks of water evaporation near to 100 and 117°C, respectively. In the curve of Ch was observed an exothermic peak that corresponds to the decomposition process. The enthalpy

variation regarding the water evaporation was higher to ChNW, what indicates a higher difficult in the water transference inside the material.

Fig. 4 DSC curves of Ch and ChNW.

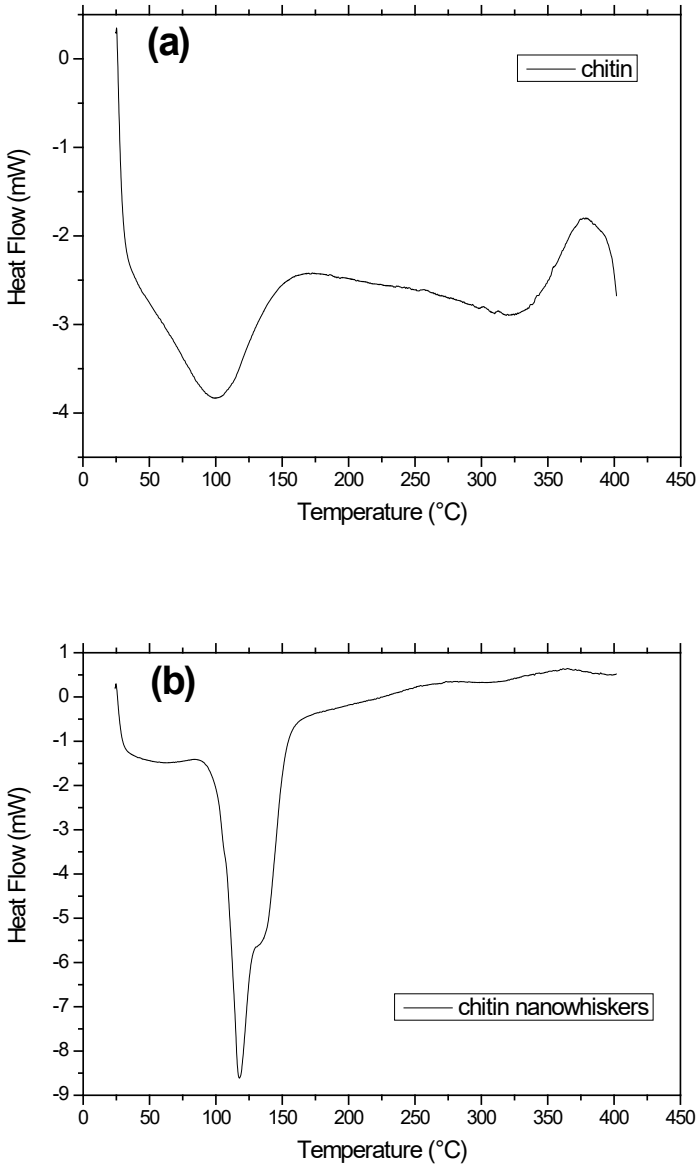

The SEM images of Ch and ChNW are presented in Figure 5. Figure 5a and Figure 5b shows that Ch has a smooth, homogeneous and highly compacted surface without the presence of pores (DOTTO et al., 2015a; DOTTO et al., 2015b; CÔRTES et al., 2015). In the Figure 5c and Figure 5d can be seen that ChNW have a rod–like shape at nanometer level, which contributes to a greater dispersibility and its in accordance with the literature (ZENG et al., 2012; FAN et al., 2008, GOPI et al., 2016). This shape of ChNW also contributes to the

adsorption process, since facilitates the occupation of the adsorption sites by the dye molecules, which in the raw chitin can be difficult due the lower area–volume relation.

Fig. 5 SEM images of Chitin and Chitin nanowhiskers: (a) Ch 100×, (b) Ch 10000×, ChNW 100× and ChNW 10000×.

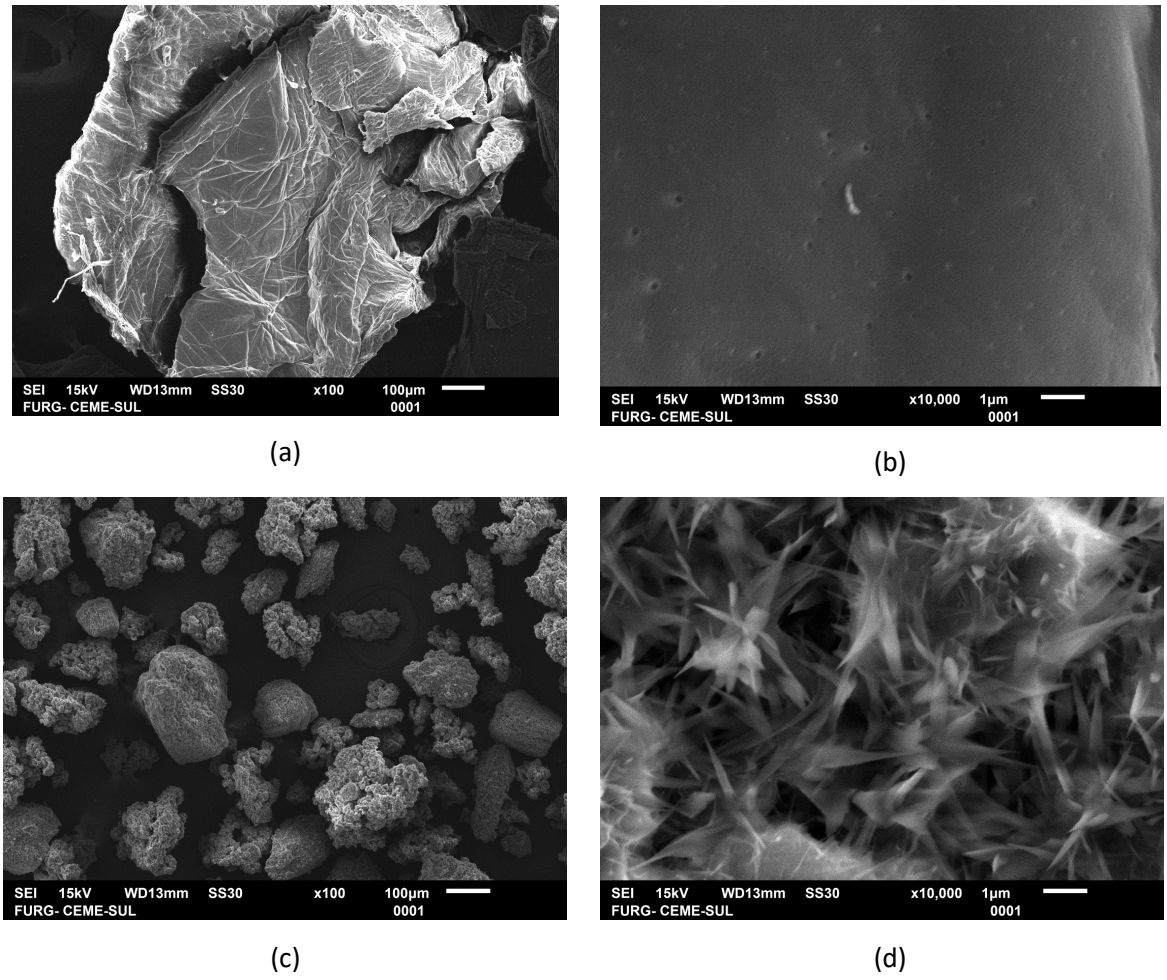

3.1.3.2 Adsorbent dosage effect

The adsorbent dosage effect of Ch and ChNW on CV removal can be seen in Figure 6. It can be seen that increasing the adsorbent dosage, there is an increase in CV removal. The increase from 1.25 to 5 g L^{-1} in Ch and ChNW dosage caused an increase of 29 to 66% and 41 to 90%, respectively, in the removal percentage. This is due to the fact that the increase in adsorption dosage causes an increase in total number of adsorption sites available to retain the dye molecules (PAVAN et al., 2014). For all adsorbent dosages, ChNW was superior in relation to Ch. This trend shows that ChNW has better adsorption characteristics than the raw Ch. These results can be mainly attributed to the higher average pore size, area–volume

relation and also the rod–like shape and nanometric size of ChNW. Based on these results the following tests were performed using 5 g L^{-1} of ChNW.

3.1.3.3 pH effect

The results of pH effect, in terms of removal percentage (%), are depicted in Figure 7. The pH effect was investigated from 2.0 to 10.0. It can be observed that an increase in pH from 2.0 to 7.0 results in an increase in CV removal percentage from 75.90 to 91.63%. However from pH 7 there is no significant variation on values of CV removal percentage. Under low pH values, there is a competition between the H^+ ions with the CV cationic dye (BRIÃO et al., 2017; SILVA et al., 2017), leading to a lower adsorption values. When the pH is increased, this competition decreases and in parallel, the ChNW organic functional groups tend to be deprotonated. These facts cause an increase in adsorption. Thus, it was chosen to follow the experiments using the original pH of the CV solution (pH = 8).

Fig. 6 Adsorbent dosage effect on CV adsorption by Ch and ChNW (298 K, C_0=25 mg L^{-1}, 250 rpm, 2 h).

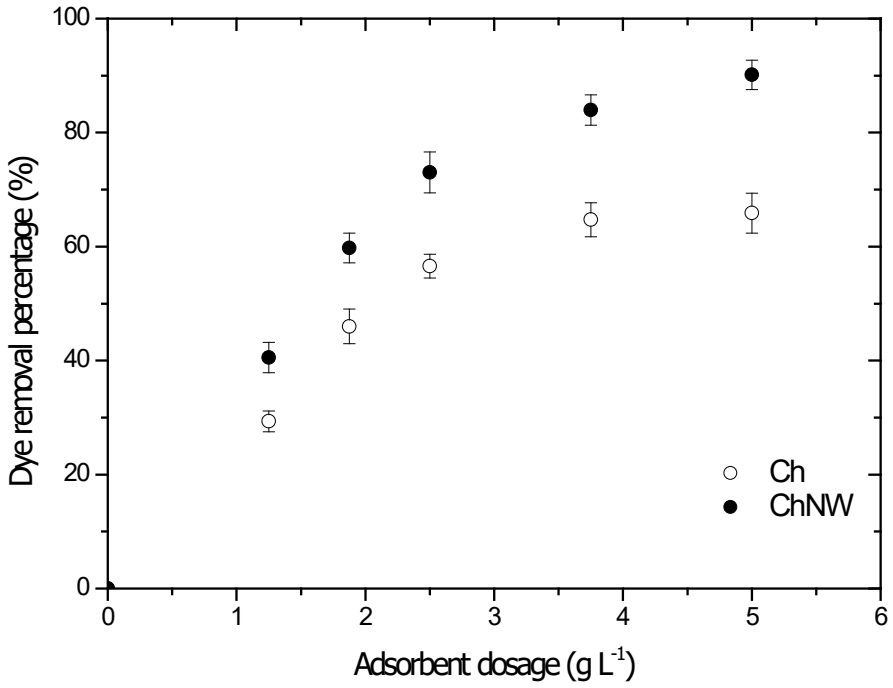

Fig. 7 pH effect on CV adsorption by ChNW (298 K, C_0=25 mg L^{-1}, 250 rpm, 2 h, adsorbent dosage of 5 g L^{-1}).

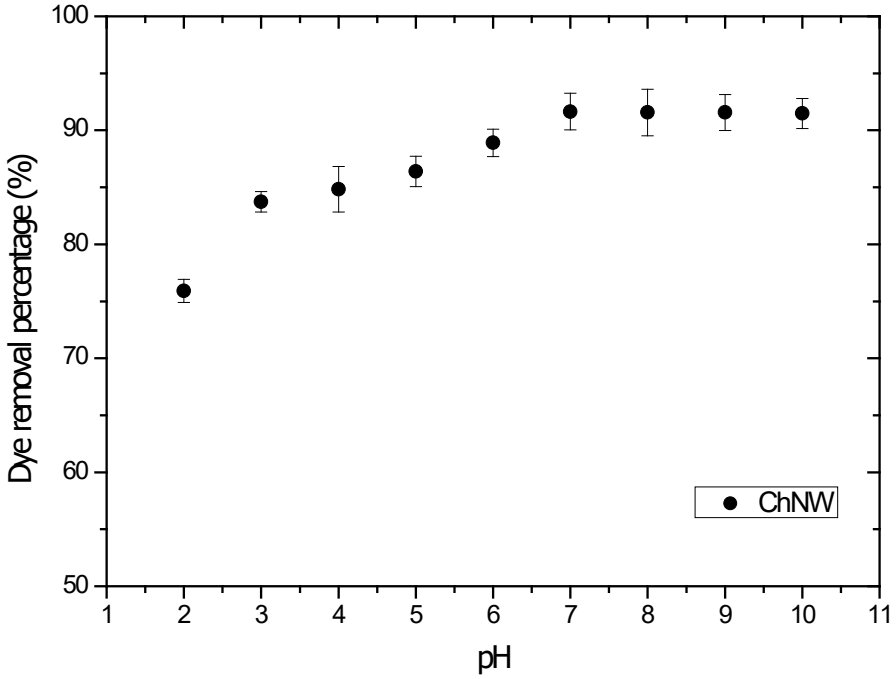

3.1.3.4 Kinetic studies

The adsorption kinetic curves can be seen in Figure 8. The kinetic curves were constructed with initial CV concentrations of 25, 50, 100, 150 and 200 mg L^{-1}, using an adsorbent dosage of 5 g L^{-1}, pH of 8 and contact time ranging from 0 to 180 min. Figure 8 shows that typical kinetic curves were obtained. It can be observed that in the first 10 min a fast step occurred and after, that the adsorption rate gradually decreased. Also it can be observed that adsorption sites were occupied progressively by the dye molecules and the higher values of initial CV concentration resulted in higher values of adsorption capacity.

The kinetic behavior was investigated by the adjustment of the pseudo–first order and pseudo–second order models. The kinetic parameters for CV adsorption on ChNW are presented in Table 1. The coefficient of determination, adjusted coefficient of determination and average relative error were considered adequate for the two models investigated. However, pseudo–second order model presented better values of adjustment quality indicators and was considered the most adequate to represent the adsorption kinetic of CV on ChNW.

Fig. 8 Kinetic curves for CV adsorption on ChNW (298 K, pH of 8, adsorbent dosage of 5 g L^{-1}).

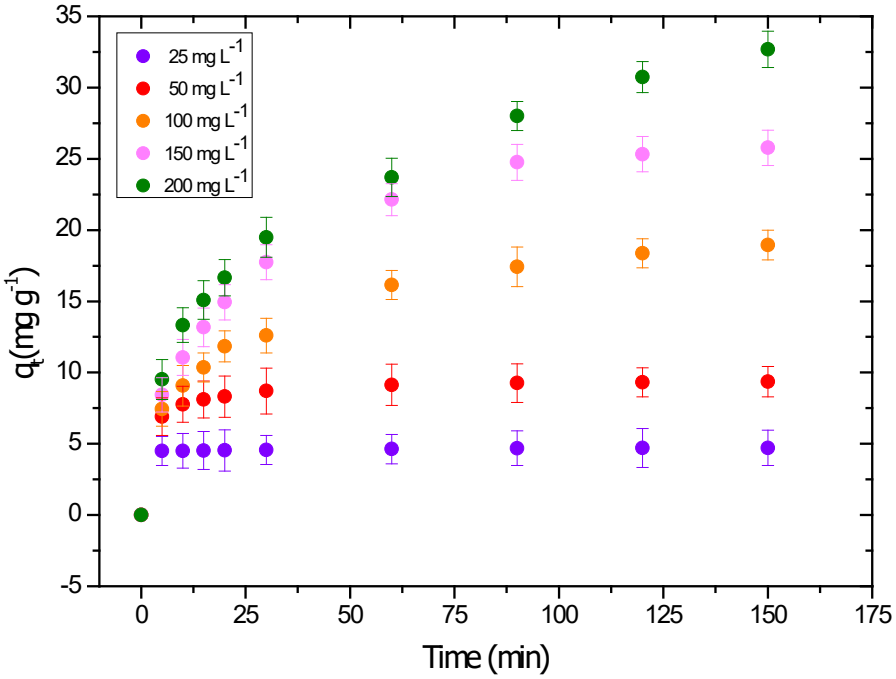

Table 1 Kinetic parameters for CV adsorption on ChNW.

Kinetic Model	Initial dye concentration (mg L^{-1})				
	25	50	100	150	200
Pseudo–first order					
q_1 (mg g^{-1})	4.62	8.98	17.87	25.03	30.51
k_1 (min^{-1})	0.6982	0.2509	0.0586	0.0491	0.0408
R^2	0.9983	0.9872	0.9731	0.9879	0.9721
R^2_{adj}	0.9981	0.9858	0.9701	0.9866	0.9690
ARE	0.03	0.03	3.30	3.52	5.00
Pseudo–second order					
q_2 (mg g^{-1})	4.67	9.41	19.90	28.41	35.39
k_2 (g mg^{-1} min^{-1})	0.7491	0.0524	0.0040	0.0022	0.0014
R^2	0.9992	0.9989	0.9911	0.9965	0.9891
R^2_{adj}	0.9991	0.9987	0.9901	0.9961	0.9879
ARE	0.01	0.02	1.35	1.33	2.54
q_e (mg g^{-1})	4.74	9.41	18.75	25.77	32.68

The values of q_2 increased from 4.67 to 35.39 mg g^{-1} with the increase of the initial CV concentration from 25 to 200 mg L^{-1}, as expected. The values of q_2 closed very well with the experimental values of q_e for all CV concentrations, which indicates the good fit of the model.

3.1.3.5 Equilibrium studies

Equilibrium isotherms for CV adsorption on ChNW were obtained at 298, 308 and 318 K, using an adsorbent dosage of 5 g L^{-1}, pH of 8 and initial CV concentration ranging from 25 to 200 mg L^{-1}. The equilibrium curves are shown in Figure 9. According to the initial slope, all curves can be classified as Langmuir type curves ("L" curves). Based on the shapes of the upper parts of the isotherms, the curve obtained at 298 K can be classified as a "L_2" type isotherm, while the curves obtained at 308 and 318 K were typical "L_1" type isotherms (GILES et al., 1960). Curves "L_2" type commonly occurs in cases of adsorption from dilute solutions. The initial curvature in this type of isotherm shows that it becomes more difficult to the dye molecules to find a site available as the sites in the adsorbent are filled. Thus the plateau suggests that a monomolecular layer of CV on the ChNW surface is forming. For curves "L_1" type, the q_e tends to increase progressively with the increase of equilibrium concentration, which suggests that there is no complete occupation of all adsorption sites (Dotto et a., 2015a; Giles et al., 1960; Peres et al., 2018).

Fig. 9 Equilibrium curves for CV adsorption on ChNW (pH of 8, adsorbent dosage of 5 g L^{-1}).

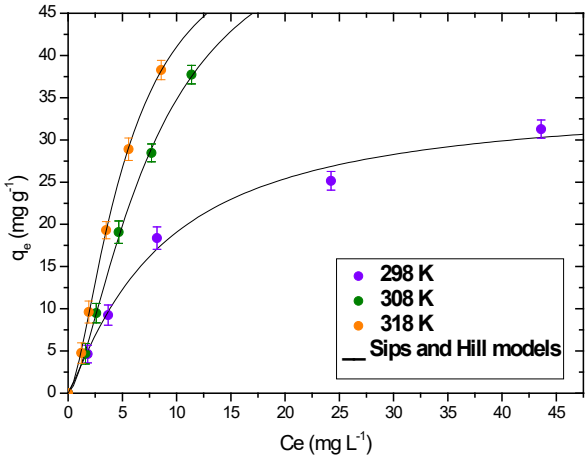

The equilibrium curves of CV adsorption on ChNW were represented by Langmuir, Freundlich, Sips and Hill models. The estimated equilibrium parameters are shown in Table 2.

Table 2 Isotherm parameters for CV adsorption on ChNW.

Equilibrium models	Temperature (K)		
	298	308	318
Freundlich			
k_F (mg g^{-1})(mg L^{-1})$^{-1/nF}$	5.65	4.37	5.91
$1/n_F$	0.4618	0.8972	0.8840
R^2	0.9851	0.9954	0.9941
R^2_{adj}	0.9813	0.9942	0.9926
ARE (%)	10.85	8.19	9.15
Langmuir			
q_m (mg g^{-1})	38.12	184.55	168.88
k_L (L mg^{-1})	0.0944	0.0230	0.0350
R^2	0.9956	0.9969	0.9961
R^2_{adj} (%)	0.9945	0.9961	0.9952
ARE	4.13	8.42	9.38
Sips			
q_{mS} (mg g^{-1})	34.91	56.36	59.52
k_S (L mg^{-1})	0.1175	0.1257	0.1856
m_S	1.1512	1.4894	1.5573
R^2	0.9960	0.9997	0.9999
R^2_{adj}	0.9951	0.9996	0.9999
ARE	1.93	1.08	0.76
Hill			
q_H (mg g^{-1})	34,91	59,52	56,69
n_H	1,1513	1,4894	1,5573
K_D (mg L^{-1})	11,7615	21,9448	13,7761
R^2	0.9960	0.9997	0.9999

R^2_{adj}	0.9951	0.9996	0.9999
ARE	1.93	1.08	0.76

By analyzing the statistical indicators (R^2, R^2_{adj} and ARE) the three models can be classified as suitable to represent the isotherms. However, Hill and Sips models presented higher values of coefficient of determination and adjusted coefficient of determination and lower value of average relative error, so it was considered the most adequate to represent the adsorption isotherms of CV on ChNW. The k_s parameter increased with the temperature increase and the adsorption was better at 318 K, so the increase of the temperature is favorable to the adsorption. Also, the q_{ms} parameter increased with the temperature, indicating higher adsorption capacity at 318 K. The binding of CV on ChNW was considered as a positive cooperative interaction, since the Hill coefficient n_H was higher than 1 (RINGOT et al., 2007).

The maximum adsorption capacity of CV in ChNW was 59.52 mg g^{-1}. Kumari et al. (KUMARI et al., 2017) obtained a maximum adsorption capacity of about 15 mg g^{-1} for a *Typha latifolia* activated charcoal and chitosan composite used to remove CV from aqueous solutions. Dhodapkar et al. (DHODAPKAR et al., 2007) developed the Janshakti® polymer and applied it as adsorbent for the removal of CV, obtaining a maximum capacity of 12.90 mg g^{-1}. Sugarcane fiber and pinus bark powder were also used to remove CV of aqueous solutions, and presented maximum adsorption capacities of 10.44 and 32.78 mg g^{-1}, respectively (PARAB et al., 2012; AHMAD et al., 2009). Comparing the maximum adsorption capacity value obtained for ChNW with those obtained using the adsorbent materials cited, ChNW can be classified as an attractive adsorbent for the treatment of effluents containing CV dye.

3.1.3.6 Adsorption thermodynamics

The adsorption thermodynamics was evaluated by the standard values of Gibbs free energy (ΔG^0, kJ mol^{-1}), enthalpy (ΔH^0, kJ mol^{-1}) and entropy (ΔS^0, kJ mol^{-1} K^{-1}) changes. The thermodynamic parameters estimated are presented in Table 3.The adsorption process was favorable and spontaneous, since the values of ΔG^0 were negative. The adsorption was more favorable at 318 K due the more negative value of ΔG^0, which is agrees with equilibrium studies. The CV adsorption on ChNW was an endothermic process, since $\Delta H^0$was positive. Based on the magnitude of ΔH^0 it is possible to affirm that electrostatic interactions occurred between CV and ChNW surface (TRAN et al., 2017; PERES et al., 2018).

Table 3 Adsorption thermodynamic parameters.

Temperature (K)	ΔG^0 (kJ mol^{-1})	ΔH^0 (kJ mol^{-1})	ΔS^0 (kJ mol^{-1} K^{-1})
298	–20.60		
308	–22.83		
318	–24.46	36.94	0.19

3.1.4 Conclusion

In this work, ChNW was prepared from Ch by acid hydrolysis and used as an alternative adsorbent to removal CV from aqueous solutions. The characterization techniques as XRD, FT–IR, N_2 adsorption/desorption isotherms (BET and BJH), DSC and SEM were used to show the modifications that occurred on Ch during the hydrolysis. The significant increase in average pore size, the rod–like shape and also the nanometric size of ChNW were probably the characteristics that most contributed to the increase in CV adsorption.

The ChNW presented higher CV adsorption potential when compared to raw Ch. The adsorption was favored at 5 g L^{-1} and pH of 8.0. The kinetic curves followed the pseudo–second order model and, Sips equilibrium model was able to fit the CV adsorption on ChNW, being the maximum adsorption capacity 59.52 mg g^{-1}. The thermodynamic studies indicated that electrostatic interactions occurred between CV and ChNW and that adsorption processes was endothermic, favorable and spontaneous. Finally, according to this research, ChNW have potential to be used as an adsorbent in the treatment of colored wastewater containing the crystal violet dye.

REFERENCES

Al–SAGHEER, F. A. et al. Extraction and characterization of chitin and chitosan from marine sources in Arabian Gulf. **Carbohydr. Polym.**, v.77, p. 410-419,2009.

BRIÃO, G. V. et al. Adsorption of Crystal violet dye onto a mesoporous ZSM–5 zeolite symthetized using chitin as template. **J. Colloid. Interf. Sci.**, v. 508, p. 313–322, 2017.

BROWN, M. E.**Introduction to thermal analysis**: Techniques and applications, Springer, 2001.

CADAVAL, T. R. S. Jr. et al. Vanadium removal from aqueous solutions by adsorption onto chitosan films. **Desalin. Water. Treat.**, v. 57, p. 16583–16591,2015b.

CADAVAL, T. R. S. Jr. et al. Equilibrium isotherms, thermodynamics, and kinetic studies for the adsorption of food azo dyes onto chitosan films. **Chem. Eng. Commun.**, v. 202, p. 1316–1323, 2015a.

CAI, T. et al. Efficient flocculation of an anionic dye from aqueous solutions using a cellulose–based flocculant. **Cellulose**, v. 22, p. 1439–1449, 2015.

CÔRTES, L. N. Biosorption of gold from computer microprocessor leachate solutions using chitin. **Waste Manage**, v. 45, p. 272–279, 2015.

CRINI, G. &BADOT, P. M. Application of chitosan, a natural aminopolysaccharide, for dye removal from aqueous solutions by adsorption processes using batch studies: A review of recent literature. **Prog. Polym. Sci.,** v. 33, p. 399–447, 2008.

DHODAPKAR, R. Adsorption of cationic dyes on super absorbent polymer and photocatalytic regeneration of the adsorbent. **React. Funct. Polym.**, v. 67, p. 540–548, 2007.

DOTTO, G. L. et al. Kinetics and Mechanism of Tartrazine Adsorption onto Chitin and Chitosan.**Ind. Eng. Chem. Res.**, v. 51, p. 6862–6868, 2012.

DOTTO, G. L. et al. Kinetic studies on the biosorption of phenol by nanoparticles from Spirulina sp. LEB 18. **J. Environ. Chem. Eng.**, v. 1, p. 1137–1143, 2013.

DOTTO, G. L. et al. Adsorption of Methylene Blue by ultrasonic surface modified chitin. **J. Colloid. Interf. Sci.**, v. 446, p. 133–140, 2015a.

DOTTO, G. L. et al. Surface modification of chitin using ultrasound–assisted and supercritical CO_2 technologies for cobalt adsorption. **J. Hazard. Mater.**, v. 295, p. 29–36, 2015b.

DOTTO, G. L.et al. Adsorption rate of Reactive Black 5 on chitosan based materials: geometry and swelling effects. **Adsorption,** v. 22, p. 973–983, 2016a.

DOTTO, G. L. et al. Ultrasound–assisted treatment of chitin: evaluation of physicochemical characteristics and dye removal potential. **E–Polymers**, v. 16, p. 49–56, 2016b.

DOTTO, G. L. et al. Chitosan/polyamide nanofibers prepared by Forcespinning® technology: A new adsorbent to remove anionic dyes from aqueous solutions. **J. Clean. Prod.**, v. 144, p. 120–129, 2017.

FABRYANTY, R. et al. Removal of Crystal violet dye by adsorption using bentonite – alginate composite. **J. Environ. Chem. Eng.**, v. 5, p. 5677–5687, 2017.

FAN, Y. et al. Preparation of chitin nanofibers from squid pen b–chitin by simple mechanical treatment under acid conditions. **Biomacromolecules**, v. 9, p. 1919–1923, 2008.

FOO, K. Y. &HAMEED, B. H. Insights into the modeling of adsorption isotherm systems. **Chem. Eng. J.**, v. 156, p. 2-10, 2010.

FORGACS, E. et al. Removal of synthetic dyes from wastewaters: a review. **Environ. Int.**, v. 30, p. 953–971, 2004.

FRANTZ,T. S. et al. Cu(II) adsorption from copper mine water by chitosan films and the matrix effects. **Environ. Sci. Pollut. Res.**, v. 24, p. 5908–5917, 2017.

FREUNDLICH, H. M. F. Over the adsorption in solution. **Z Physic. Chem. *A***, v. 57, p. 385–470, 1906.

GILES, C. H. et al. A system of classification of solution adsorption isotherms, and its use in diagnosis of adsorption mechanisms and in measurement of specific surface areas of solids. **J. Chem. Soc.**, p. 3973–3993, 1960.

GOLDSTEIN, J. et al. **Scanning Electron Microscopy and X–Ray Microanalysis**.3. ed. New York: Kluwer Academic/Plenum Publishers,2003.

GOPI, S. et al. Enhanced adsorption of crystal violet by synthesized and characterized chitin nanowhiskers from shrimp shell. **J. Water. Process. Engin.**, v. 14, p. 1–8, 2016.

GOSWAMI, M. &PHUKAN, P. Enhanced adsorption of cationic dyes using sulfonic acid modified activated carbon. **J. Environ. Chem. Eng.**, v. 5, p. 3508–3517, 2017.

KUMARI, H. J.et al. An efficient removal of crystal violet dye from waste water by adsorption onto TLAC/Chitosan composite: A novel low cost adsorbent. **Int. J. Biol. Macromol.**, v. 96, p. 324–333, p. 2017.

LANGMUIR, I. The adsorption of gases on plane surface of glass, mica and platinum. **J. Am. Chem. Soc.**, v. 40, p. 1361–1403, 1918.

MOURA, J. M.et al. Comparison of chitosan with different physical forms to remove Reactive Black 5 from aqueous solutions. **J. Environ. Chem. Eng.**, v. 4, p. 2259–2267, 2016.

NASCIMENTO, R. F. do et al. **Adsorção**: Aspectos teóricos e aplicações ambientais. Imprensa Universitária, 2014.

NATARAJ, S. K. et al. Nanofiltration and reverse osmosis thin film composite membrane module for the removal of dye and salts from the simulated mixtures. **Desalination**, v. 249, p. 12–17, 2009.

PARAB, H. et al. Use of Agro-Industrial Wastes for Removal of Basic Dyes from Aqueous Solutions. **Clean. (Weinh)**, v. 37, p. 963–969, 2009.

PAVAN, F. A.et al. Formosa papaya seed powder (FPSP): Preparation, characterization and application as an alternative adsorbent for the removal of crystal violet from aqueous phase. **J. Environ. Chem. Eng.**, v. 2, p. 230–238, 2014.

PEREIRA, A. G. B. et al. Chitosan–sheath and chitin–core nanowhiskers. **Carbohyd. Polym.**, v. 107, p. 158–166, 2014.

PERES, E. C. et al. Microwave synthesis of sílica nanoparticles and its application for methylene blue adsorption. **J. Environ. Chem. Eng.**, v. 6, p. 649–659, 2018.

QIU, H. et al. Critical review in adsorption kinetic models. **Zhejiang Uni. Sci. A**, v. 10, p. 716–724, 2009.

RINGOT, D.et al. *In vitro* biosorption of ochratoxin A on the yeast industry by-products: Comparison of isotherm models. **Bioresour. Technol.**, v. 98, p. 1812-1821, 2007.

ROSU, M. C.et al. Azo dyes degradation using TiO2–Pt/graphene oxide and TiO2–Pt/reduced graphene oxide photocatalysts under UV and natural sunlight irradiation. **Solid. State. Sci.**, v. 70, p. 13–20, 2017.

SILVA, J. M. et al. Development of chitosan/spirulina bio–blend films and its biosorption potential for dyes. **J. Appl. Polym. Sci.**, v. 134, p. 44580, 2017.

SILVERSTEIN, R. et al. **Spectrometric Identification of Organic Compounds**. New York: John Wiley & Sons,2005.

SIPS, R. The Structure of a Catalyst Surface. **J. Chem. Phys.**, v. 16, p. 490–495, 1948.

TAN, K. B.et al. Adsorption of dyes by nanomaterials: Recent developments and adsorption mechanisms. **Sep. Purif. Technol.**, v. 150, p. 229–242, 2015.

THOMMES, M.et al. Physisorption of gases, with special reference to the evaluation of surface area and pore size distribution (IUPAC Technical Report). **Pure Appl. Chem.**, v. 87, p. 1051-1069, 2015.

TRAN, H. N. et al. Mistakes and inconsistences regarding adsorption of contaminants from aqueous solutions: A critical review. **Water Res.**, v. 120, p. 88–116, 2017.

YAGUB, M. T. et al. Dye and its removal from aqueous solution by adsorption: a review. **Adv. Colloid Interface. Sci.**, v. 209, p. 172–184, 2014.

WANG, J. et al. Enzymatic construction of antibacterial ultrathin membranes for dyes removal. **Chem. Eng. J.**, v. 323, p. 56–63, 2017.

WU, F. C.et al. Characteristics of pseudo–second–order kinetic model for liquid–phase adsorption: A mini–review. **Chem. Eng. J.**, v. 151, p. 1–9,2009.

WAN NGAH, W. S. et al. Adsorption of dyes and heavy metal ions by chitosan composites: A review. **Carbohyd. Polym.**, v. 83, p. 1446–1456, 2011.

Zeng, J.et al. Chitin whiskers: An overview. **Biomacromolecules**, v. 13, p. 1–11,2012.

3.2 ARTIGO 2

Chitin-psyllium based aerogel for the efficient removal of crystal violet from aqueous solutions

Susanne Pedroso Druzian[1], Natalia Pollon Zanatta[1], Renata König Borchardt[1], Letícia Nascimento Côrtes[1], Angélica Fátima Mantelli Streit[1], Eric da Cruz Severo[1], Janaína Oliveira Gonçalvez[1], Edson Luiz Foletto[1], Éder Cláudio Lima[2], Guilherme Luiz Dotto[1]

[1]Chemical Engineering Department, Federal University of Santa Maria, UFSM, Roraima Avenue, 1000, 97105–900, Santa Maria, RS, Brazil.
[2]Institute of Chemistry, Federal University of Rio Grande do Sul, UFRGS, Av. Bento Gonçalves 9500, 91501-970, Porto Alegre, RS, Brazil.

Abstract A new alternative aerogel was prepared from low-cost chitin and psyllium biopolymers to adsorb crystal violet (CV) dye from liquid media and possibly treat effluents containing other dyes. The aerogel was characterized by X-ray diffraction (XRD), Fourier-transform infrared spectroscopy (FTIR), and scanning electron microscopy (SEM), which demonstrated that aerogel has a typical structure of amorphous materials and presented a randomly interconnected porous structure that resembles an open pore network. 2.5 g L^{-1} of aerogel was able to remove 86.00% of CV from solutions, and the natural pH of the CV solution was considered the more adequate for adsorption. The pseudo-second-order (PSO) model satisfactorily described the adsorption kinetics, and the Freundlich model was suitable to represent the adsorption equilibrium. The experimental maximum capacity achieved was 227.11 mg g^{-1}, which indicates that aerogel is very efficient and competitive with several adsorbents. Tests using a simulated effluent showed that aerogel has excellent potential to treat real colored effluents.

Keywords: aerogel; chitin; psyllium; crystal violet; adsorption.

3.2.1 Introduction

Water is an essential element for life and human activities. This resource is limited, and it is threatened mainly by unsustainable consumption in agriculture and industry (AZIZULLAH et al., 2011). According to Mekonnen e Hoekstra, there are temporal and spatial variations in freshwater availability globally. Around two-thirds of the global population already faces severe water scarcity conditions at some time of the year

(MEKONNEN&HOEKSTRA, 2016). It is estimated that in 2050, without new ambitious policies on water resource management, the growth of 55% in global water demand could increase pollution and depletion of groundwater, eutrophication, damage to aquatic biodiversity, and the number of people living under severe water stress (OECD, 2009). Industrial activity is one of the leading causes of these problems due to the great demand for water and the extensive use of toxic chemicals in its production process (CHOUDHARY et al., 2020; TOUNSADI et al., 2020).

The textile industry is classified as one of the most problematic industrial sectors because, in addition to being one of the largest consumers of freshwater, they use a wide variety of chemicals in their production process (TOUNSADI et al., 2020). This type of industry's effluents contains various organic and inorganic pollutants, such as heavy metals, detergents, pigments, and dyes, which can bioaccumulate, persist, and cause more toxic by-products (MATHEW et al., 2019; HUSSAIN et al., 2018). Crystal violet - a triphenylmethane dye - is a water-soluble, recalcitrant, toxic organic molecule that causes serious environmental pollution problems (CHERUIYOT et al., 2019; PATIL et al., 2020). Its presence in water bodies directly affects the aquatic ecosystem and human life. It results in low light penetration that harms the photosynthetic activities and, in extreme cases, can cause permanent blindness and kidney and respiratory failure in humans (MOHANTY et al., 2006; ALI & MUHAMMAD, 2008; MIRZA & AHMAD, 2020). Despite that, crystal violet is widely used as a coloring agent by several industrial sectors, mainly by the textile industry. It is used for the coloring of nylon, wool, silk, and cotton (OLOO et al., 2020). Therefore, removing crystal violet from industrial effluents before discharge in aquatic systems is extremely important to avoid water resource depletion (GOPI et al., 2016; FABRYANTY et al., 2017, ABBASI et al., 2019).

The conventional effluent treatments, such as biological treatment, show significant results in removing organic materials; however, they are not as efficient in discoloration of effluents due to the high stability and resistance of dyes to microbiological degradation (BUSCIO et al., 2019).In the last few decades, there has been an effort by the global scientific community to the development of new technologies that contribute to the decontamination, management, and reuse of water (DOTTO & McKAY, 2020). Several processes can treat wastewater containing dye - such as physical, chemical, and biological (Al-MAMUNA et al., 2019; MATHEW et al., 2019). Oxidation processes are the chemical processes most used for the degradation of dyes due to their easy application and ability to degrade molecules; however, sludge formation can present itself as a relevant disadvantage (HOLKAR et al.,

2016). Among physical processes, adsorption stands out as a highly competent technology for the purification and recycling of water containing dyes (MATHEW et al., 2019). Advantages such as high efficiency, low cost, ease of implementation, and operation make this operation highly demanded in treating colored effluents. However, the main point for configuring an adsorption process for water treatment is the choice, development, and characterization of the adsorbent material, which must have, among other characteristics, high adsorption capacity and fast kinetics (DOTTO& McKAY, 2020).

Chitin is a low-cost, available, biodegradable polysaccharide used as an adsorbent in the last years (AHMED et al., 2020; FRANCO et al., 2020). Despite these advantages, chitin has poor textural features, and some researchers have been performed to improve it (YAZIDI et al., 2020; GHOURBANPOUR et al., 2019; LI et al., 2019; HOU et al., 2019). An alternative is the preparation of aerogels. Aerogels have excellent physical properties such as extremely low density, which can approach $1.2x10^{-4}$ g cm^{-3}, and a high specific surface area, exceeding 1000 m^2 g^{-1}(ZHAO et al., 2018). They were produced for the first time in 1931 through supercritical drying of hydrogels. Since then, they have been produced from various precursor materials and used in the most diverse applications, including adsorption (KISTLER, 1931; ZAMAN et al., 2020; TIAN et al., 2019).

Based on this context, aerogels obtained from chitin and psyllium were prepared by lyophilization to study the removal of crystal violet dye from aqueous solutions. XRD, FTIR, and SEM analytical techniques were used to characterize the obtained aerogel. The adsorbent potential of the aerogel was investigated by studying the effect of the adsorbent dosage and the effect of the solution's initial pH. The models of pseudo-first-order, pseudo-second-order, general-order, and Avrami were used to describe adsorption's kinetic profile. The adsorption isotherms were determined at three different temperatures and evaluated using the Langmuir, Freundlich, and Sips models. In general, the results obtained from the experimental data analysis allow attributing new ideas in the treatment of colored waters using natural polymers.

3.2.2 Material and methods

3.2.2.1 Reagents

Psyllium husks were acquired from a local market in Santa Maria – RS (Santa Maria – RS, Brazil).The analytical grade Crystal violet dye (color index 42,555, molar weight 407.98 g mol^{-1}, purity 99.0%, and λ_{max} 584 nm)was obtained from INLAB (Brazil). The structural formula of crystal violet dye is depicted in Fig. 1.Shrimp (*Penaeus brasiliensis*) wastes were

donated from a fishing industry located on the south coast of Brazil and stored in a freezer at -18°C.The other chemical reagents and solvents used to develop the experiments had an analytical degree and were acquired from Sigma-Aldrich and VETEC.

Figure 1 – a) Structural formula of crystal violet dye; pKa values indicated in the figure; b) Optimized three-dimensional structural formula of crystal violet. The dimension of the chemical molecule was calculated using MarvinSketch version 20.20. Molecular weight 407.213 g mol^{-1}; Van der Waals surface area 585.94 $Å^2$ (pH 7.0); Polar surface area 9.49 $Å^2$ (pH 7.0), Van der Waals volume 45.63 $Å^3$; Dipole moment 5.65 Debye; polarizability 45.64 $Å^3$, Hydrophilic-lipophilic balance 1.00.

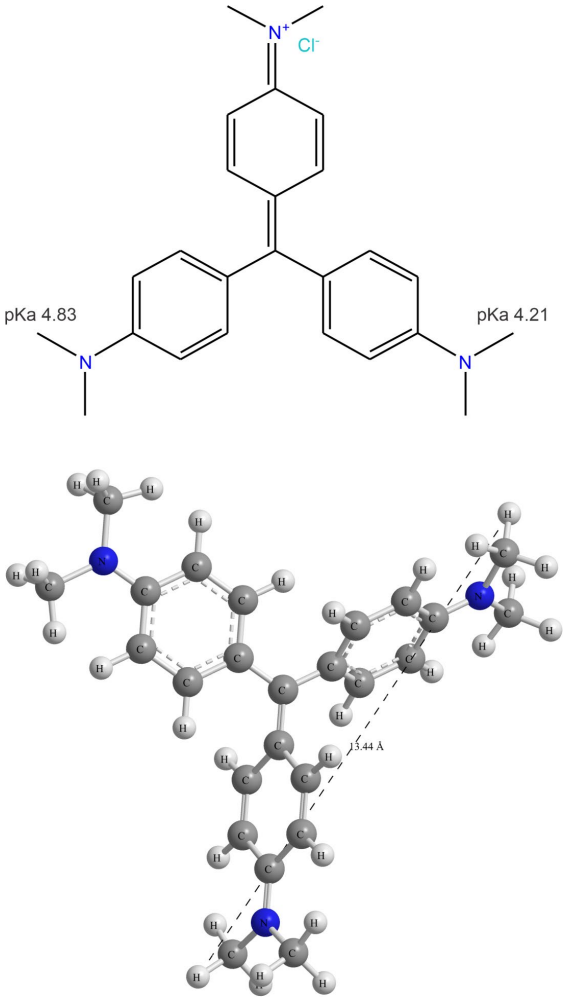

3.2.2.2 Chitin obtainment

The chitin used to prepare the aerogel was obtained from shrimp wastes using the methodology proposed by Dotto et al. (DOTTO et al., 2013a). Shrimp shells were subjected to demineralization, deproteinization, and deodorization to reduce ash content, protein

nitrogen content, and material odor, respectively. The material obtained was dried in an oven, ground, and sieved to obtain particles between 425 and 850 μm in size.

3.2.2.3 Aerogel preparation

Fig. 2 presents the scheme of the development of the aerogel. First, the gel was obtained by mixing chitin and psyllium in deionized water in a proportion of 1g: 5g: 300mL, respectively. A 1 mL aliquot of glutaraldehyde for every 50 mL of deionized water was added to the mixture as a crosslinking agent. The mixture was kept for 30 min under vigorous stirring and was heated to 50°C using a magnetic stirrer with coupled heating. After gel formation, it was cooled to room temperature (20°C), transferred to Petri dishes, and frozen in an ultra-low temperature freezer (FV-500, Eppendorf New Brunswick, Canada) for 48 h. The gel was subjected to freeze-drying at -55°C and under vacuum for 48 h, using a freeze dryer (L 101, Liotop, Brazil), coupled to a vacuum pump. The aerogel obtained was cut into small fillets of approximately 1 cm^2 and stored at room temperature in a closed plastic package protected from light. This procedure was developed for our research group based on several experimental tests.

Figure 2 – Scheme for development of the aerogel.

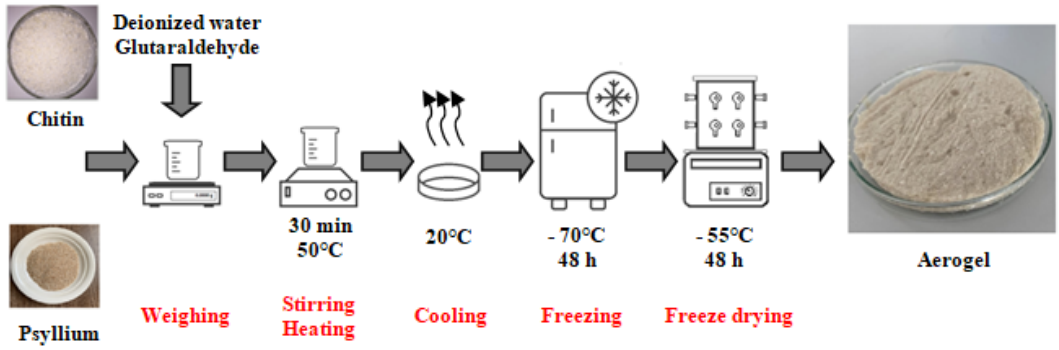

3.2.2.4 Characterization of chitin and aerogel

Chitin and aerogel were characterized by FT-IR (Shimadzu, Prestige 21, Japan), XRD (Rikagu, Miniflex 300, Japan), and SEM (JEOL, JSM-6060, Japan). FT-IR was used to verify the functional groups present in the materials in a wavelength range from 4500 to 450 cm^{-1}, and the sample preparation was done using the KBr pastille technique. The XRD patterns were evaluated using a diffractometer equipped with Ni-filtered copper radiation (Cu-Kαλ=1.54051 Å – 10 mA and 30 kV) to obtain information about the crystallographic

structure of chitin and aerogel. SEM images were obtained to observe the samples' morphological and textural aspects using a scanning electron microscope.

3.2.2.5 Adsorption assays

All adsorption assays were carried out in batch mode using Erlenmeyer flasks coupled to a thermostatic shaker (Marconi, MA 093, Brazil). Crystal violet solutions were prepared by diluting a stock solution of 1 g L^{-1} in deionized water. The adsorbent dosage effect on removing the crystal violet dye from the aqueous solution was evaluated under conditions of a temperature of 298 K and a rotational speed of 150 rpm. The chitin and aerogel dosages evaluated were 1.25, 2.5 and 5.0 g L^{-1}, and each test lasted 2 h. The pH and initial concentration of the dye solutions used were 8 and 25 mg L^{-1}, respectively. The violet crystal solution's pH effect on its removal was evaluated at 298 K and under 150 rpm for 2 h and using a 2.5 g L^{-1} aerogel dosage. The initial pH of the solution ranged from 2.0 to 10.0. Solutions of 0.1 mol L^{-1} of NaOH and HCl were used to adjust the pH solution before the beginning of the tests. Kinetic curves were constructed for the initial CV concentrations of 25, 50, 100, 150, and 200 mg L^{-1}. The tests were performed at 298 K, under 150 rpm, and pH 8, and the times in which the samples were collected were 5 to 180 min. Finally, equilibrium curves were constructed with initial CV concentrations of 25 to 1000 g L^{-1} at 298, 308, and 318 K after 180 min. The initial pH of the solutions was 8, and the samples' agitation speed was 150 rpm.

The CV concentration in the solutions was estimated using a spectrophotometer (Biospectro, SP-22, Brazil) and using a spectrophotometric method at the maximum absorption wavelength (584 nm). The separation of the remaining solution from the solid phase was performed by centrifugation using a centrifuge (Centribio, 80-2B, Brazil) at 4000 rpm for 15 min. All tests were performed in triplicate and with blank control to guarantee the reliability of the experimental data. The adsorption capacity at time t (q_t, mg g^{-1}) (FRANTZ et al., 2017), the adsorption capacity at equilibrium (q_e, mg g^{-1}) (DOTTO et al., 2016), and the percentage of CV removal (R,%) (CADAVAL et al., 2015) were determined from equations 1, 2 and 3, respectively, presented in Table 1.

Table 1 –The adsorption capacity at time "t," adsorption capacity at equilibrium, and percentage of CV removal equations.

Name	Equation		Parameters
Adsorption capacity at time "t"(q_t, mg g^{-1})	$q_t = \frac{V(C_0 - C_t)}{m}$	(1)	V (L) volume of solution; C_0 (mg L^{-1}) initial CV concentration in liquid phase; C_t (mg L^{-1}) the CV concentration in liquid phase at time "t"; m (g) adsorbent amount.
Adsorption capacity at equilibrium (q_e, mg g^{-1})	$q_e = \frac{V(C_0 - C_e)}{m}$	(2)	V (L) volume of solution; C_0 (mg L^{-1}) initial CV concentration in liquid phase; C_e (mg L^{-1}) the equilibrium CV concentration in liquid phase; m (g) adsorbent amount.
Percentage of CV removal (R,%)	$R = \frac{V(C_0 - C_t)}{C_0}100$	(3)	V (L) volume of solution; C_0 (mg L^{-1}) initial CV concentration in liquid phase; C_t (mg L^{-1}) the CV concentration in liquid phase at time "t";

3.2.2.6 Kinetic and equilibrium of CV adsorption on the Chitin-psyllium based aerogel

The kinetic model equations and parameters to estimate each model are presented in Table 2 (QIU et al., 2009; WU et al., 2009; ALENCAR et al., 2012; LOPES et al.; 2003). Table 3 presents the isotherm equations and parameters estimated for each equilibrium model (LANGMUIR, 1918; FREUNDLICH, 1906; SIPS, 1948).

Nonlinear regression of the experimental data was used to estimate the kinetic and equilibrium parameters, based on the minimization of the least square function and using the Gauss-Newton method on Statistic 10.0 software (Statsoft, EUA). The coefficient of determination (R^2), the adjusted coefficient of determination (R^2_{adj}), the sum of square error (SSE),the average relative error (ARE), and Akaike's information criterion (AIC) were used to evaluate the fit quality (DOTTO et al., 2013b; BONILLA-PETRICIOLET et al., 2017).

Table 2 – Equation and parameters to be estimated of PFO, PSO, PnO, and Avrami models.

Model	Equation		Parameters
PFO	$q_t = q_1\left(1 - exp(-k_1 t)\right)$	(4)	q_1(mg g^{-1}) theoretical value for adsorption capacity; k_1 (min^{-1}) rate constant of the PFO model.
PSO	$q_t = \frac{t}{\left(\frac{1}{k_2 q_2^2}\right) + \left(\frac{t}{q_2}\right)}$	(5)	q_2 (mg g^{-1}) theoretical value for adsorption capacity; k_2 (g mg^{-1} min^{-1}) rate constant of the PSO model.
PnO	$q_t = q_n - \frac{q_n}{[k_n (q_n)^{n-1} t(n-1) + 1]^{\frac{1}{n-1}}}$	(6)	q_n (mg g^{-1}) theoretical values for adsorption capacity; k_n (min^{-1}(g mg^{-1})$^{n-1}$) rate constant of PnO model; n the reaction order.
Avrami	$q_t = q_{AV}\{1 - exp[-(k_{AV} t)]^{n_{AV}}\}$	(7)	q_{AV} (mg g^{-1}) theoretical values for adsorption capacity; k_{AV} (min^{-1}) the Avrami kinetic constant; n_{AV} constant related to adsorption mechanism.

3.2.2.7 Treatment of simulated textile effluent

The aerogel was used to treat a simulated textile effluent to verify its effectiveness in treating colored solutions closer to the real conditions. Table 4 presents the chemical composition of the simulated textile effluent, according to Côrtes et al.(CÔRTES et al., 2019). The adsorption tests using simulated effluent were carried out at the room temperature and natural pH of the dyes and inorganic compounds solution. The simulated textile effluent treatment lasted 60 min and the aerogel dosage used was 5 g L^{-1}. A spectrophotometer (Biospectro, SP-22, Brazil) was utilized to scanning the untreated simulated effluent and the simulated effluent treated with aerogel. The samples were scanned from 700 to 400 nm, and the percentage of color removed was related to the ratio between the areas under the spectral curves (LIMA et al., 2017; GEORGIN et al., 2018).

Table 3 –Equation and parameters to be estimated of Langmuir, Freundlich, Sips, and Hill models.

Model	Equation		Parameters
Langmuir	$q_e = \frac{q_m k_L C_e}{1 + k_L C_e}$	(8)	q_m (mg g^{-1}) the maximum adsorption capacity of Langmuir model; k_L (L mg^{-1}) the Langmuir constant.
Freundlich	$q_e = k_F C_e^{\frac{1}{n_F}}$	(9)	k_F ((mg g^{-1})(mg L^{-1})$^{-1/nF}$) the Freundlich constant. $1/n_F$ heterogeneity factor
Sips	$q_e = \frac{q_{mS}(k_S C_e)^{mS}}{1 + (k_S C_e)^{mS}}$	(10)	q_{mS} (mg g^{-1}) the maximum adsorption capacity of Sips model; k_S(L mg^{-1}) the Sips constant; mS the fractional exponent.

Table 4 – Chemical composition of the simulated textile effluent.

Dyes and inorganic compounds	Concentration (mg L^{-1})	λ_{max} (nm)
Crystal violet	50	584
Methylene blue	10	664
Alizarin cyanin green	50	644
Sodium chloride (NaCl)	100	-
Sodium bicarbonate ($NaHCO_3$)	50	-

3.2.3 Results and discussions

3.2.3.1 Characteristics of chitin and aerogel

XRD, FTIR, and SEM analytical techniques were used to characterize the chitin and aerogel. The XRD patterns give us information about chitin and aerogel's crystallographic structure, shown in Fig. 3.

Figure 3 –XRD patterns of chitin and aerogel.

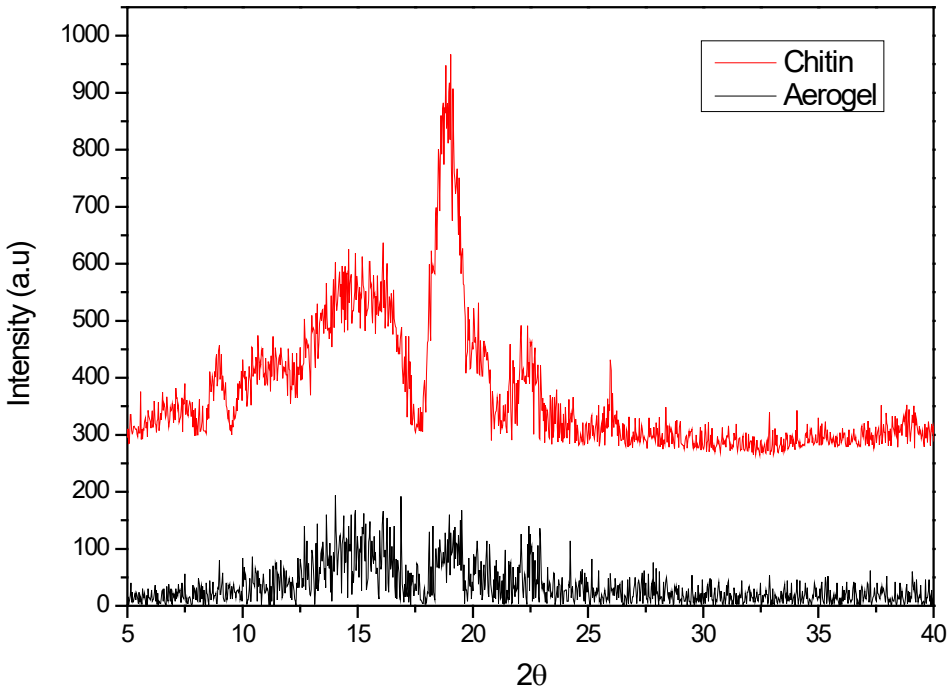

Chitin presented diffraction peaks near 9° and 20° related to the shrimp's orthorhombic crystal structure (Al–SAGHEER et al, 2009; DOTTO et al., 2015a). On the other hand, aerogel presented a profile typical of amorphous materials, which indicates that the aerogel has an amorphous structure, probably due to the material's uncontrolled growth. For dyes adsorption, an amorphous structure is more suitable and desirable since this type of structure facilitates dye-binding (PERES et al., 2018a; DOTTO et al., 2015b).

FT-IR was used to determine the main functional groups present in the structure of chitin, aerogel, and aerogel after CV adsorption. The FTIR spectra for these organic materials can be seen in Fig. 4.

In Fig 4a, it is presented the vibrational bands of chitin. There is a broadband 3100-3500 cm^{-1} assigned to OH of alcohols presented in the chitin, mixed with the N-H band stretching of the amide (HU et al., 2018). The band centered in 3450 cm^{-1} is the stretching of the O-H bond, and the two bands at 3267 and 3108 are due to the N-H stretching (DOTTO et al., 2015b). The bands at 2962, 2932 cm^{-1} are asymmetric C-H stretching (NANDIYANTO et al., 2019), and 2889 cm^{-1} is due to symmetric C-H stretch (SEMWAL & RAMANDEEP, 2014). The two bands at 1660 and 1628 are due to the C=O stretch of amide group (NANDIYANTO et al., 2019) present in the chitin structure. The band at 1560 cm^{-1} should be attributed to NH_2 bending (scissors) and NH bending in the plane (KUMIRSKA et al., 2010).

The bands at 1419 and 1379 cm^{-1} are assigned to the C-N stretch (IBITOYE et al., 2018). The vibrational bands at 1316 and 1260 cm^{-1} are assigned to C-C-O stretching of chitin's glycosidic ring (SILVERSTEIN et al., 2005; SABNIS & BLOCK, 1997; PEREIRA et al., 2014). The bands at 1158, 1074, and 1026 cm^{-1} are assigned to O-C-C stretching of the glycosidic ring (NANDIYANTO et al., 2019; Tan et al., 2020). The band at 896 cm^{-1} is due to the out-of-plain bend of the NH_2 group (KUMAR & RAI, 2010).

Figure 4 – FT-IR vibrational spectra of chitin, aerogel and aerogel after adsorption.

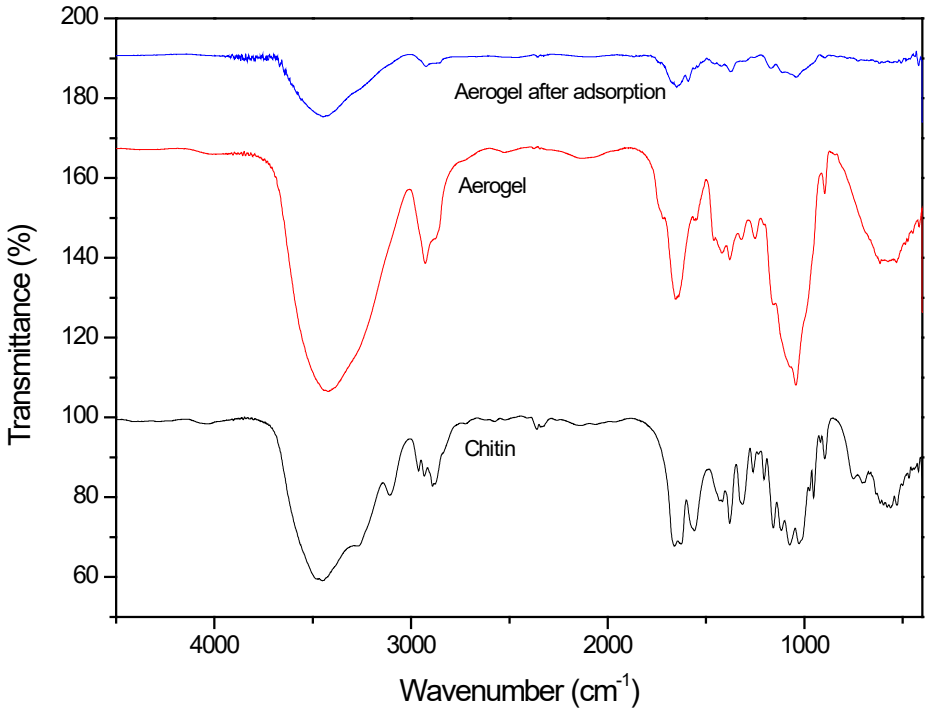

In Fig. 4b, the aerogel formed by chitin and the lignocellulosic fiber (psyllium) will present a mixture of bands of chitin and lignocellulosic materials. The bands of NH in the region of 3267 and 3108 cm^{-1} are overlapped with the OH groups of lignocellulosic fiber, appearing as broadband at 3422 cm^{-1} that is typical of O-H stretching of lignocellulosic materials (KUMAR et al., 2019). The bands at 2928 and 2873 cm^{-1} are due to asymmetric and symmetric C-H stretch. At 1649 cm^{-1} is the C=O band of the chitin that practically is the same chitin value (see Fig.4a). The vibrational band at 1548 and 1419 cm^{-1} could be assigned to the modes of the aromatic ring of lignocellulosic material that suffered an overlap with bands of C-N stretching and N-H bending of chitin. At 1370 cm^{-1}, the band is assigned to the C-N stretch of chitin, which suffered a small shift compared with the pure chitin (Fig.4a). The

vibrational band at 1320 and 1250 $cm^{-1}$are assigned to C-C-O stretching of chitin's glycosidic ring as well as the lignocellulose matrix. The bands at 1161 and 1043 cm^{-1} are assigned to O-C-C stretching of the glycosidic ring and lignocellulosic matrix. At 897 cm^{-1} is due to the out-of-plain bend of the NH_2 group and bending of the C-H group of the aromatic ring.

The analysis of Figs. 4a and 4b show that the aerogel formed (Fig. 4b) is a material with some chemical composition of chitin and lignocellulosic material, where the FTIR bands suffered small shift and overlap.

Fig. 4c shows the vibrational FTIR spectra of aerogel after the adsorption of the dye CV. The most significant change in the spectra is the OH band of the adsorbent before the adsorption (3422 cm^{-1}) to after the adsorption (3443 cm^{-1}). Considering the FTIR spectrophotometer's resolution of 4 cm^{-1}, any band shift < 12 cm^{-1} is within the instrumental error. Other significant band shift occurred at 2857 cm^{-1} after adsorption compared to 2873 cm^{-1} before adsorption. This band corresponds to the symmetric C-H stretching. The shoulder at 1590 cm^{-1} that appears in Fig. 4c should be a band shift from the C=O group after the CV's adsorption onto the aerogel surface. Another significant band shift that occurred in the aerogel after the adsorption is the band at 1161 cm^{-1} (before the adsorption) shift to 1110 cm^{-1}. This band is assigned to O-C-C bands. Based on FTIR results, it is possible to infer that the OH groups, and probably N-H groups (that were overlapped) at basic conditions (see further experiments of adsorption), should present a negative charge that would electrostatically attract the positively charged CV dye. Some hydrophobic interactions such as van der Waals attraction should also occur, explaining the C-H band's band shift.

The SEM images of chitin (a,b) and aerogel (c,d) are shown in Fig. 5. It is possible to observe in Fig. 5 (a,b) that chitin has a highly compacted and relatively smooth surface. There are no visible holes, cavities or protuberances on its surface, even at a magnification of 2000 times. Grooves, cavities and protuberances are interesting for adsorption as they allow the solvent passage through the adsorbent, reflecting an increase in the adsorption capacity (SOLTANI et al., 2015; LATA & SAMADDER, 2014; DOTTO et al., 2015b). On the other hand, aerogel (Fig. 5(c,d)) presented randomly interconnected holes, with grooves and cavities. Due to the uncontrolled growth of ice crystals during freezing, the aerogel has a structure that resembles an open channels network, with pores of non-uniform sizes (ZAMAN et al., 2019). These morphological characteristics contribute to an increase in the sorption capacity of the adsorbent.

Figure 5 –SEM images of chitin and aerogel: **a** Chitin × 100, **b** Chitin × 2000, **c** Aerogel × 100, **d** Aerogel × 1000.

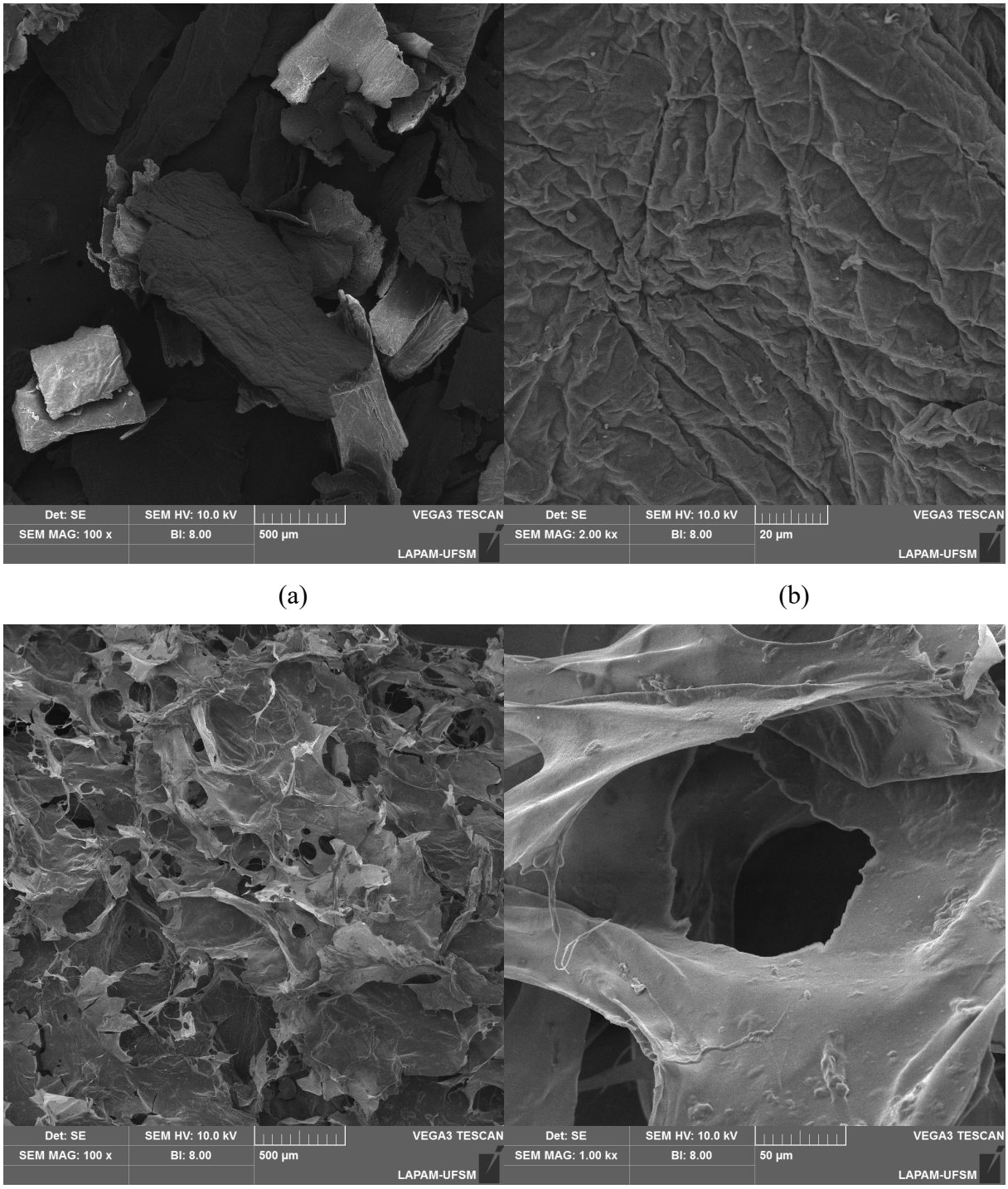

3.2.3.2 Adsorbent dosage effect on CV adsorption by the aerogel

The dosage effect of chitin and aerogel on the adsorption of CV dye is presented in Fig. 6.

Figure 6 –Adsorbent dosage effect on CV adsorption by aerogel.

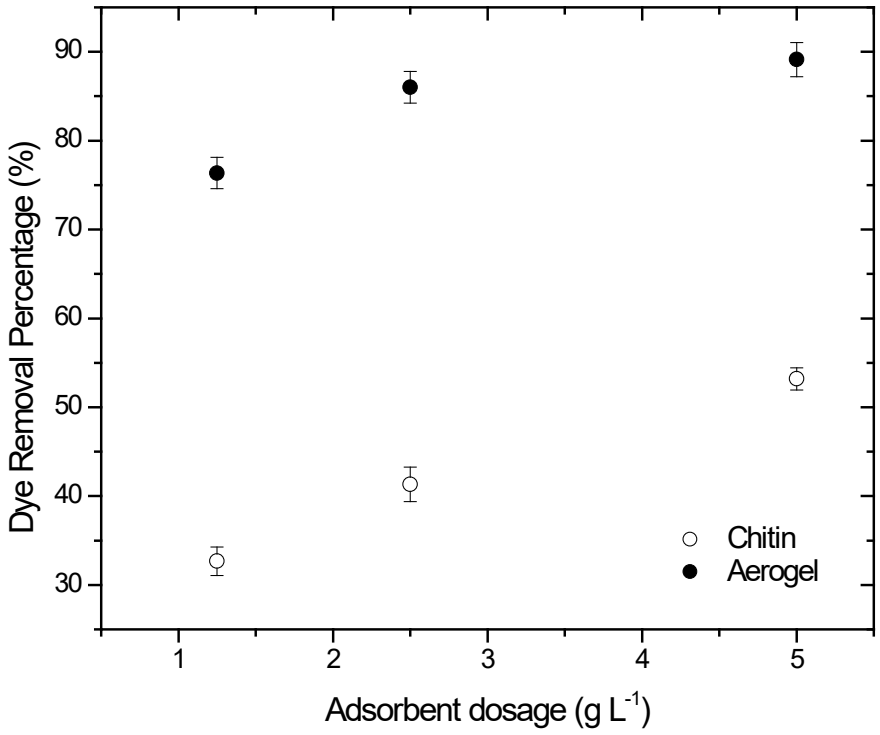

The chitin and aerogel dosages evaluated were1.25, 2.5, and 5 g L^{-1}, and the values of dye removal percentage obtained ranged from approximately 33-53% for chitin and 76-89% for aerogel. As expected, an increase in adsorbent dosage increases CV removal from the aqueous solution for both materials. This increase occurs because, at higher chitin and aerogel dosages, a higher amount of adsorption sites are available to retain CV dye molecules presented in liquid medium (DRUZIAN et al., 2019; PAVAN et al., 2014). When aerogel was used as an adsorbent material, the dye removal percentage values were higher than using chitin, regardless of the adsorbent's dosage. From this, it can be determined that, under the conditions studied, aerogel is more suitable to attain greater efficiencies in removing CV from aqueous solutions than chitin. The dye removal percentage values obtained using 1.25, 2.5, and 5 g L^{-1} of aerogel were 76.36, 86.00, and 89.12%. It was observed that by doubling the aerogel dosage values from 1.25 to 2.5, an increase of 12.62% was obtained in the dye removal percentage. However, the same for chitin resulted in an increase of only 3.63% in dye removal percentage. Therefore, the dosage considered most suitable for the continuity of CV adsorption in aerogel tests was 2.5 g L^{-1}.

3.2.3.3 pH effect

The initial pH of liquid medium effect on CV adsorption using aerogel as adsorbent is depicted in Fig. 7.

Figure 7 – pH effect on CV adsorption by aerogel.

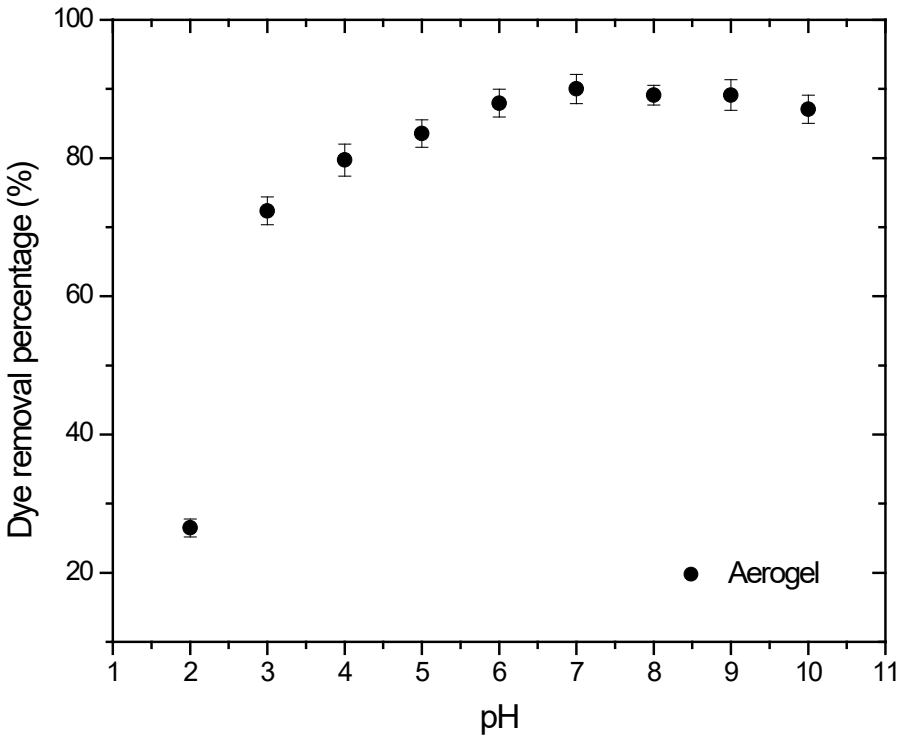

The pH effect was investigated, in terms of the dye removal percentage, covering the range of 2.0 to 10.0, encompassing the pH range of real effluents containing dyes (5.5 to 8.5) and severe conditions (HESSEL et al., 2007). It can be observed that the increase in pH from 2 to 10 caused a significant increase in dye removal percentage from approximately 26 to 87%, reaching a maximum value of 90% (pH 7). This behavior can be explained by the fact that there is a competition between the H^+ ions and the CV cationic dye ions under acidic conditions. Under low pH conditions, the H^+ ions occupy the available sites in the adsorbent that should retain the dye molecules, which leads to low removal percentage values. As the medium's pH increases, the competition between these ions decreases, which increases the removal of dye molecules from the liquid medium (PERES et al., 2018b, BRIÃO et al., 2017). Under conditions of neutrality and alkalinity of the pH range evaluated, it can be observed that there were no significant differences in the values of the percentage of dye

removal. Therefore, the subsequent adsorption tests were performed at pH 8, which corresponds to the CV dye solution's original pH in water.

3.2.3.4 Kinetic studies

The kinetic curves for CV adsorption on aerogel are presented in Fig. 8.

Figure 8 – Kinetic curves for CV adsorption on aerogel.

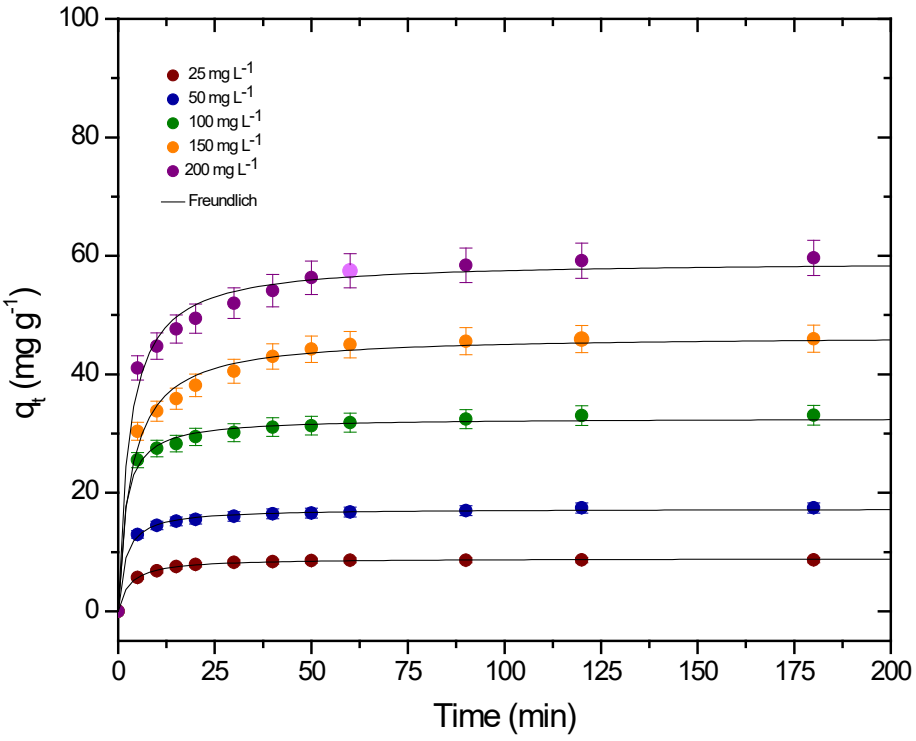

The adsorption kinetics of CV with initial concentrations of 25, 50, 100, 150, and 200 mg L^{-1} were performed under 150 rpm and 298 K, using contact times from 0 to 180 min. According to previous tests, the conditions of adsorbent dosage and pH of the liquid medium were established (2.5 g L^{-1} and 8). It can be seen that typical kinetic curves were obtained (Fig. 8), observing the CV molecules that were gradually occupying the adsorption sites in the aerogel until the equilibrium was established. In the first 5 min, there was a high adsorption rate. After the first 5 min, the adsorption rate gradually decreases over time, until equilibrium is reached at around 180 min for all studied concentrations.

Pseudo-first-order, pseudo-second-order, pseudo-n order, and Avrami models were investigated to represent the kinetic data. The kinetic parameters estimated using each model, followed by the model fit's quality measures, are shown in Table 5.

Table 5 –Kinetic parameters for CV adsorption on aerogel.

Kinetic model	Initial dye concentration (mg L^{-1})				
	25	**50**	**100**	**150**	**200**
Pseudo-first order					
q_1 (mg g^{-1})	8,43	16,50	31,14	43,49	55,42
k_1 (min^{-1})	0,1882	0,2708	0,2984	0,1714	0,2044
R^2	0,9933	0,9889	0,9857	0,9742	0,9734
R^2_{adj}	0,9926	0,9878	0,9842	0,9716	0,9707
ARE	0,23	0,05	0,14	0,24	0,02
SSE	0,90	5,59	25,70	93,00	154,61
AIC	-22,07	-1,95	14,84	28,98	34,57
Pseudo-second order					
q_2 (mg g^{-1})	8,93	17,30	32,62	46,57	59,14
k_2 (g mg^{-1} min^{-1})	0,0391	0,0311	0,0182	0,0063	0,0059
R^2	0,9995	0,9987	0,9972	0,9948	0,9941
R^2_{adj}	0,9994	0,9986	0,9969	0,9942	0,9936
ARE	0,02	0,01	0,01	0,06	0,03
SSE	0,07	0,65	5,12	19,04	34,43
AIC	-49,98	-25,57	-2,91	11,54	18,05
Pseudo-n order					
q_n (mg g^{-1})	8,80	16,28	37,33	53,81	69,10
k_n(min^{-1}(g mg^{-1})$^{n-1}$)	0,05557	13,97629	0,00002	0,00001	0,000001
n	1,79	7,53	4,24	3,63	3,90
R^2	0,9996	0,9653	0,9998	0,9976	0,9986
R^2_{adj}	0,9996	0,9618	0,9997	0,9974	0,9985
ARE	0,01	0,71	0,45	4,99	16,18
SSE	0,05	17,27	0,66	53,67	796,83
					(conclusão)
AIC	-50,32	14,39	-21,53	26,86	56,54
Avrami					

q_{AV} (mg g^{-1})	8,43	16,50	31,14	43,49	55,42
k_{AV} (min^{-1})	0,0137	0,0005	0,0005	0,0004	0,0005
n_{AV}	13,72	520,38	546,19	413,89	452,03
R^2	0,9933	0,9889	0,9857	0,9742	0,9734
R^2_{adj}	0,9926	0,9878	0,9842	0,9716	0,9707
ARE	0,23	0,05	0,14	0,24	0,02
SSE	0,90	5,59	25,70	93,00	154,61
AIC	-18,14	1,98	18,76	32,91	38,50
q_e (mg g^{-1})	8,65	17,45	33,08	46,00	59,65

Values higher than 0.99 for the coefficient of determination (R^2>0.99) and adjusted coefficient of determination (R_{adj}^2), and low values of average relative error, the sum of square error and Akaike's information criterion indicates that the Pseudo-second-order model satisfactorily described the adsorption process and was considered the more adequate to represent CV adsorption on aerogel. The PSO model's theoretical values for adsorption capacity increased from 8.93 to 59.14 mg g^{-1} with the CV concentration increase (25-200 mg L^{-1}) and were very close to the experimental adsorption capacity values, with indicates a good fit of the model.

3.2.3.5 Equilibrium studies

The equilibrium adsorption isotherms of CV using chitin-psyllium based aerogel are presented in Fig. 9.

The isotherms were obtained at different temperatures (298, 308, and 318 K) with CV concentration ranging from 0 to 1000 mg L^{-1}, aerogel dosage of 2.5 g L^{-1}, 150 rpm, and pH 8. Fig. 9 shows that the temperature decrease favored adsorption. At 298 K, high values of adsorption capacity were verified. However, at 308 and 318 K, the adsorption capacity values were close to zero, which indicates that the adsorption of the CV dye in the aerogel did not occur.

According to the isotherm classification system and due to the initial slope, the adsorption isotherm at 298 K can be a Langmuir type curve ("L" curve). Based on the upper part of the curve's shapes, this curve can also be classified as a typical "L_1" isotherm (GILES et al., 1960). The adsorption capacity at equilibrium tends to increase progressively with the increase of equilibrium concentration, but the plateau was not attained, which indicates that the aerogel contains empty adsorption sites (DOTTO et al., 2015b; PERES et al., 2018a).

Figure 9 –Equilibrium curves for CV adsorption on aerogel.

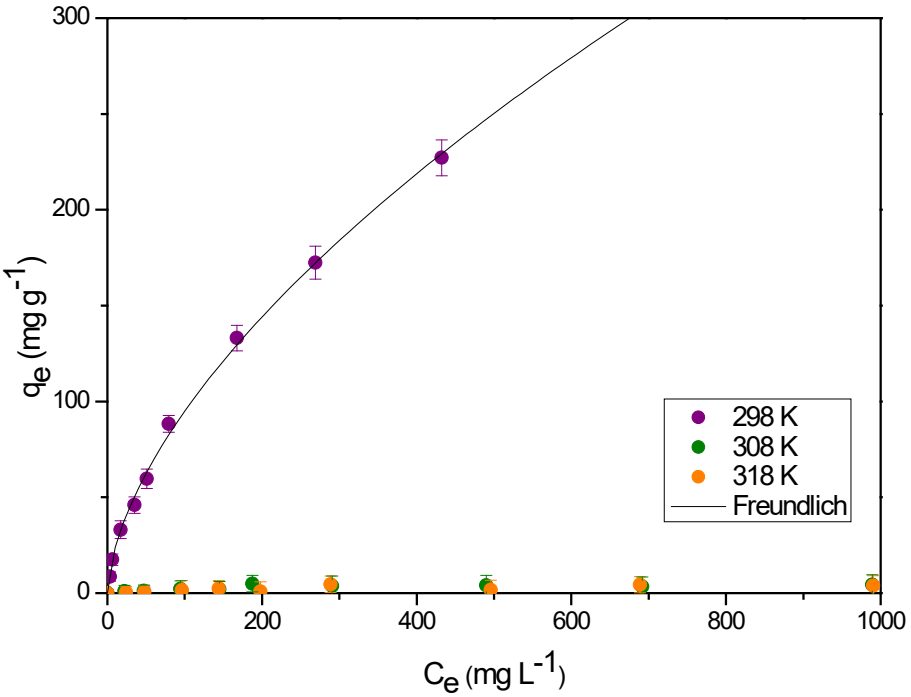

Based on the isotherm curve's shape, the equilibrium curve of CV adsorption on aerogel was represented by Langmuir, Freundlich, and Sips models. The estimated parameters of each model are shown in Table 6.

Based on the high values of coefficient of determination (R^2>0.99), adjusted coefficient of determination (R^2_{adj}>0.99) and on the low values of average relative error (<ARE), the sum of squares (<SSE) and Akaike's information criterion (<AIC), it can be affirmed the Freundlich model was suitable to represent the CV adsorption onto chitin-psyllium based aerogel.

The experimental maximum adsorption capacity of CV onto aerogel was 227.11 mg g^{-1}, and this parameter was used to compare the efficiency of aerogel with several other adsorbents used to remove crystal violet from aqueous solutions. Table 4 shows the maximum adsorption capacity of several adsorbents materials from literature. It can be stated that aerogel is very efficient and competitive with several adsorbents in remove CV from aqueous solutions, in terms of adsorption capacity, comparing the aerogel with the other adsorbents from Table 7.

Table 6 – Isotherm parameters for CV adsorption on aerogel.

Equilibrium models	Temperature (K)
	298
Langmuir	
q_m (mg g^{-1})	343.12
k_L (L mg^{-1})	0.0041
R^2	0.9963
R^2_{adj}	0.9958
ARE	14.79
SSE	386.33
AIC	41.84
Freundlich	
k_F ((mg g^{-1})(mg L^{-1})$^{-1/nF}$)	5.9192
$1/n_F$	0,60
R^2	0.9991
R^2_{adj}	0.9989
ARE	5.86
SSE	98.42
AIC	27,53
Sips	
q_{mS} (mg g^{-1})	87.31
k_S (L mg^{-1})	63304.35
mS	16.83
R^2	0.3625
R^2_{adj}	0.2828
ARE	162.62
SSE	45360.09
AIC	87.53

Table 7 – Comparation of the aerogel with other adsorbents for CV adsorption.

Adsorbent	q_{max} (mg g^{-1})	Reference
Chitin-psyllium based aerogel	227.11	This work
Typhalatifolia activated charcoal and chitosan composite	15.00	Kumari et al., 2017
Janshakti® polymer	12.90	Dhodapkar et al., 2007
Sugarcane fiber	10.44	Parab et al., 2009
Pinus bark powder	32.78	Ahmad et al., 2009
Chitin nanowhiskers	59.52	Druzian et al., 2019
Palmpetiole-derived biochar	209.00	Chahinez et al., 2020
Gumarabic-cl-poly(acrylamide) nanohydrogel	90.90	Sharma et al., 2018
Datepalmleaves	37.74	Ghazali et al., 2018
Chitosananilinecomposite	100.60	Tahir et al., 2017
Artocarpusheterophyllus (jackfruit) leaf powder	43.39	Saha et al., 2012
NaOH-modified rice husk	44.87	Chakraborty et al., 2011
Jutefibercarbon	27.99	Porkodi& Kumar, 2007

3.2.3.6 The potential of aerogel to treat textile effluents

The potential of aerogel to treat real textile effluents was evaluated in terms of color removal using a simulated effluent containing different dyes and compounds. Fig. 10 shows the simulated effluent's visible spectra before and after treatment with 5 g L^{-1} of aerogel.

Measuring the areas under the curves between wavelength ranges from 700 to 400 nm, it was possible to estimate that 60% of the color was removed in only 60 min of treatment with aerogel. Based on the fact that the simulated effluent had a high concentration of dyes and the treatment time was relatively short, it can be inferred that aerogel has a high potential to treat real effluents containing dyes and can perform even better with the adjustment of operation conditions, as treatment time and adsorbent dosage.

Figure 10 –Visible spectra of the simulated textile effluent before and after treatment with aerogel.

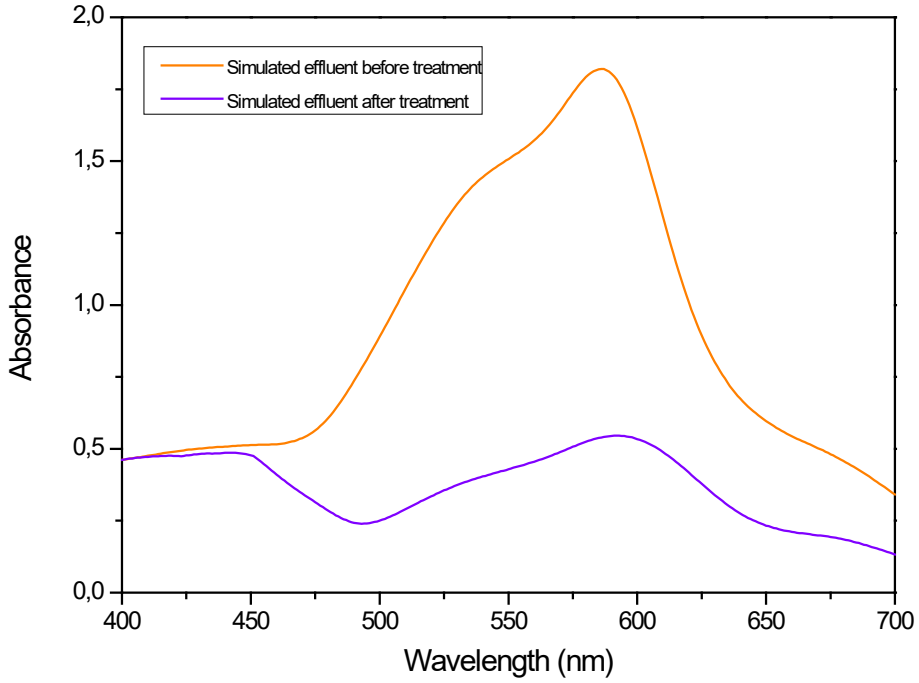

3.2.4 Conclusion

In this work, an aerogel was synthesized using natural polymers as chitin and psyllium. The aerogel developed was used to evaluate its ability to adsorb molecules of crystal violet dye present in aqueous solutions and its potential to treat real effluents containing dyes. Based on this investigation, it can be concluded that:

- The aerogel's characterization demonstrated that this material has a typical structure of amorphous materials and presented a randomly interconnected hole and channel structure that resembles an open pore network. These characteristics contribute to adsorption of dye molecules and may be a consequence of the uncontrolled growth of ice crystals during freezing;
- The adsorption was dependent on the adsorbent dosage, and 2.5 g L^{-1} of aerogel was able to remove 86.00% of CV dye from aqueous solution;
- The increase in pH caused a significant increase in dye removal percentage, reaching 90%. Because of cost-benefits, the pH original of the CV solution (pH = 8) was considered more suitable for adsorption;
- The Pseudo-second order model well represented the adsorption kinetics;

- The Freundlich model was suitable to represent the equilibrium data and the maximum adsorption capacity achieved was 227.11 mg g^{-1}, which indicates that aerogel is very efficient and competitive with several adsorbents in remove CV from aqueous solutions;
- In conclusion, the tests using aerogel to remove the color from a simulated effluent containing different dyes and compounds indicate that aerogel has a high potential to treat real colored effluents.

REFERENCES

ABBASI, F. et al. Keratin nanoparticles obtained from human hair for removal of crystal violet from aqueous solution: Optimized by Taguchi method. **Int. J. Biol. Macromol.**, v. 143, p. 492-500, 2019.

AHMAD, R. Studies on adsorption of crystal violet dye from aqueous solution onto coniferous pinus bark powder (CPBP). **J. Hazard. Mater.**, v. 171, p. 767–773, 2009.

AHMED, M. J. et al. Review on recent progress in chitosan/chitin-carbonaceous material composites for the adsorption of water pollutants. **Carbohydr. Polym.**, v. 247, 116690, 2020.

ALENCAR, W. S. et al. Application of aqai stalks as biosorbents for the removal of the dye Procion Blue MX-R from aqueous solution. **Sep. Sci. Technol.**, v. 47, p. 513- 526, 2012.

ALI, H. &MUHAMMAD, S. K. Biosorption of crystal violet from the water on leaf biomass of *Calotropisprocera*. **Environ. Sci. Technol.**, v. 1, p. 143-150, 2008.

Al-MAMUNA, M. R. et al. Photocatalytic activity improvement and application of UV-TiO_2 photocatalysis in textile wastewater treatment: A review. **J. Environ. Chem. Eng.**, v. 7, 103248, 2019.

Al–SAGHEER, F. A. et al. Extraction and characterization of chitin and chitosan from marine sources in Arabian Gulf. **Carbohydr. Polym.**, v. 77, p. 410–419, 2009.

AZIZULLAH, A. et al. Water pollution in Pakistan and its impact on public health--a review. **Environ. Int.**, v. 37, n. 2, p. 479-497, 2011.

BONILLA-PETRICIOLET, A. et al. **Adsorption Processes for Water Treatment and Purification**. Springer, 2017.

BRIÃO, G. V. et al. Adsorption of Crystal violet dye onto a mesoporous ZSM–5 zeolite synthesized using chitin as a template. **J. Colloid Interf. Sci.**, v. 508, p. 313–322, 2017.

BUSCIO, V. et al. Reducing the environmental impact of textile industry by reusing residual salts and water: ECUVal system. **Chem. Eng. J.**, v. 373, p. 161-170, 2019.

CADAVAL, T. R. S. Jr. et al. Equilibrium isotherms, thermodynamics, and kinetic studies for the adsorption of food azo dyes onto chitosan films. **Chem. Eng. Commun.**, v. 202, p. 1316-1323, 2015.

CHAHINEZ, H-O.et al. One-stage preparation of palm petiole-derived biochar: Characterization and application for adsorption of crystal violet dye in water. **Environ. Technol. Inno.**, 100872, 2020.

CHAKRABORTY, S. et al. Adsorption of crystal violet from aqueous solution onto NaOH-modified rice husk. **Carbohydr. Polym.**, v. 86, n. 4, p. 1533-1541, 2011.

CHERUIYOT, G. K. et. al. Adsorption of toxic crystal violet dye using coffee husks: Equilibrium, kinetics, and thermodynamics study. **Scientific African**, v. 5, e00116, 2019.

CHOUDHARY, M.et al. Activated biochar derived from *Opuntiaficus-indica* for the efficient adsorption of malachite green dye, Cu^{2+}, and Ni^{2+} from water. **J. Hazard Mater.**, v. 392, 122441, 2020.

CÔRTES, L. N. et al. Preparation of carbonaceous materials from pyrolysis of chicken bones and its application for fuchsine adsorption. **Environ. Sci. Pollut. R.**, v. 26, p. 28574-28583, 2019.

DHODAPKAR, R. et al. Adsorption of cationic dyes on super absorbent polymer and photocatalytic regeneration of the adsorbent. **React. Funct. Polym.**, v. 67, p. 540–548, 2007.

DOTTO, G. L. & McKay, G. Current scenario and challenges in adsorption for water treatment. **J. Environ. Chem. Eng.**, v. 4, 103988, 2020.

DOTTO, G. L. et al. Adsorption of methylene blue by ultrasonic surface-modified chitin. **J. Colloid Interf. Sci.**, v. 446, p. 133-140, 2015b.

DOTTO, G. L. et al. Adsorption rate of Reactive Black 5 on chitosan-based materials: geometry and swelling effects. **Adsorption**, v. 22, p. 973–983, 2016.

DOTTO, G. L. et al. Kinetic studies on the biosorption of phenol by nanoparticles from Spirulina sp. LEB 18. **J. Environ. Chem. Eng.**, v. 1, p. 1137–1143, 2013b.

DOTTO, G. L. et al. Surface modification of chitin using ultrasound-assisted and supercritical CO_2 technologies for cobalt adsorption. **J. Hazard. Mater.**, v. 295, p. 29-36, 2015a.

DOTTO, G. L. et al. Treatment of chitin effluents by coagulation-flocculation with chitin and aluminum sulfate. **J. Environ. Chem. Eng.**, v. 1, n. 1-2, p. 50-55, 2013a.

DRUZIAN, S. P. et al. Preparation of chitin nanowhiskers and its application for crystal violet dye removal from wastewaters. **Environ. Sci. Pollut. Res.**, v. 26, p. 28548-28557, 2019.

FABRYANTY, R. et al. Removal of crystal violet dye by adsorption using bentonite–alginate composite. **J. Environ. Chem. Eng.**, v. 5, p. 5677–5687, 2017.

FRANCO, D. P. et al. Interpretations on the mechanism of In(III) adsorption onto chitosan and chitin: A mass transfer model approach. **J. Mol. Liq.**, v. 304, 112758, 2020.

FRANTZ, T. S. et al Cu(II) adsorption from copper mine water by chitosan films and the matrix effects. **Environ. Sci. Pollut. Res.**, v. 24, p. 5908-5917, 2017.

FREUNDLICH, H. M. F. Over the adsorption in solution. **Z Phys. Chem. A**, v. 57, p. 385-470, 1906.

GEORGIN, J. et al. Biosorption of cationic dyes by Pará chestnut husk (*Bertholletiaexcelsa*). **Water Sci. Technol.**, v. 77, p. 1612–1621, 2018.

GHAZALI, A. et al. Optimization of crystal Violet adsorption onto date palm leaves as a potent biosorbent from aqueous solutions using response surface methodology and ant colony. **J. Environ. Chem. Eng.**, v. 6, n. 4, p. 3942-3950, 2018.

GHOURBANPOUR, J. et al. Effective dye adsorption behavior of poly(vinyl alcohol)/chitin nanofiber/Fe(III) complex. **Int. J. Biol. Macromol.**, v. 137, p. 296-306, 2019.

GILES, C. H. et al. A system of classification of solution adsorption isotherms, and its use in the diagnosis of adsorption mechanisms and in the measurement of specific surface areas of solids. **J. Chem. Soc.**, p. 3973–3993, 1960.

GOPI, S. et al. Enhanced adsorption of crystal violet by synthesized and characterized chitin nanowhiskers from shrimp shell. **J. Water Process. Eng.**, v. 14, p. 1–8, 2016.

HESSEL, C. et al. Guidelines and legislation for dye house effluents. **J. Environ. Manage**, v. 83, n. 2, p. 171-180, 2007.

HOLKAR, C. R. et al. A critical review on textile wastewater treatments: Possible approaches. **J. Environ. Manage.**, v. 182, p. 351-366, 2016.

HOU, F. et al. Enhanced adsorption of Congo red using chitin suspension after sonoenzymolysis. **Ultrasonics Sono. Chem.**, v. 70, 105327, 2019.

HU, Z. et al. Investigation of the effects of molecular parameters on the hemostatic properties of chitosan. **Molecules**, v. 23, n. 12, 3147, 2018.

HUSSAIN, Z. et al. Treatment of the textile industry effluent in a pilot-scale vertical flow constructed wetland system augmented with bacterial endophytes. **Sci. Total Environ.**, v. 645, p. 966-973, 2018.

IBITOYE, E. B. et al. Extraction and physicochemical characterization of chitin and chitosan isolated from house cricket. **Biomed. Mater.**, v. 13, 025009, 2018.

KISTLER, S. Coherent Expanded Aerogels and Jellies. **Nature**, v. 127, p. 741-741, 1931.

KUMAR, D. et al. Synthesize and characterization of binary grafted psyllium for removing toxic mercury (II) ions from aqueous solution. **Mater. Sci. Eng. C**, v. 104, 109900, 2019.

KUMAR, S. & Rai, S. B. Spectroscopic studies of L-arginine molecule.Indian. **J. Pure Appl. Phys.**, v. 48, p. 251-255, 2010.

KUMARI, H. J. et al. An efficient removal of crystal violet dye from wastewater by adsorption onto TLAC/Chitosan composite: A novel low-cost adsorbent. **Int. J. Biol. Macromol.**, v. 96, p. 324–333, 2017.

KUMIRSKA, J. et al. Application of spectroscopic methods for structural analysis of chitin and chitosan. **Mas. Drugs.**, v. 8, p. 1567-1636,2010.

LANGMUIR, I.The adsorption of gases on plane surfaces of glass, mica, and platinum. **J. Am. Chem. Soc.**, v. 40, p. 1361-1403, 1918.

LATA, S. &SAMADDER, S. R. Removal of heavy metals using rice husk: A review. **J. Environ. Res. Develop.**, v. 4, p. 165-170, 2014.

LI, Z. et al. Adsorption of indium (III) from aqueous solution on raw, ultrasound- and supercritical-modified chitin: Experimental and theoretical analysis. **Chem. Eng. J.**, v. 373, p. 1247-1253, 2019.

LIMA, D. R. et al. Application of ultrasound modified corn straw as an adsorbent for malachite green removal from synthetic and real effluents. **Environ. Sci. Pollut. Res. Int.**, v. 24, p. 21484–21495, 2017.

LOPES, E. C. N. et al. An alternative Avrami equation to evaluate kinetic parameters of the interaction of Hg (II) with thin chitosan membranes. **J. Colloid Interface Sci.**, v. 263, p. 542-547, 2003.

MATHEW, M. L. et al. Low-cost multilayered green fiber for the treatment of textile industry wastewater. **J. Hazard. Mater.**, v. 365, p. 297-305, 2019.

MEKONNEN, M. M. &HOEKSTRA, A. Y. Four billionpeopleare facing severe water scarcity. **Sci. Adv.**, v. 2, n. 2, e1500323, 2016.

MIRZA, A. &AHMAD, R. An efficient sequestration of toxic crystal violet dye from aqueous solution by Alginate/Pectin nanocomposite: A novel and eco-friendly adsorbent. **Groundw. Sustain. Dev.**, v. 11, 100373, 2020.

MOHANTY, K. et al. Removal of crystal violet from wastewater by activated carbons prepared from rice husk. **Ind. Eng. Chem. Res.**, v. 45, p. 5165–5171, 2006.

NANDIYANTO, A. B. D. et al. How to read and interpret FTIR spectroscope of organic materials. **Indones. J. Sci. Technol.**, v. 4, n. 1, p. 97-118,2019.

OECD - Organization for Economic Co-operation and Development. **Eco-Innovation in Industry**: Enabling Green Growth. Paris: OECD Innovation Strategy, 2009.

OLOO, C. M. et al. Adsorptive removal of hazardous crystal violet dye from aqueous solution using *Rhizophoramucronata*stem-barks: Equilibrium and kinetics studies. **Environmental Chemistry and Ecotoxicology**, v. 2, p. 64-72, 2020.

PARAB, H. et al. Use of AgroIndustrial Wastes for Removal of Basic Dyes from Aqueous Solutions. **Clean (Weinh)**, v. 37, p. 963–969, 2009.

PATIL, S.R. et al. Sorption of crystal violet from aqueous solution using live roots of *Eichhorniacrassipes*: Kinetic, isotherm, phyto, and cyto-genotoxicity studies. **Environ. Technol. Innov.**, v. 18, 100648, 2020.

PAVAN, F. A. et al. Formosa papaya seed powder (FPSP): Preparation, characterization, and application as an alternative adsorbent for the removal of crystal violet from the aqueous phase. **J. Environ. Chem. Eng.**, v. 2, p. 230–238, 2014.

PEREIRA, A. G. B. et al. Chitosan-sheath and chitin-core nanowhiskers. **Carbohyd. Polym.**, v. 107, p. 158-166,2014.

PERES, E. C. et al. Bio-nano-silica obtained from rice husk using ultrasound and its potential for dye removal. **Mater. Lett.**, v. 231, p. 72-75, 2018b.

PERES, E. C. et al. Microwave synthesis of sílica nanoparticles and its application for methylene blue adsorption. **J. Environ. Chem. Eng.**, v. 6, p. 649-659, 2018a.

PORKODI, K. &KUMAR, V. Equilibrium, kinetics and mechanism modeling and simulation of basic and acid dyes sorption onto jute fiber carbon: Eosin yellow, malachite green and crystal violet single component systems. **J. Hazard. Mater.**, v. 143, n. 1-2, p. 311-327, 2007.

QIU, H. et al. Critical review in adsorption kinetic models. **Zhejiang Uni. Sci.A**, v. 10, p. 716-724, 2009.

SABNIS, S. &BLOCK, L. H. Improved infrared spectroscopic method for the analysis of the degree of N-deacetylation of chitosan. **Polym. Bull.**, v. 39, p. 67-71, 1997.

SAHA, P. D. et al. Batch and continues (fixed-bed column) biosorption of crystal violet by *Artocarpus heterophyllus* (jackfruit) leaf powder. **Colloid Surface B**, v. 92, p. 262-270, 2012.

SEMWAL, A. &RAMANDEEP, S. Preparation, characterization, and biological evaluation of chitosan-moxifloxacin prodrugs for pharmaceuticals. **Marmara Pharm. J.**, v. 1, n. 18, 36-42, 2014.

SHARMA, G. et al. Fabrication and characterization of Gum arabic-cl-poly(acrylamide) nanohydrogel for effective adsorption of crystal violet dye. **Carbohydr. Polym.**, v. 202, p. 444-453, 2018.

SILVERSTEIN, R. et al. **Spectrometric Identification of Organic Compounds**. New York: John Wiley & Sons, 2005.

SIPS, R.On the structure of a catalyst surface. **J. Chem. Phys.**, v. 16, p. 490-495, 1948.
Soltani, N. et al. Review on the physicochemical treatments of rice husk for production of advanced materials. **Chem. Eng. J.**, v. 264, p. 899-935, 2015.

TAHIR, N. et al. Biopolymers composites with peanut hull waste biomass and application for Crystal Violet adsorption. **Int. J. Biol. Macromol.**, v. 94, p. 210-220, 2017.

TAN, Y. N. et al. Dual Extraction of crustacean and fungal chitosan from a single mucor circinelloides fermentation. **Fermentation**, v. 6, n. 2, 40, 2020.

TIAN, X. et al. Adsorption of antibiotics from aqueous solution by different aerogels.**J. Non. Cryst. Solids.**, v. 505, p. 72-78, 2019.

TOUNSADI, H. et al. Impact of chemical substances used in the textile industry on the employee's health: Epidemiological study. **Ecotoxicol. Environ. Saf.**, v. 197, 110594, 2020.

WU, F. C. et al. Characteristics of the pseudo-second-order kinetic model for liquid-phase adsorption: a mini-review. **Chem. Eng. J.**, v. 151, p. 1-9, 2009.

YAZIDI, A. et al. Ternary adsorption of cobalt, nickel and methylene blue on a modified chitin: Phenomenological modeling and physical interpretation of the adsorption mechanism. **Int. J. Biol. Macromol.**, v. 158, p. 595-604, 2020.

ZAMAN, A. et al. Preparation, properties and applications of natural cellulosic aerogels: A review. **Energy and Built Environment**, v. 1, n. 1, p. 60-76,2019.

ZHAO, S. et al. Biopolymer Aerogels and Foams: Chemistry, Properties, and Applications. **Angew. Chem. Int. Ed.**, v. 57, n. 57, p. 2-31, 2018.

CAPÍTULO 4: DISCUSSÕES E CONCLUSÃO

4.1 DISCUSSÕES

O trabalho desenvolvido nesta tese de doutorado propiciou a elaboração de dois artigos de pesquisa que tiveram como objetivo principal desenvolver diferentes materiais adsorventes a partir da quitina para a aplicação na remoção de violeta cristal de soluções aquosas por adsorção. Os adsorventes desenvolvidos neste trabalho apresentaram bons resultados comparados a outros materiais adsorventes descritos na literatura utilizados no tratamento de águas contendo violeta cristal, e se mostraram promissores para serem utilizados no tratamento de efluentes contendo corantes. Além disso, os materiais desenvolvidos apresentarem um importante viés para a gestão de resíduos sólidos, uma vez que a quitina pode ser obtida a partir de resíduos da indústria de pesca.

No primeiro artigo, nanowhiskers de quitina foram preparadas, caracterizadas e aplicadas como adsorvente para remover violeta cristal de meio aquoso. O material foi caracterizado por XRD, FT-IR, DSC, SEM, BET e BJH. Além disso, através dos testes de adsorção foram avaliados os efeitos da dosagem de adsorvente, efeito do pH, cinética, isoterma e termodinâmica. A caracterização provou que os nanowhiskers apresentam uma forma de haste e um significante aumento no tamanho de poro médio quando comparada a quitina. Os testes de adsorção mostraram que a adsorção foi favorável utilizando-se 5 g L^{-1} de nanowhiskers de quitina a um pH igual a 8. Os modelos de pseudossegunda ordem e Sips foram os mais adequados para descrever os dados de cinética e equilíbrio, respectivamente. O estudo da termodinâmica mostrou que o processo foi favorável, endotérmico e espontâneo. A capacidade máxima de adsorção apresentada pelos nanowhiskers foi de 59,52 mg g^{-1}, e que este material apresenta potencial para ser utilizado para tratar efluentes contendo violeta cristal.

No segundo artigo, um novo aerogel foi criado a partir da criodessecação de um gel de quitina e psyllium para ser utilizado como adsorvente na adsorção de violeta cristal de soluções aquosas. O aerogel foi caracterizado por XRD, SEM e FT-IR e as variáveis analisadas foram efeito da dosagem de adsorvente, efeito do pH, tempo de contato e temperatura. O aerogel apresentou uma estrutura porosa interconectada aleatoriamente, que se assemelha a uma rede de poros abertos, e foi classificado como um típico material amorfo. Dentro das condições estudadas, 2,5 g L^{-1} e o pH natural da solução de violeta cristal foram consideradas as condições mais adequadas para a adsorção. O modelo de pseudossegunda ordem apresentou o melhor ajuste dos dados da cinética de adsorção, enquanto o modelo de

Freundlich foi o mais adequado para representar as dados de equilíbrio. A capacidade máxima de adsorção experimental obtida foi 227,11 mg g^{-1}, e os testes de adsorção utilizando efluente têxtil simulado mostraram que o aerogel remove em torno de 60% da cor em 60 minutos. A partir disso, pode-se concluir que o aerogel é eficiente e competitivo quando comparado a outros adsorventes da literatura utilizados para o mesmo fim e apresenta excelente potencial para tratar efluentes coloridos reais.

Por fim, de uma maneira geral, pode-se afirmar que a quitina, mesmo com características como baixa porosidade e baixa área de superfície, pode originar materiais com alta aplicabilidade na adsorção de corantes. Ambos os materiais desenvolvidos neste trabalho foram aptos e eficientes na remoção de violeta cristal de soluções aquosas por adsorção. Contudo, o aerogel de quitina e psyllium apresentou uma capacidade máxima de adsorção (227,11 mg g^{-1}) relativamente maior quando comparada a dos nanowhiskers de quitina (59,52 mg g^{-1}), e logo pode ser classificado como aquele com maior potencial para tratar efluentes contendo violeta cristal. Assim, sugere-se para trabalhos futuros, a realização de testes utilizando estes materiais desenvolvidos para a remoção de outros corantes, e também para a remoção de outros poluentes emergentes, como fármacos e pesticidas.

4.2 CONCLUSÃO

Neste trabalho, nanowhiskers e aerogel foram preparados a partir de quitina para serem utilizados na adsorção de violeta cristal em solução aquosa. O aproveitamento de um resíduo sólido, como as cascas de camarão, para a obtenção de quitina, configura-se como uma alternativa para a destinação destes resíduos e contribui para a redução de impactos ambientais causados pelo seu descarte. Os nanowhiskers que foram desenvolvidos a partir da quitina obtida apresentaram forma de haste e um aumento no tamanho médio de poros quando comparados ao material precursor. A capacidade máxima de adsorção do violeta cristal utilizando este material foi 59,52 mg g^{-1}, classificando-o como um material adsorvente com potencial para o tratamento de efluentes contendo corantes. Também foi desenvolvido a partir da quitina um novo aerogel muito eficiente na remoção de violeta cristal de soluções aquosas, com uma capacidade máxima de adsorção de 227,11 mg g^{-1}. Os testes utilizando o aerogel para tratar efluente têxtil simulado mostraram que este material apresenta grande potencial para tratar efluentes reais contendo cor, pois foi capaz de remover 60% da cor em 60 minutos de tratamento. Por fim, pode-se concluir que o desenvolvimento de materiais adsorventes a partir da quitina contribui fortemente para as pesquisas relacionadas ao desenvolvimento de tecnologias eficazes e de baixo custo para o tratamento de efluentes contendo corantes.